Journal of Medicinal Chemistry

Article

pubs.acs.org/jmc

Indole-Derived Psammaplin A Analogues as Epigenetic Modulators with Multiple Inhibitory Activities

Raquel Pereira,[†,#] Rosaria Benedetti,[‡,#] Santiago Pérez-Rodríguez,[†] Angela Nebbioso,[‡] José García-Rodríguez,[†] Vincenzo Carafa,[‡] Mayra Stuhldreier,[†] Mariarosaria Conte,[‡] Fátima Rodríguez-Barrios,[†] Hendrik G. Stunnenberg,[∥] Hinrich Gronemeyer,[⊥] Lucia Altucci,*[,‡,§] and Ángel R. de Lera*[,†]

[†]Departamento de Química Orgánica, Universidade de Vigo, 36310 Vigo, Spain

[‡]Dipartimento di Patologia Generale, Seconda Università degli Studi di Napoli, Vico L. de Crecchio 7, 80138 Napoli, Italy

[§]Institute of Genetics and Biophysics (IGB), CNR, Via P. Castellino 111, 80131 Napoli, Italy

[∥]NCMLS, Department of Molecular Biology, Radboud University, 6525 GA Nijmegen, The Netherlands

[⊥]Department of Cancer Biology, Institut de Génétique et de Biologie Moléculaire et Cellulaire (IGBMC), CNRS, INSERM, ULP, BP 163, 67404 Illkirch Cedex, C. U. de Strasbourg, France

Supporting Information

ABSTRACT: A SAR study has been carried out around a modified scaffold of the natural product psammaplin A obtained by replacing the *o*-bromophenol unit by an indole ring. A series of indole psammaplin A constructs were generated in a short synthetic sequence that starts with the functionalization of the C3 indole position with in situ generated nitrosoacrylate, and this is followed by protection of the *β*-indole-*α*-oximinoesters, saponification, condensation with symmetrical diamines, and deprotection. Biochemical and cellular characterization using U937 and MCF-7 cells confirmed that many of these analogues displayed more potent actitivies than the parent natural product. Moreover, in addition to the reported HDAC and DNMT dual epigenetic inhibitory profile of the parent compound, some analogues, notably **4a** (UVI5008), also inhibited the NAD^+-dependent SIRT deacetylase enzymes. The SAR study provides structural insights into the mechanism of action of these multiple epigenetic ligands and paves the way for additional structural exploration to optimize their pharmacological profiles. Because of their multi(epi)target features and their action in ex vivo samples, the indole-based psammaplin A derivatives are attractive molecules for the modulation of epigenetic disorders.

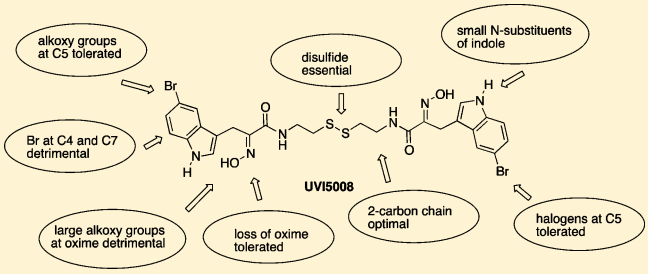

INTRODUCTION

In addition to its structural role in shaping the degree of DNA compaction, chromatin is considered the signal transduction interpreter that regulates all genome functions.[1] The basic unit of chromatin is the nucleosome, the 146 base-pair stretch of DNA wrapped 1.7 times around an octameric protein core containing two molecules each of histones H2A, H2B, H3, and H4. The flexible and highly conserved basic tail regions of the histones can be post-translationally modified primarily by acetylation, methylation, ADP-ribosylation, phosphorylation, sumoylation, and ubiquitylation.[2,3] The covalent modifications of DNA and histone proteins, most of which are reversible,[4,5] control the degree of compaction or relaxation of chromatin and act as recognition sites for regulatory factors/machineries. Ultimately, these events result in the regulation of fundamental cellular processes (such as replication, chromatin remodeling, repair, and transcription) through recognition, recruitment, and assembly of supramolecular structures (histone−histone and histone−DNA).[6] Because the alterations on gene expression are induced by mechanisms other than changes in DNA sequence, they are termed "epigenetic". The enzymes responsible for the most important covalent modifications of DNA and histones with small chemical marks are DNA methyltransferases (DNMTs), histone acetyltransferases (HATs), histone deacetylases (HDACs), histone methyltransferases (HMTs), and histone demethylases (HDMs).[7]

Emerging evidence suggests that the disruption of the balance of epigenetic networks and its interaction with the genome and the environment contribute to several major pathologies.[8−14] During onset and/or progression of disease, alterations of both the effectors of chromatin changes (e.g., histone and DNA modifiers)[15] and upstream signaling pathways[16−18] can occur.

DNA methylation at the cytosine C5 position within CpG dinucleotide-rich regions (CpG islands)[19] is promoted by the DNMT protein family,[20−22] which includes in mammals the

Received: May 3, 2012
Published: October 3, 2012

dx.doi.org/10.1021/jm300618u | J. Med. Chem. 2012, 55, 9467−9491

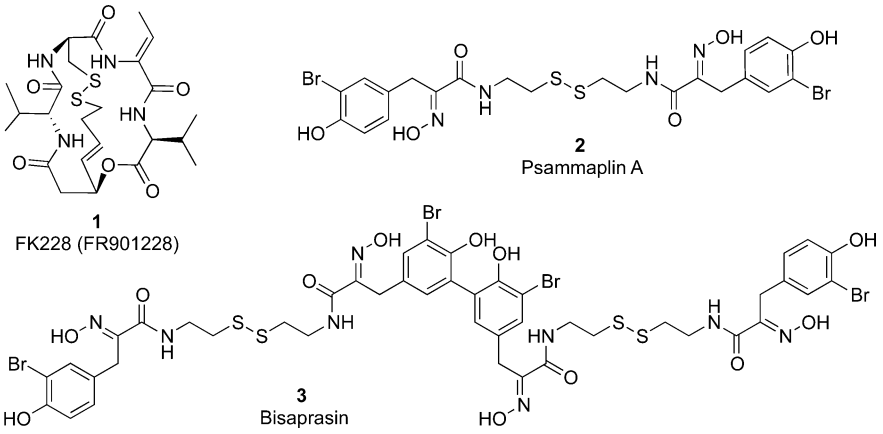

Figure 1. Disulfide-containing natural HDACis.

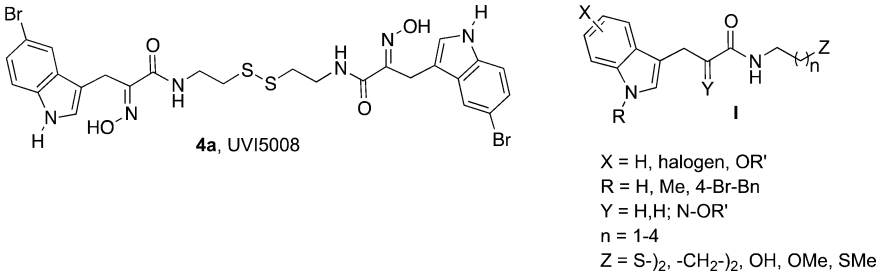

Figure 2. General structure of the indole derivatives prepared in the SAR study leading to the discovery of **4a**.

maintenance DNMT1 and the de novo methyltransferases DNMT2 and DNMT3 (a, b, and L).[23] The aberrant expression of DNMT1 induces site-specific hypermethylation and global hypomethylation of CpG islands, which are biological signatures of cancer.[9,24−29] Methylation of CpG islands in the promoter regions of tumor suppressor genes is associated with a silencing state.[30,31,28] Hypermethylation of DNA promoter and coding sequences is a major epigenetic mechanism that contributes to cancer progression by causing the inactivation of a number of tumor suppressor genes in a wide range of tumor types,[32] which is the most common molecular lesion of cancer cells.[12]

Post-translational reversible acetylation of histone lysine residues regulates gene expression and cell cycle progression. Many non-histone proteins also undergo acetylation,[33] and this modification alters, among other functions, DNA-binding activity, microtubule stabilization, protein−protein interactions, and small-molecule action. At the chromatin level, acetylation is controlled by the opposite activities of histone acetyltransferases (HATs) and histone deacetylases (HDACs).

Eighteen mammalian deacetylase enzymes comprise the superfamily of HDACs, which is conveniently divided into two families that differ in the overall mechanism of lysine deacetylation: the Zn^{2+}-dependent hydrolases (11 members consisting of class I with HDAC1, -2, -3, and -8; class IIa with HDAC4 and -10; class IIb with HDAC5, -6, -7, and -9; class IV with HDAC11) and the NAD^{+}-dependent deacetylases or sirtuins (7 members consisting of SIRT1−7).[34−36]

The Zn^{2+}-dependent HDAC hydrolases deacetylate the ε-acetylamidolysine by a nucleophilic attack of bound water to the Zn^{2+}-activated carbonyl group, creating a tetrahedral zinc alkoxide intermediate stabilized by enzyme residues which releases the acetyl group and the lysine product. Class I/II/IV HDAC inhibitors[37−39] contain three regions: a Zn^{2+}-chelating headgroup[40] (hydroxamates, benzamides, short-chain fatty acids, and thiolates, among others, are part of the metal-binding structure[38,39]), a linker/spacer that occupies the binding pocket of the native lysine, and a highly variable cap group that extends along the rim of the pocket. Sirtuins regulate a variety of cellular functions such as conservation of the genome, longevity, and metabolism of organisms ranging from bacteria to eukaryotes.[36,41−45] An increasing number of reports indicate the implication of multiple epigenetic enzymes in the onset or progression of cancer,[13] among them the sirtuins.[43]

The modulation of epigenetic enzymes by small molecules has been correlated with the induction of differentiation, cell cycle and growth arrest, and apoptosis in cancer cells.[46,47] Chromatin regulators ("epi drugs")[19,48,49] thus represent novel promising anticancer drugs.[8,13,50−52] Indeed, two DNMT inhibitors (DNMTis) (5-aza-cytidine, Vidaza; 5-aza-deoxycytidine, Dacogen)[21,53] have been approved for the treatment of myelodisplastic syndrome (MDS),[54] and two HDACis, namely, SAHA (suberoylanilide hydroxamic acid, vorinostat) and FK-228 **1** (depsipeptide), have also been marketed for the treatment of cutaneous T cell lymphoma (CTCL).

Depsipeptide **1** is a natural product isolated from *Chromobacterium violaceum* No. 968.[55] Its approval for therapy demonstrates that natural products continue to be a source of new medicines or the inspiration for the discovery of new drug leads.[56−60] It has been demonstrated that the disulfide bond of FK228 **1** (for other depsipeptides with disulfide bonds in bicyclic structures, such as the spiruchostatins and FR901375, see[58]) becomes reduced in cells by the activity of glutathione to afford a thiolate termed redFK, which then would interact with the Zn^{2+} ion in the active site of HDAC.[61]

A disulfide bond is also present in the dimeric natural product psammaplin A (**2**, Figure 1), a representative member of the symmetrical bromotyrosine−cysteine modified tetrapeptides. Isolated in 1987 from an unidentified sponge[62−64] and later,

dx.doi.org/10.1021/jm300618u | J. Med. Chem. 2012, 55, 9467−9491

Scheme 1[a]

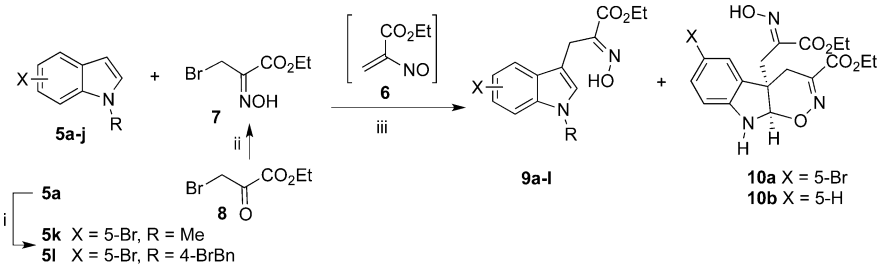

[a]Reagents and conditions: (i) MeI or 4-$BrC_6H_4CH_2Br$, KOH, DMF, 0 °C, 30 min (**5k**, 91%; **5l**, 53%); (ii) **8**, $CHCl_3$, $NH_2OH{\cdot}HCl$, MeOH/H_2O (1:1), 25 °C, 22 h (86%); (iii) K_2CO_3, CH_2Cl_2, 25 °C, 20 h (**9a–l**, Table 1).

Scheme 2[a]

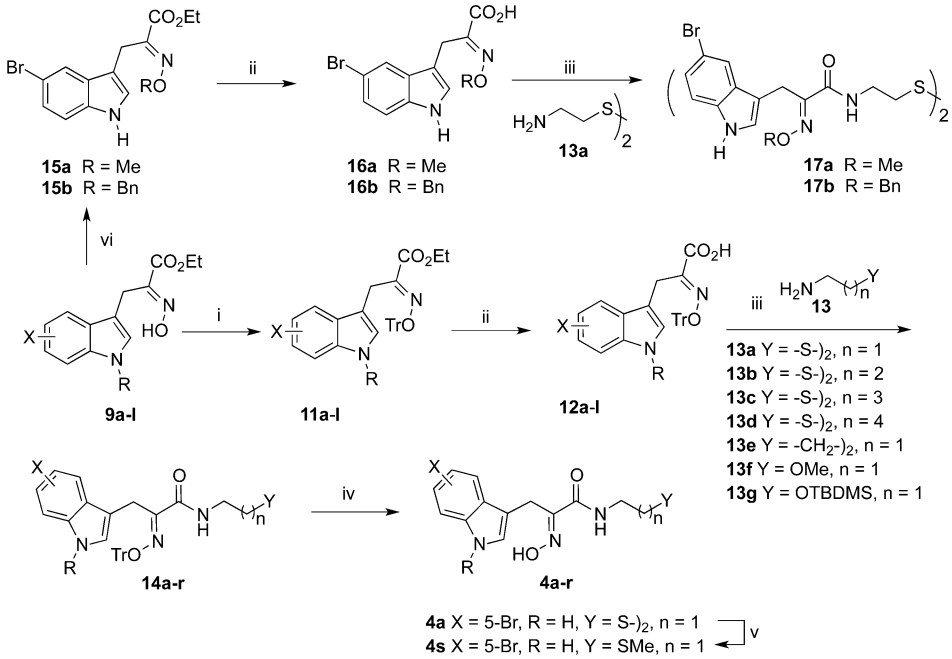

[a]Reagents and conditions: (i) K_2CO_3, CH_2Cl_2, TrCl, 25 °C, 20 h; (ii) $LiOH{\cdot}H_2O$, THF/H_2O (1:1), 25 °C, 20 h (**12a–l**, Table 1, combined yield for the two steps); **16a**, 84%; **16b**, 99%; (iii) (i) EDC, NHS, dioxane, 25 °C, 2 h; (ii) cystamine **13a**, Et_3N, MeOH, dioxane, 25 °C, 15 h (**17a**, 80%; **17b**, 84%) or amines **13b–f**, Et_3N, MeOH, dioxane, 25 °C, 15 h; (iv) 1 M HCl in Et_2O, CH_2Cl_2, 25 °C, 2 h (**4a–r**, Table 1, combined yield for the two steps); (v) (i) $NaBH_4$, NaOH, EtOH, 25 °C, 0.5 h; (ii) MeI, 25 °C, 16 h (**4s**, 80%); (vi) MeI, Ag_2O, acetone, 25 °C, 14 h or BnBr, KO^{t}Bu, DME, 25 °C, 12 h (**15a**, 42%; **15b**, 72%).

together with **3**, from Verongid sponges (refs 65 and 66 and references cited therein), psammaplin A was shown to display antibacterial and antitumor activities.[67] In particular, **2** exhibited significant cytotoxicity against human lung (A549), ovarian (SKOV- 3), skin (SK-MEL-2), CNS (XF498), and colon (HCT15) cancer cell lines.[66] The dual inhibition of histone deacetylase (HDAC) and DNA methyltransferase (DNMT) enzymes reported for **2**[65] (note that DNMT inhibition by psammaplin A has been debated, being reported in refs 68–70 but not observed in a recent SAR study[71]) captured our interest,[72] given the promising results of ongoing clinical trials with combination therapies using HDACis and DNMTis.[20,73]

Inspired by the structure and likely mechanism of action of psammaplin A (**2**), we recently reported the synthesis and characterization of **4a** (Figure 2)[74] which, in addition to displaying a more potent inhibition of HDAC and DNMT than parent **1**, also targets at least one other family of epigenetic enzymes (SIRT). Here we report on the development of **4a** and SAR studies on this family of epigenetic modulators.

DESIGN AND SYNTHESIS

The structure of psammaplin A **2** contains a symmetrical tetrapeptide formed by condensation of two modified 2-bromotyrosine and cystamine units. It was considered that other amide moieties derived from heteroaryl-containing aminoacids incorporated into the scaffold could improve the reported HDAC and DNMT inhibitory profile of the parent compound. This assumption was supported by the discovery of highly potent HDACis with the indoleamide hydroxamic acid structure.[75,76]

Our purpose to undertake SAR studies called for a synthetic approach to these modified tetrapeptides that could yield analogues (general structure **I**, Figure 2) at the various positions by slight modifications of the sequence. Initial exploratory studies focused on the variations of the substituents at the indole ring including the group at N, the oxime functionality, and the size of the chain connecting the amide to the disulfide. Addressing some of these structural modifications, we expected

dx.doi.org/10.1021/jm300618u | J. Med. Chem. 2012, 55, 9467–9491

Table 1. Yields (%) for the Compounds of the Synthetic Sequence of Indole Psammaplins

9, 12	yield, 9	yield, 12	4	yield
a, X = 5-Br, R = H	60	73	**a**, X = 5-Br, R = H, Y = $(S\text{-})_2$, n = 1	70
b, X = H, R = H	67	87	**b**, X = H, R = H, Y = $(S\text{-})_2$, n = 1	50
c, X = 5-F, R = H	87	71	**c**, X = 5-F, R = H, Y = $(S\text{-})_2$, n = 1	38
d, X = 5-Cl, R = H	42	73	**d**, X = 5-Cl, R = H, Y = $(S\text{-})_2$, n = 1	30
e, X = 5-I, R = H	82	77	**e**, X = 5-I, R = H, Y = $(S\text{-})_2$, n = 1	13
f, X = 5-OMe, R = H	51	64	**f**, X = 5-OMe, R = H, Y = $(S\text{-})_2$, n = 1	4
g, X = 5-OBn, R = H	75	59	**g**, X = 5-OBn, R = H, Y = $(S\text{-})_2$, n = 1	20
h, X = 4-Br, R = H	65	61	**h**, X = 4-Br, R = H, Y = $(S\text{-})_2$, n = 1	54
i, X = 6-Br, R = H	43	49	**i**, X = 6-Br, R = H, Y = $(S\text{-})_2$, n = 1	41
j, X = 7-Br, R = H	43	37	**j**, X = 7-Br, R = H, Y = $(S\text{-})_2$, n = 1	30
k, X = 5-Br, R = Me	68	60	**k**, X = 5-Br, R = Me, Y = $(S\text{-})_2$, n = 1	71
l, X = 5-Br, R = 4-BrBn	68	45	**l**, X = 5-Br, R = 4-BrBn, Y = $(S\text{-})_2$, n = 1	32
			m, X = 5-Br, R = H, Y = $(S\text{-})_2$, n = 2	19
			n, X = 5-Br, R = H, Y = $(S\text{-})_2$, n = 3	42
			o, X = 5-Br, R = H, Y = $(S\text{-})_2$, n = 4	38
			p, X = 5-Br, R = H, Y = $(CH_2\text{-})_2$, n = 2	82
			q, X = 5-Br, R = H, Y = OMe, n = 1	37
			r, X = 5-Br, R = H, Y = OH, n = 1	37
			s, X = 5-Br, R = H, Y = SMe, n = 1	80

to additionally get further insights into the mechanism of action of **4a** in its epigenetic inhibitory activities, and for this purpose the terminal group was also chemically modified.

The synthesis of **4a** (Schemes 1 and 2) is representative of the preparation of the entire collection of indole psammaplins. It started with the attachment of the functionalized oxime ester side chain to indole derivative **5a** to provide **9a** using the method described by Gilchrist.[77] This entails reaction of **5a** with nitrosoacrylate **6**,[77] generated in situ from oxime **7**, itself prepared by the reaction of ethyl bromopyruvate **8** with hydroxylamine hydrochloride. Either an inverse electron-demand hetero-Diels–Alder cycloaddition or a Friedel–Crafts reaction followed by indole aromatization is fully compatible with the outcome of the condensation of **5a** and **6**. Other analogues **9b–e** were similarly obtained (Scheme 1, Table 1) starting from commercial and noncommercial bromoindoles. The latter compounds were synthesized by application of the Leimgruber–Batcho methodology[78] or by the Bartoli procedure.[79] N-Substituted indoles **5k** and **5l** were instead synthesized using the protocol described by Stadlwieser.[80]

Minor amounts of the cycloadducts **10** resulting from 2-fold condensation at the C3-position of indole and **7** were isolated and characterized in the case of X = 5-Br (**10a**, 4%) and X = H (**10b**, 7%). X-ray analysis of compounds **9b** and **10b** confirmed the *E* geometry of the oxime and for **10b** the *cis*-fusion of the indole and oxazine rings (Supporting Information). The amount of **10** could be minimized using an excess of indole derivative (2 equiv) and base (5.5 equiv) relative to oxime **7**.

Initial attempts to couple the oxime indole derivatives **9a** with amines using a variety of reaction conditions (DCC, HOBt,[81,82] PyBOP, $ClCO_2Et$[83]) were either unsuccessful or produced the product in low yields (<50% with DCC, *N*-hydroxyphthalimide).[84] Therefore, protection of the oxime of **9a** (Scheme 2, Table 1) as trityl derivative **11a** was required before saponification (to produce acid **12a**) and condensation with cystamine **13a** via activation as the *N*-succinimidyl ester, a sequence that produced disulfides **14**.[85] Cleavage of the trityl protecting group[85] afforded compound **4a** (Table 1).

Following identical sequence, indoles **9b–l** were transformed into disulfides **4b–l** using either cystamine **13a** or amines **13b–g** (Scheme 2, Table 1), some of which were synthesized using the general methodology described by Pfammatter.[86] Deprotection of the silyl ether of **14r** took place concomitantly with trityl deprotection. On the other hand, methyl sulfide **4s** was obtained by reduction of disulfide **4a** with $NaBH_4$ and methylation with MeI (Scheme 2).[87]

The same sequence provided the benzyl[88] and methyl[89] oximes (**15b** and **15a**, respectively, Scheme 2) following benzylation and methylation of **9a**, and along similar steps analogues **17a,b** were obtained from these intermediates.

Analogues **20a** and **20b**, which lack the oxime function, were synthesized by a similar sequence using a $ZrCl_4$-catalyzed[90] Friedel–Crafts type alkylation of 5-bromoindoles **5a** and **5k** with methyl acrylate followed by hydrolysis and condensation of acids **19a** and **19b** with cystamine **13a** via activation as the *N*-hydroxysuccinimidyl ester (Scheme 3).

Scheme 3[a]

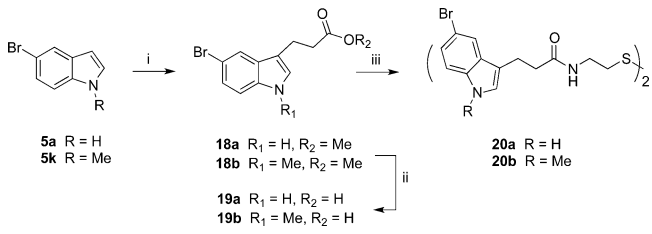

[a]Reagents and conditions: (i) methyl acrylate, $ZrCl_4$, CH_2Cl_2, 25 °C, 5 h; (ii) $LiOH{\cdot}H_2O$, THF/H_2O (1:1), 25 °C, 20 h (**19a**, 57%; **19b**, 75%; combined yield); (iii) (i) EDC, NHS, dioxane, 25 °C, 2 h; (ii) cystamine **13a**, Et_3N, MeOH, dioxane, 25 °C, 15 h (**20a**, 65%; **20b**, 42%).

BIOLOGICAL EFFECTS OF PSAMMAPLIN A DERIVATIVES IN CELLULAR CANCER MODELS

Following the confirmation of the epigenetic activities of psammaplin A **2** using in vitro assays on isolated enzymes and cellular experiments,[72] we undertook the search for more potent analogues, with a focus on the β-indole-α-oximinoamido scaffold. The series of indole derivatives synthesized (Schemes

dx.doi.org/10.1021/jm300618u | J. Med. Chem. 2012, 55, 9467–9491

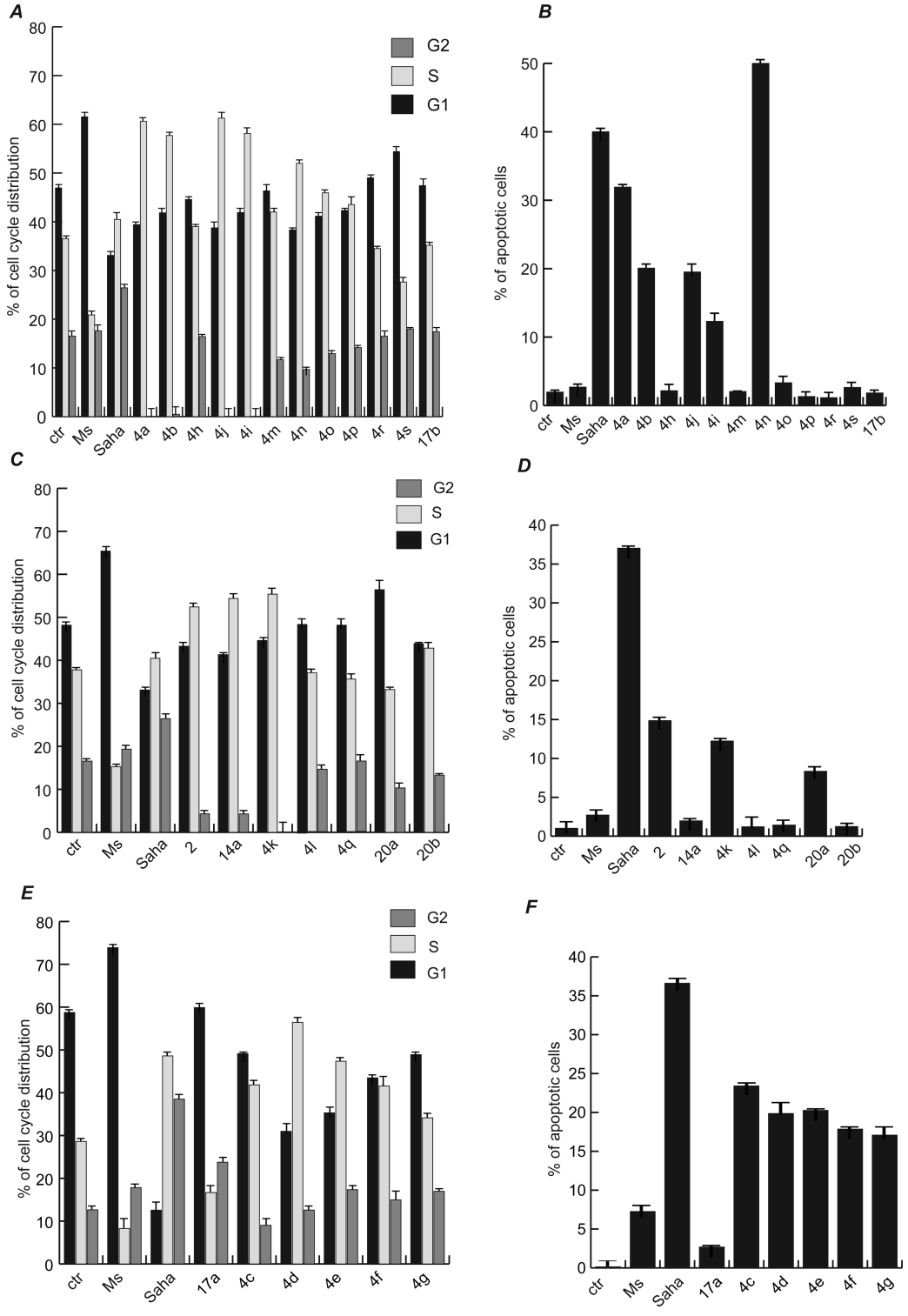

Figure 3. Analysis of the effects of cell cycle and apoptosis of U937 cells treated with indole-based psammaplin A analogues: (A, C, E) cytofluorimetric cell cycle analysis after treatment with the compounds at 5 μM for 24 h; (B, D, F) apoptosis analysis after treatment with the compounds at 5 μM for 30 h. MS-275 and SAHA (5 μM) were used as controls. Error bars represent standard deviation (SD) of biological triplicates.

2 and 3) were aimed at understanding the role of structural elements and functional groups in the modulation of different epigenetic enzymes and at the identification of the pharmacophore(s) of these inhibitors. We also addressed whether (i) the dimeric structure or just the monomer is necessary for their biological activity, (ii) if the disulfide bridge is dispensable, and (iii) if an uncleavable dimeric compound displays similar activities. By use of the U937 acute myeloid leukemia (AML) cell line, the activity readouts systematically investigated were cell cycle arrest and $p21^{WAF1/CIP1}$ induction, induction of differentiation, acetylation of histone H3, and for HDAC6 inhibition, the levels of α-tubulin acetylation.

As shown in Figure 3B, after 24 h of stimulation with the analogues at 5 μM, derivatives **4a** and **4n** showed a greater

dx.doi.org/10.1021/jm300618u | J. Med. Chem. 2012, 55, 9467−9491

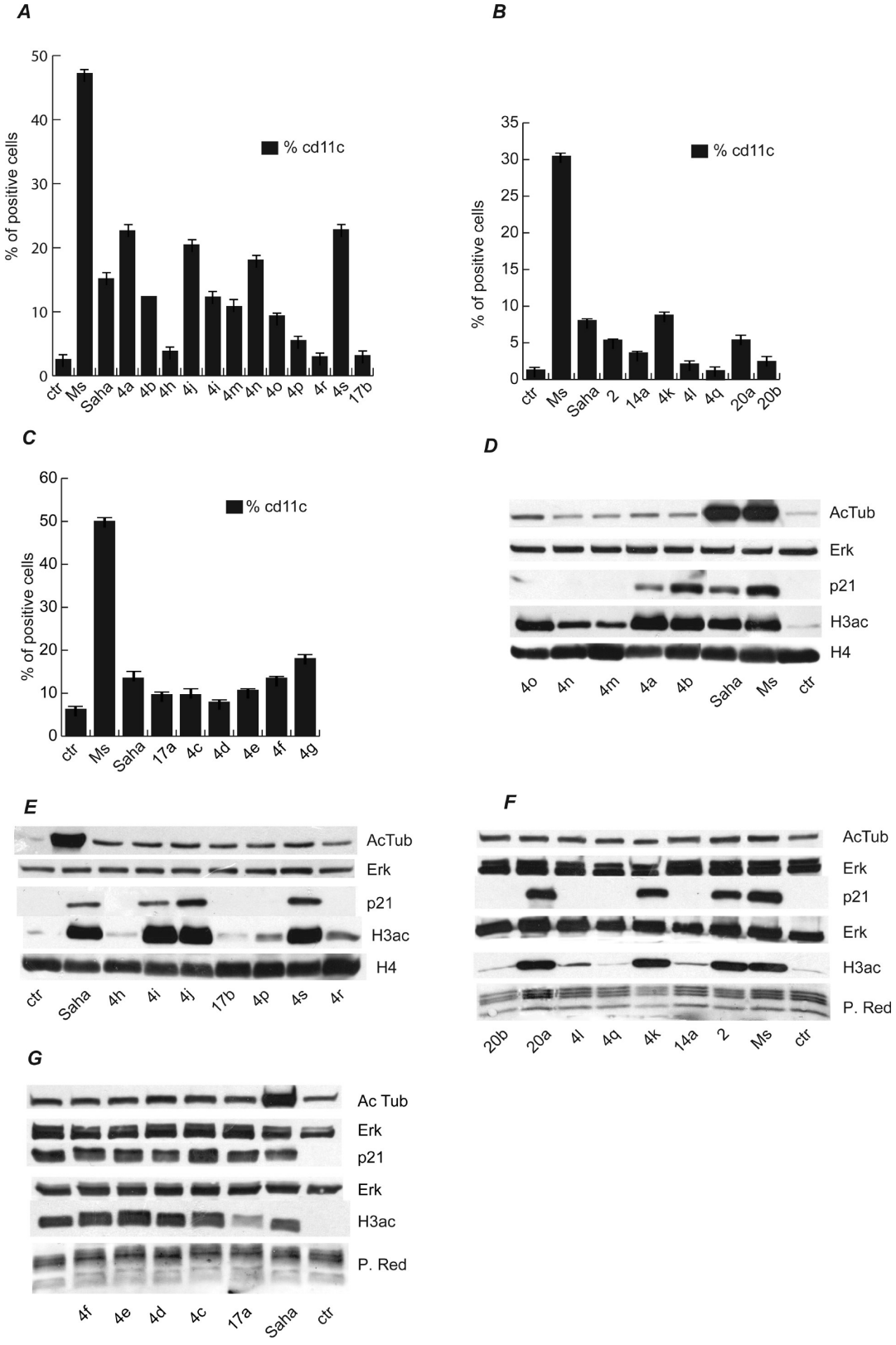

Figure 4. Analysis of cell differentiation (A–C) and Western blot analysis (D–G) of functional readouts of indole-based psammaplin A analogues. (A–C) Effects on granulocytic differentiation by cytofluorimetric analysis of CD11c expression after treatment of U937 acute myeloid leukemia cells with indole-based psammaplin A analogues at 5 μM for 30 h. SAHA and MS-275 (5 μM) were used as positive control. The data represent the average value of independent triplicates. Error bars represent standard deviation (SD) of biological triplicates. (D–G) Western blot analysis of p21, histone H3 acetylation, and α-tubulin acetylation in U937 cells after treatment with the indicated compounds at 5 μM for 24 h. Total ERKs were used to normalize for equal loading of total protein extraction. Total H4 or Ponceau red staining was used to normalize for equal loading of histone extracts. SAHA and MS-275 (5 μM) were used as controls.

dx.doi.org/10.1021/jm300618u | J. Med. Chem. 2012, 55, 9467–9491

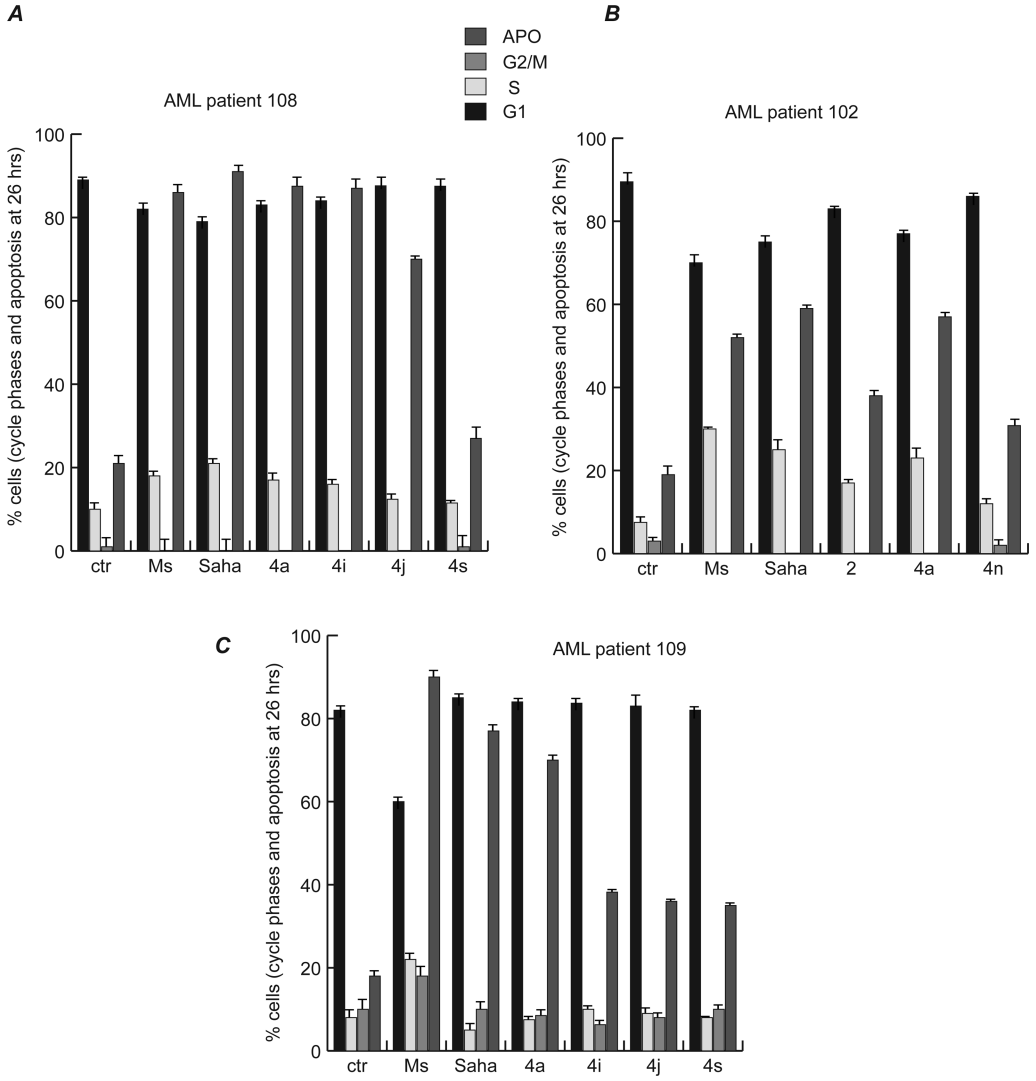

Figure 5. (A–C) Cell cycle analysis of ex vivo patient's blasts treated with selected indole-based psammaplin A analogues. Analysis of cell cycle and apoptosis was carried out with selected compounds at 5 μM in different AML patient blasts (indicated as numbers). SAHA and MS-275 (5 μM) were used as controls. Error bars represent standard deviation (SD) of biological triplicates.

induction of cell death than psammaplin A **2** (Figure 3D). To confirm these biological activities, cell cycle analyses were performed after 24 h of induction with psammaplin A **2** and its derivatives (Figure 3A,C). The proapoptotic activities of psammaplin A **2** and analogues **4a** and **4n** were also validated in the solid cancer cell lines derived from breast (ZR75.1, data not shown) and prostate (LnCap, data not shown) tumors. Cell death was observed for compounds **4i**, **4j**, **4k**, **20a**, **4c–g** (see Figure 3D and Figure 3F), but a lower number of cells underwent apoptosis compared to **4n**. Some compounds induced changes in the relative percentage of cells in the different phases of the cell cycle (Figure 3C and Figure 3E).

The parent compound formally derived from tryptophan (**4b**) displayed lower proapoptotic activity than the C5-bromoindole derivative (**4a**), but changing the substitution from C5 to C6 (**4i**) or C7 (**4j**) had only a minor effect on cell cycle arrest and apoptosis (Figure 3A and Figure 3B) and rather increased the induction of differentiation measured by expression of the CD11c marker (Figure 4A).

Figure 4A–C shows that most compounds (**4n**, **4i**, **4j**, **4s**, **4k**, **4f**, **4g**, and **4m**) derived from **4a** and **4b** induced the expression of CD11c (prodifferentiation surface marker), which is indicative of the differentiation of U937 cells to granulocytes.

Cell-based assays confirmed that the presence of one or two sulfur atoms and/or the disulfide bridge and/or the cell cleavage thiols derived from **2** and **4a** is required for cell cycle arrest, induction of apoptosis, and differentiation. Interestingly however, the methylthioether **4s** is inactive at inducing apoptosis (Figure 3B) and G2M phase accumulation but it induces cell arrest at G1 (Figure 3A) and the corresponding enhanced expression of $p21^{WAF1/CIP1}$, as shown in Figure 4A and Figure 4E. Further studies will be necessary to define the molecular pathways that are apparently differently affected by **4a** and **4s**.

Indole psammaplin A derivatives induced α-tubulin acetylation (a marker of HDAC6 inhibition), in some cases at levels similar to psammaplin A (**2**), as shown by Western blot analysis (Figure 4D–G). Moreover, most of the compounds increased histone H3 acetylation levels, with **4a** being clearly more efficient (Figure 4D). Note that despite its action on α-tubulin acetylation, **4n** did not show hyperacetylation of histone H3, suggesting a different mechanism of action.

dx.doi.org/10.1021/jm300618u | J. Med. Chem. 2012, 55, 9467–9491

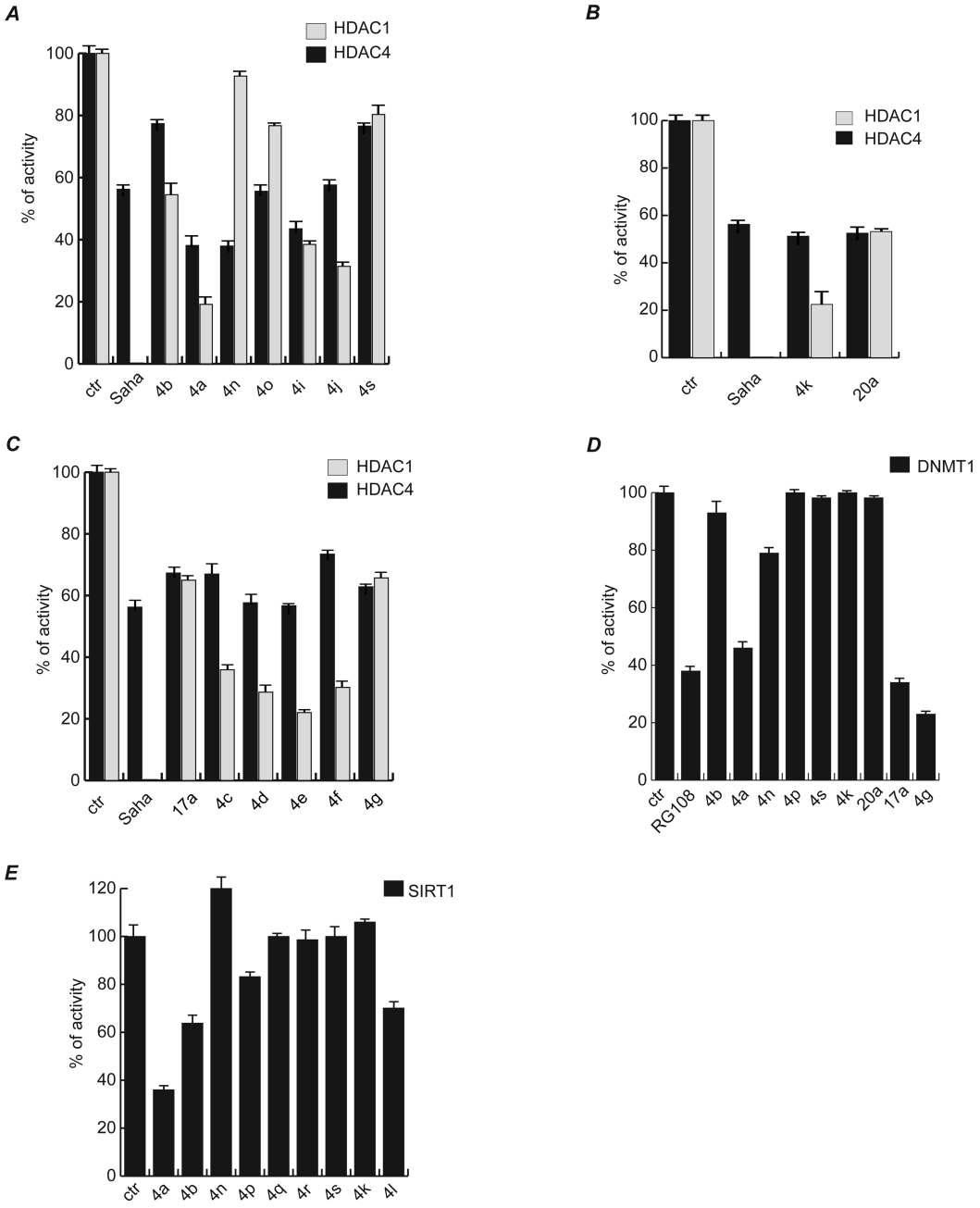

Figure 6. Modulation of epigenetic enzymes by indole-based psammaplin A analogues: (A−C) U937 cell-based HDAC1 and HDAC4 assay carried out with the indicated compounds at 5 μM; (D) in vitro DNMTs assay carried out in U937 extracts treated with the indicated compounds at 5 μM; (E) in vitro human recombinant SIRT1 assays with the indicated compounds at 5 μM. SAHA and RG-108 (5 μM) were used as controls. Error bars represent standard deviation (SD) of biological triplicates.

A correlation between hyperacetylation of histone H3 and expression of p21 protein exists. Indeed, as shown in Figure 4D−G, compounds for which the H3ac level is greater (**4b**, **4a**, **4i**, **4j**, **4s**, **4k**, **20a**, **4c**−**g**) also showed a stronger induction of p21 and the greatest percentage of cell death.

With regard to the effect of other substituents at the C5-indole ring position (OMe, **4f**; OBn, **4g**), including other halogens (F, **4c**; Cl, **4d**; I, **4e**), the biological evaluation indicates that the original scaffold is quite lenient at that position, since most of the C5-substituted indole derivatives showed the ability to induce p21, histone H3, and α-tubulin acetylation levels (Figure 4G) and, with the exception of **4c**, also p16 (see Figure 7).

Finally, the *N*-methyl derivative **4k** was found to induce apoptosis, change the cell cycle distribution, induce the acetylation of histone H3 and α-tubulin, and overexpress p21 (at levels comparable to **4a**), but the larger *N*-*p*-bromobenzyl analogue **4l** is quite inactive in these biological assays, showing a weak induction of p21 after 24 h of treatment of U937 cells (Figure 3C,D and Figure 4B,F).

INDOLE PSAMMAPLIN A DERIVATIVES INDUCE APOPTOSIS IN AML PATIENT'S BLASTS

The intriguing anticancer potential of these indole-based psammaplin A derivatives prompted us to test their activity in ex vivo AML patient blasts. As shown in Figure 5 B, **4a** induced

dx.doi.org/10.1021/jm300618u | *J. Med. Chem.* 2012, 55, 9467−9491

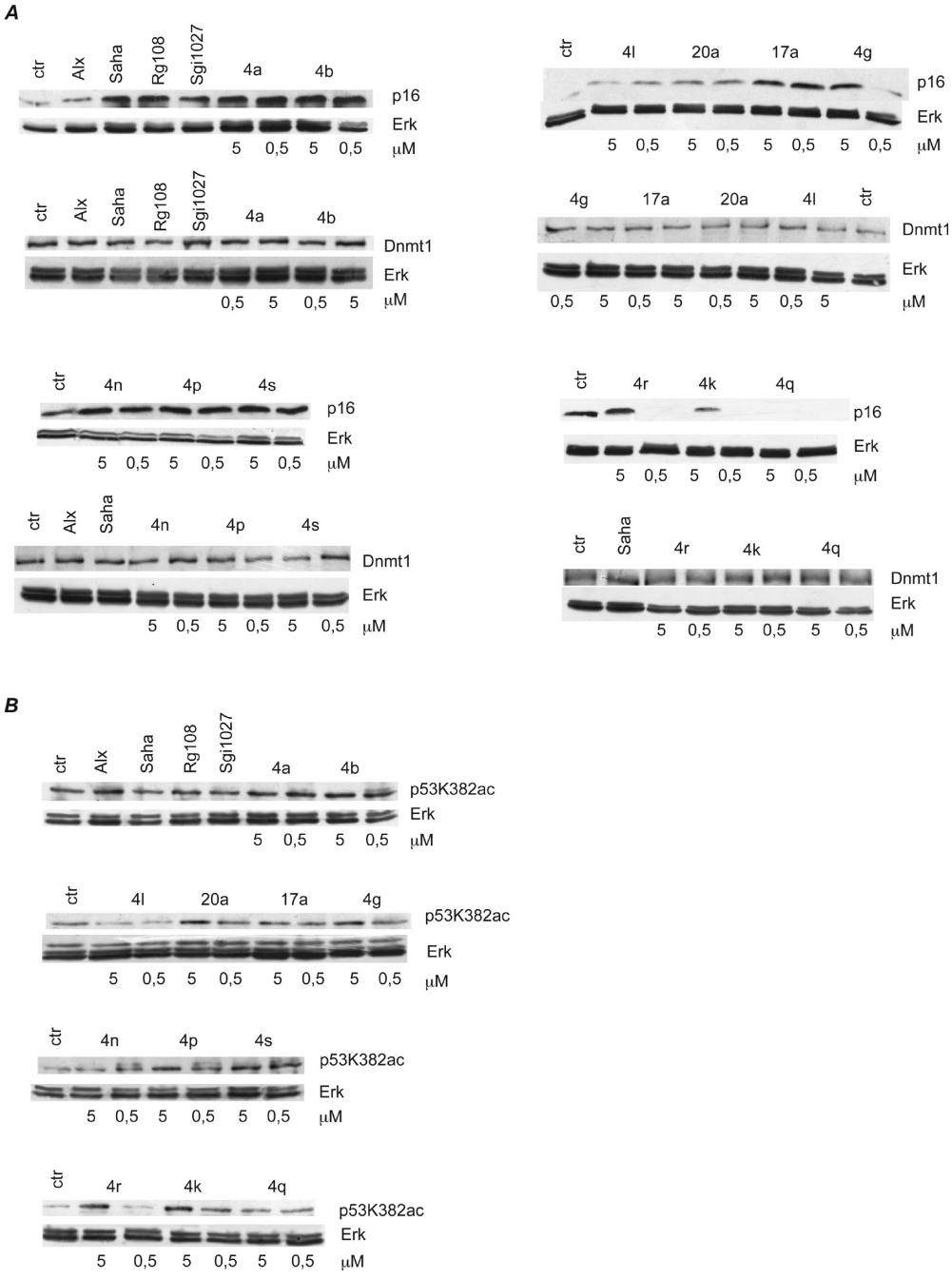

Figure 7. (A) Western blot analysis of p16 and DNMT1 levels after treatment of U937 cells with the indicated compounds at 5 and 0.5 μM for 24 h. Total ERKs were used to normalize for equal loading of total protein extraction. SAHA, RG108 (5 μM), SGI1027 (5 μM), and ALX (1 μM) were used as controls. (B) Western blot analysis of p53 acetylation on lysine 382 after treatment of MCF7 cells with the indicated compounds at 5 and 0.5 μM for 24 h. Total ERKs were used to normalize for equal loading of total protein extraction. SAHA, RG108 (5 μM), SGI1027 (5 μM), and ALX (1 μM) were used as controls.

cell cycle block and apoptosis as measured by FACS in AML no. 102 ex vivo blasts, similar to psammaplin A **2**. Known HDACis such as MS-275 (Entinostat) and SAHA (Vorinostat) displayed activities similar to that of **4a**. To verify the action of the selected derivatives on AML patient blasts, the activity of compounds **4a**, **4i**, **4j**, and **4s** was tested at 5 μM. As shown in Figure 5A,C, all these derivatives showed proapoptotic activity in two different samples of AML patient's blasts (no. 108 and no. 109). Methylthioether **4s** showed a weak induction of apoptosis, confirming data obtained with the U937 cell line.

INHIBITION OF EPIGENETIC ENZYMES BY INDOLE PSAMMAPLIN A DERIVATIVES

Having established the activity of the indole psammaplin A analogues in biological assays, the active compounds were also tested in vitro (on enzyme-based assays). Because acetylation levels of many targets were found to be modified after the treatment with selected compounds (see Figure 4D–G), those leading to the expression of p21, acetylation of histone H3, and acetylation of α-tubulin were tested (at 5 μM) as inhibitors of HDAC1 and HDAC4 enzymes.

dx.doi.org/10.1021/jm300618u | J. Med. Chem. 2012, 55, 9467–9491

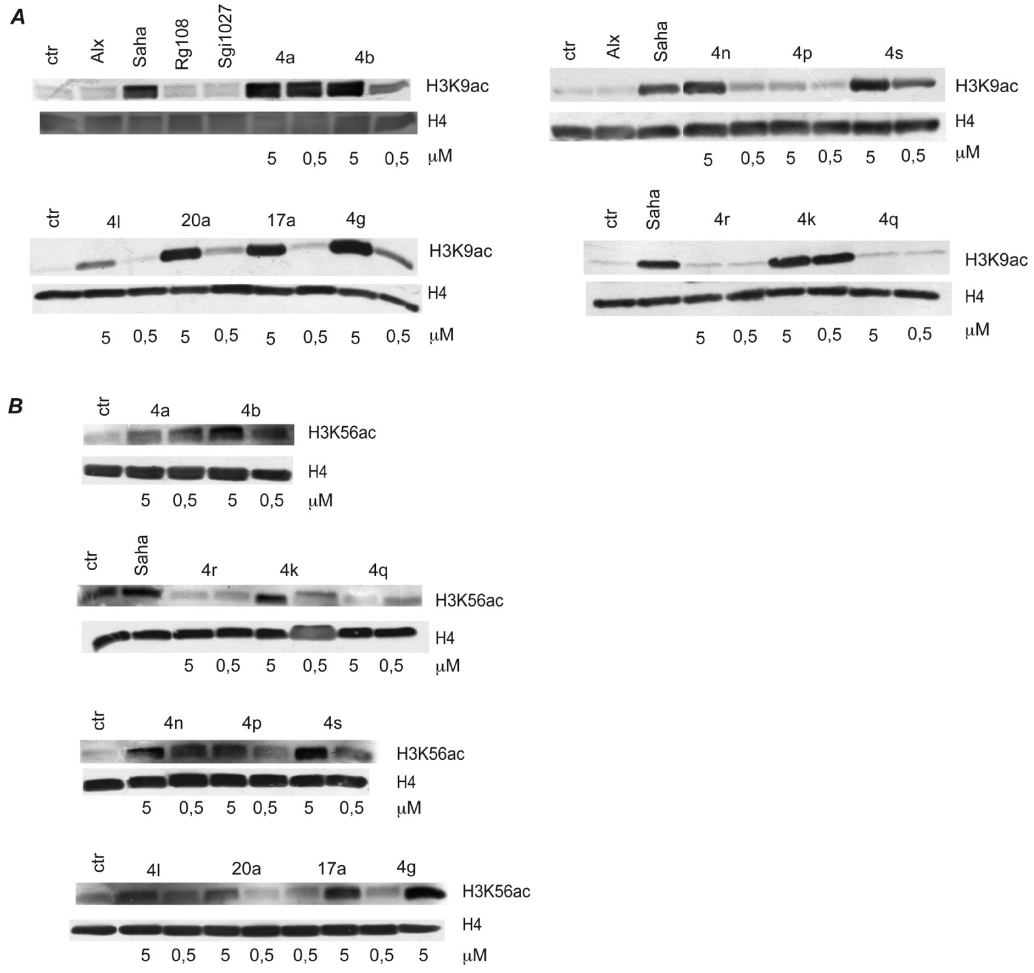

Figure 8. Western blot analysis of H3 acetylation on lysine K9 (A) and lysine K56 (B) after treatment of U937 cells with the indicated compounds at 5 and 0.5 μM for 24 h. Total H4 was used to normalize for equal loading of histone extracts. SAHA, RG108 (5 μM), SGI1027 (5 μM), and ALX (1 μM) were used as controls.

As shown in Figure 6A, compounds **4a**, **4i** and **4j** showed inhibitory activities (around 60−80%) against HDAC1. The same compounds were also active against HDAC4 (see black and gray bars in Figure 6A), although with lower potency (40−60% for compounds **4a** and **4j**). Other analogues followed the same trend (better inhibitors of HDAC1 than HDAC4) but were less effective inhibitors of both enzymes, with percentages of inhibition ranging from 20% (HDAC4) to 40% (HDAC1).

Compounds **4n** and **4o** were instead rather inactive against HDAC1 but acted as inhibitors of HDAC4 (in particular compound **4n**, for which the percentage of inhibition of HDAC4 is around 60%). Compounds **4k** and **20a** (see cell-based data in Figure 3C,D and Figure 4B,F) showed inhibition of HDAC4 (Figure 6B) and to a lesser extent of HDAC1 (**4k**).

The series of halogen and ether analogues at C5 (**4c−g**) reduced the activity of HDAC1 and HDAC4 in a variable way (different for each derivative) but in general showed a greater activity against HDAC1 than HDAC4 (Figure 6C). The inhibition induced by the methyloxime **17a** (Figure 6C) was similar to that of **4g**.

Likewise, the activity of mechanistically relevant analogues on other epigenetic enzymes was analyzed, in particular as inhibitors of DNMTs and SIRTs, in order to relate structure and activities. By use of recombinant DNMT1 enzyme and labeled *S*-adenosymethionine, the cofactor for methyl transfer (Figure 6D), it was shown that the desoximino compound (**20a**) was inactive but the methylated oxime (**17a**) was as active as **4a**, and the 5-OBn derivative (**4g**) exhibited even greater activity than **4a** and also than the known DNMT1 inhibitor RG-108.

As shown in Figure 6 E, **4a** displayed the greatest potency of the series on SIRT1 inhibition, with the presence of C5-Br being less important (**4b**) than other modifications. Whereas the *N*-Me-indole derivative **4k** proved to be inactive, the *N*-*p*-bromobenzyl derivative **4l** and the analogue with the all carbon connector between the amides (**4p**) showed weak activity. No SIRTi activity was noted for the corresponding monomers (**4s**, **4r**, **4q**).

INDOLE PSAMMAPLIN A ANALOGUES INDUCE CHANGES OF ACETYLATION AND EXPRESSION LEVELS OF EPIGENETIC TARGETS

Compounds that showed inhibitory activity on DNMT1 and SIRT1 enzymes were also tested in cell-based assays in order to confirm (by Western blot) if the in vitro activities correlated with changes of acetylation and expression states of selected epigenetic targets.

In Figure 7, the reactivation of p16 expression was evaluated after treatment of U937 cells for 24 h with selected compounds at two different concentrations (5 and 0.5 μM). Analogues **4a**,

dx.doi.org/10.1021/jm300618u | *J. Med. Chem.* 2012, 55, 9467−9491

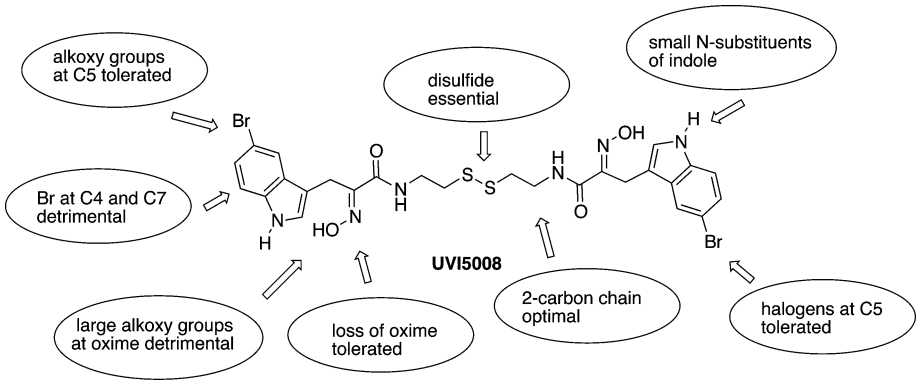

Figure 9. Summary of SAR studies on indole psammaplin A scaffold for HDAC inhibition.

17a, **4n**, **4p**, and **4s** proved to be the most active, since at 0.5 μM they induced the expression of p16 (which is causally linked to DNMT1 inhibition[74,91]). The level of DNMT1 protein remained roughly unchanged (Figure 7A). Compounds **4a**, **4g**, **4r**, and **4k** only induced p16 reactivation at 5 μM.

When compared to the data shown in Figure 6D, Figure 7 indicates a strong correlation between in vivo and cell-based assays for compounds **4a**, **4n**, **17a**, and **4g**. Surprisingly compounds **4p**, **4s**, and **4k** were inactive on in vitro DNMT1 assay (Figure 6D) but induced p16 reactivation (see Figure 7A).

The level of acetylation of SIRT1 epi-targets (as readout for SIRT inhibition) was also determined by treatment of U937 and MCF7 cells with indole psammaplin A derivatives at two concentrations. Figure 7B shows increased acetylation of p53 on residue K382 (a well-known SIRT1 target[92,93]) after treatment with selected compounds. Whereas some of those showed a dose-response trend (**4k**, **4r**, **4g**, and **20a**), others (**4s**, **4a**, and **4b**) were active only at the highest concentration (5 μM). Note that **4n** is the only compound of the series (Figure 6E) that neither increased p53K382ac levels nor inhibited SIRT in cell-based assays.

The reactivation of other reported SIRT1 targets (acetylation of H3K9[94,95] and H3K56[96]) was tested with the indole psammaplin A derivatives. Figure 8A,B shows that in general a correlation exists between concentration and level of acetylation of H3K9ac (Figure 8A) for the surveyed compounds. Compounds **4r** and **4q**, which lack the disulfide bond, did not show SIRT1 inhibition as demonstrated by their effects on H3K9 (Figure 8A) or H3K56 acetylation (Figure 8B), whereas the other analogues showed an effective proacetylation action, in particular **4k**, **4n**, **4p**, **4s**, **4l**.

SAR STUDIES ON INDOLE PSAMMAPLIN A DERIVATIVES

The biological results indicate that the indole derivatives of **2**[74] are more potent modulators of epigenetic enzymes than the natural product.[72] The 5-bromoindole analogue **4a** has been shown to highly efficiently induce cancer cell-selective death in a variety of models, and these activities were also demonstrated in several human tumor xenografts and genetic mouse models of human breast cancer in vivo.[74] Mechanistic studies proved that the anticancer activity of **4a** involves activation of death receptors and ROS production in a mutually independent manner. Importantly, cell death is efficiently induced in cells mutated or deficient for p53, Bcl-2 modifying factor, BMF, and/or TNF-related apoptosis inducing ligand, TRAIL.[74]

From the biochemical and cellular characterization of the analogues, it was concluded that positional isomers at the bromoindole ring such as **4i** and **4j** still showed cell cycle block, apoptosis induction (although to a lesser extent than **4a**), and CD11c differentiation of U937 cells (Figure 3A,B and Figure 4A,E). These derivatives increased α-tubulin acetylation and induced p21 expression similarly to **4a** and psammaplin A (**2**). On the contrary, protection of the oxime function as a trityl (**14a**) or benzyl derivative (**17b**) abolished activity (Figure 3A–D and Figure 4A,B,E,F). Furthermore **4p** (Figure 3A,B and Figure 4A,E) with a hydrocarbon linker was inactive, suggesting that the activity of these analogues must reside on the thiolate formed upon disulfide cleavage. Finally, incorporation of an alcohol functional group in place of the putative thiol as in **4r** (Figure 3A,B and Figure 4A,E) afforded a biologically inactive compound that kept a residual ability to induce α-tubulin acetylation. Altogether, the results confirm that the series of tetrapeptide disulfide dimers are prodrugs that get activated by reduction to afford the thiols, which are the functional group required for biological activity.

Capping the thiol as the methyl sulfide **4s** afforded a derivative with a distinct biological profile, since it blocked the cell cycle in G1 and induced p21 expression without increasing the differentiation of U937 cells. We note that its apoptogenic activity was only occurring in primary leukemic cells from AML patients but not in established U937 cells in culture. It will be interesting to study **4s** and other active compounds of this series in genetic mouse models for different types of (solid) human cancers, as reported for **4a**.[74]

HDAC1 and HDAC4 enzymatic inhibition studies revealed that the C5-Br could be replaced by other halogens (F, Cl, I) or oxygen substituents (OMe, OBn), since these analogues show roughly equal potency, but the absence of a substituent was detrimental. Positional isomers of the bromoindole (**4i–j**) showed reduced potency as HDAC inhibitors in enzymatic assays, as did the indole-*N*-methyl derivative (**4k**), in particular of HDAC4 (Figure 6A–C). Derivatization of the oxime as an alkyl derivative was tolerated for the small methyl group (**17a**) but not for the *O*-benzyl (**17b**) or *O*-trityl (**14a**) analogues (data not shown). The oxime group is dispensable (**20a**) if the indole N–H group is present, as the *N*-Me derivative (**20b**) lacks the activity (as confirmed by in vivo assays). Figure 9 summarizes the SAR study described in this work.

Regarding DNMT inhibition, Figure 6D shows the beneficial effect of the methylated oxime (**17a**) relative to **4a** and, more importantly, the presence of a *O*-Bn group in place of the bromine (**4g**). The data also conclude that the dimeric structure

dx.doi.org/10.1021/jm300618u | J. Med. Chem. 2012, 55, 9467–9491

Scheme 4[a]

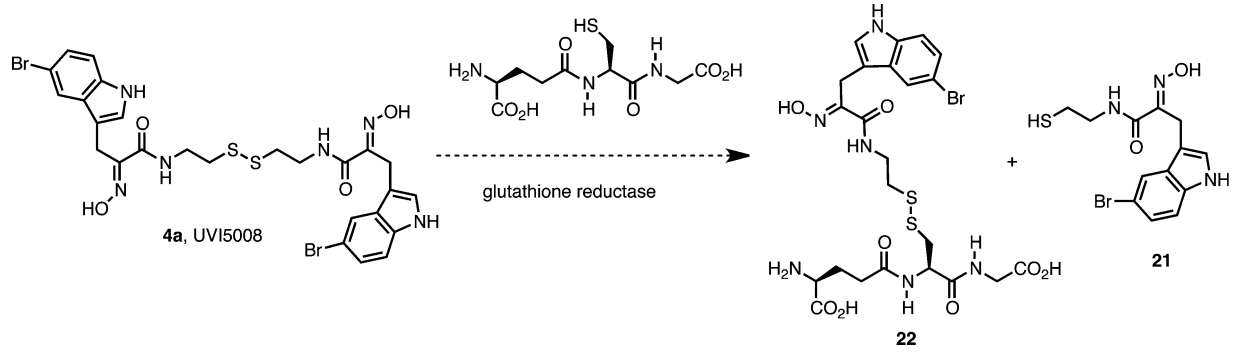

[a]In vivo conjugation of **4a** to glutathione.

is required for efficient inhibition, as monomeric analogues were inactive on DNMT1. We surmise that the disulfide could react with the enzyme after ocupation of the SAM binding pocket, perhaps undergoing capture by the invariant Cys81 active site residue[97] in a disulfide exchange reaction that might be reversible in vivo and therefore transient. Compounds that inhibited DNMT1 (**4a**, **4g**, **17a**) showed the ability to reactivate p16, an effect that was also shown by other analogues (**4n**, **4p**, **4s**; Figure 7A) but less efficiently (with the exception of **4b**).

We also studied the structural requirements for the inhibition of the SIRT NAD$^+$-dependent deacetylases by compound **4a**.[74] None of the analogues of **4a** assayed with SIRT1 showed equipotency to the parent compound (except **4b** and **4l**, Figure 6E), but the negative result also appears to suggest that the dimeric structure is required for the activity of **4a**, since the corresponding monomers (**4s**, **4r**, **4q**) proved to be inactive in our assay system, and both the *N*-*p*-bromobenzyl derivative **4l** and the analogue with the all carbon connector between the amides (**4p**) showed weak SIRT1 inhibitory activity. The modulation of SIRT1 targets (acetylation of p53 K382, H3K9, and H3K56, the last also linked to HDAC inhibition) was clearly consistent with the enzymatic assays for **4a**. The same correlation was noted for compounds **4p**, **4q**, and **4r**, for which the very weak inhibitory enzymatic activity (Figure 6E) is consistent with low levels of acetylation of H3K9 and H3K56 (Figure 8A). Complex readouts on the expression levels of the different SIRT1 targets hindered further SAR studies, although the disulfide bond also appears to be necessary for SIRT1 inhibition.

The entire data set suggests that the series of tetrapeptide disulfide dimers show greater activity in cell than in vitro assays (see Figure 6D and Figure 6C, cf. Figures 7 and 8), perhaps because of their prodrug nature. The inhibition of SIRT and DNMT enzymes is clearly indicated by the analysis of the levels of acetylation of sirtuin targets (p53 K382, H3K9, and H3K56) or by the reactivation of methylated genes (p16), respectively. The discrepancy between data from in vitro and cell-based assays could be understood and justified by the role of the disulfide group present in the molecular scaffold, which can be reduced (or undergo disulfide exchange, for example, with glutathione) upon cell uptake. This assumption is consistent with the weak activity displayed in both settings by alcohol **4r**. Other thiol-disguised prodrugs, such as the disulfide FK228 **1** and octanoyl derivative largazole, have also shown contrasting enzymatic potencies when compared to the corresponding reduced forms.[98,99]

Given their different enzymatic mechanism, sirtuins are not modulated by the inhibitors of classes I, II, and IV HDACs, such as suberoylanilide hydroxamic acid (SAHA) and trichostatin A (TSA), which have Zn^{2+} chelating groups. It is tempting to structurally relate the SIRT inhibition displayed by **4a** to the haloindole motif, which is found in related cyclic indole derivatives (EX243, GW5074, kenpaullones) that act as adenosine mimetics.[59]

MECHANISTIC INSIGHTS INTO THE MULTIPLE EPIGENETIC ACTIVITIES OF THE INDOLE-BASED PSAMMAPLIN A DERIVATIVES

With the data obtained thus far and the precedents on other sulfur containing inhibitors,[59] we surmise that the HDAC inhibition exhibited by these compounds is a consequence of disulfide reduction to the corresponding thiol-capped moiety, which likely binds the active site Zn^{2+}. Thiols such as **21** derived from the potent analogue **4a** (Scheme 4) feature the tripartite structure characteristic of most effective HDAC inhibitors, as it contains an HDAC rim-recognition element attached to an active site binding/inactivating group via a linker. The increased levels of native disulfide reductants (i.e., glutathione, thioredoxin, and thioredoxin reductase) found in many cancer cells likely render such cells particularly susceptible to the action of **4a** and analogues. Their cleavage would occur only following cellular entry after encountering a high glutathione concentration (typically 15 mM intracellular compared to 15 μM extracellular).[100]

Molecular modeling of **21** into the active site of HDAC8 shows the expected pose with the chelation of the thiol group to the Zn^{2+} ion and the additional stabilization by formation of a hydrogen bond between the indole N−H and Asp101. This model is also consistent with the inhibitory activities of the C5-indole analogue series and with the lack of activity of monomers lacking the thiol-chelating unit (Figure 10).

In support of the mechanism of action of these indole-based psammaplin A analogues, pharmacokinetic studies on lead compound **4a**[74] led to the detection by HPLC/MS of the mixed disulfide **22**, a glutathione adduct presumably formed by in-cell modification of the scissile disulfide bond as indicated in Scheme 4.

In addition to the disulfide present in other depsipeptides such as FK228 (**1**)[55] and in psammaplin A (**2**)[58] and to the octanoyl thiol ester of depsipeptide largazole,[102] the *S*-acetyl,[103] *S*-isobutyryl,[104] and *S*-2-methyl-3-phenylpropanoyl[105] thiol esters have also been developed as thiol surrogates in HDACis. Mixed disulfides have been used in lieu of the symmetrical

dx.doi.org/10.1021/jm300618u | J. Med. Chem. 2012, 55, 9467−9491

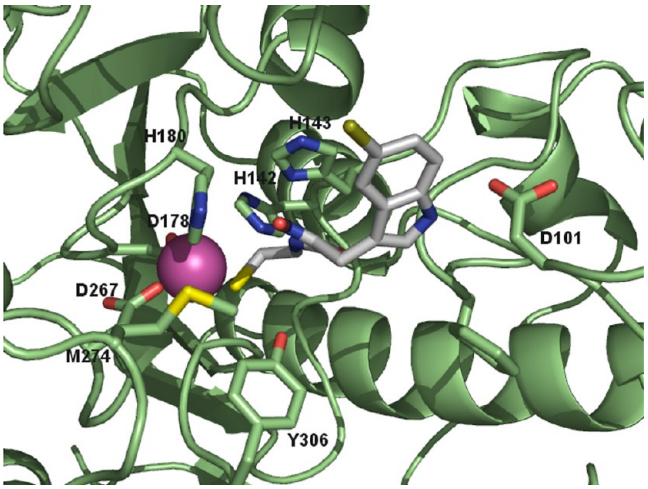

Figure 10. Proposed docking pose for **4a**-derived thiol **21** in HDAC8.[101] The Cα trace of the enzyme is displayed as a ribbon, colored in green. The side chains of His142, His143, Asp178, Asp267, His180, Met274, Tyr306 are shown as sticks, with carbon atoms colored in green. The Zn^{2+} at the catalytic site is shown as a magenta sphere. The inhibitor is displayed also as sticks but with carbon atoms colored in gray and the bromine atom colored in brown. The ab initio calculated structure of **4a**-derived thiol **21** was docked into the structure of human HDAC8[101] after removal of the trichostatin A (TSA) ligand. The highest scores using an automated docking method for the interaction with the Zn^{2+} ion in the active site was validated by the GRID maps. In these solutions, the thiolate group chelates the metal, the linker domain occupies the channel, and the bromoindole is stabilized through interaction with Tyr100 and Phe152 at the rim of the active site entrance. This positioning facilitates the formation of a hydrogen bond between the indole N−H and Asp101. The complex was refined using energy minimization, and its dynamic behavior was simulated using unrestrained MD (see Supporting Information).

dimeric structures.[106] All the above ligands are considered as prodrugs[107] that most likely release the thiolate group upon reaction with thioesterases or by thiol−disulfide exchange[108] induced by the addition of sulfhydryl groups of compounds present in the reductive environment of the cell such as glutathione. In addition, other sulfur-containing functional groups employed as headgroup of HDACis have been described, among them trithiocarbonates,[109] mercaptoacetamides,[110] mercaptoketones,[111] and methylsulfoxides.[112] The broad variety of functional groups further attests to the efficient and energetically favorable chelation of Zn^{2+} ion by sulfur-containing functional groups.[40]

CONCLUSION

To summarize, the scaffold of the psammaplin A natural product is amenable to synthetic reengineering without loss of epigenetic modulatory activity. In particular the *o*-bromophenol unit of psammaplin A **2** has been replaced by the more chemically robust and drug-friendly indole fragment. A series of indole psammaplin A constructs have been generated in a short synthetic sequence, and their biological evaluation has led to a better understanding of the structure−activity relationship of these epigenetic inhibitors (see Table 2 for a summary of enzymatic and cellular activities). Notably, the incorporation of the 5-bromoindole unit in **4a** replacing the *o*-bromophenol of **2** not only improved the potency of the parent compound with regard to the already reported HDAC and DNMT dual epigenetic inhibitory profile but interestingly added another activity, the inhibition of the NAD^+-dependent SIRT deacetylase enzymes.[74] In vivo pharmacokinetics revealed that this compound is a prodrug that gets rapidly transformed into the glutathione conjugate.[74] In keeping with the concept of targeting several pathways, it is encouraging that a large number of phase I/II clinical trials are currently exploring the combination of an HDAC together with the DNA methyltransferase inhibitor 5-aza-2′-deoxycytidine (decitabine) (http://clinicaltrials.gov). Indeed, the simultaneous block of at least three epigenetic targets offers a valid alternative to combination treatments as well as a unique strength to ensure delivery of an "all in one" drug to the cells.[59]

A major consequence of **4a**-mediated anticancer effects involves activation of different pathways of apoptosis in the cancer cells due to synergism between these inhibitory activities.[74] A balanced modulation of several epigenetic targets makes designed multiple ligands (DMLs)[113] a promising class of anticancer drugs with unanticipated therapeutic potential.[59] The fact that **4a** seems to be well tolerable in experimental mice models and that the maximal tolerable dose is higher than that of well-known HDAC inhibitors represents another important argument for its further development and use against cancer. The entire data set suggests that further investigation on the role of indole psammaplin A derivatives in controlling some biological processes, such as cellular death and regulation of epigenetic effectors/regulators, is warranted, particularly given their action on some hematological samples (Figure 5) in which, compared to other epi-drugs, selected compounds were able to efficiently induce cell death.

EXPERIMENTAL SECTION

General. Solvents were dried according to published methods and distilled before use. HPLC grade solvents were used for HPLC purification. All other reagents were commercial compounds of the highest purity available. All reactions were carried out under argon atmosphere, and those not involving aqueous reagents were carried out in oven-dried glassware. Analytical thin layer chromatography (TLC) was performed on aluminum plates with Merck Kieselgel 60F254 and visualized by UV irradiation (254 nm) or by staining with a solution of phosphomolybdic acid. Flash column chromatography was carried out using Merck Kieselgel 60 (230−400 mesh) under pressure. Infrared spectra were obtained on a JASCO FTIR 4200 spectrophotometer, from a thin film deposited onto a NaCl glass. ^{1}H NMR spectra were recorded in $CDCl_3$, CD_3OD, DMSO-d_6, and $(CD_3)_2CO$ at ambient temperature on a Bruker AMX-400 spectrometer at 400 MHz with residual protic solvent as the internal reference ($CDCl_3$, δ_H = 7.26 ppm; $(CD_3)_2CO$, δ_H = 2.05 ppm; CD_3OD, δ_H = 3.31; DMSO-d_6, δ_H = 2.50). Chemical shifts (δ) are given in parts per million (ppm), and coupling constants (J) are given in hertz (Hz). The proton spectra are reported as follows: δ (multiplicity, coupling constant J, number of protons, assignment). ^{13}C NMR spectra were recorded in $CDCl_3$, CD_3OD, DMSO-d_6, and $(CD_3)_2CO$ at ambient temperature on the same spectrometer at 100 MHz, with the central peak of $CDCl_3$ (δ_C = 77.0 ppm), CD_3OD (δ_C = 49.0 ppm), DMSO-d_6 (δ_C = 39.4 ppm), or $(CD_3)_2CO$ (δ_C = 30.8 ppm) as the internal reference. DEPT135 sequence was used to aid in the assignment of signals in the ^{13}C NMR spectra. Melting points were determined on a Stuart SMP10 apparatus. Elemental analyses were determined on a Carlo Erba EA 1108 analyzer. Crystallographic information was obtained from the corresponding single crystals analyzed by X-ray diffraction. Crystallographic data were collected on a single crystal Bruker SMART CCD6000 FR591 diffractometer equipped with a charge-coupled device (CCD) detector at 20 °C using graphite monochromated Mo Kα radiation (λ = 0.710 73 Å) and were corrected for Lorentz and polarization effects.

Mass Spectrometry. Experiments were performed on an APEX III FT-ICR MS instrument (Bruker Daltonics, Billerica, MA) equipped

Table 2. Summary of Compounds Activities[a]

	Cell cycle	Death	Cd11c	Acetylation	Expression	HDACs	SIRT1	DNMT1
2	■	■		■	■			
14a	■							
17a				■	■	■		■
17b								
20a			■	■	■	■		
20b								
4a	■	■	■	■	■	■	■	■
4b	■	■	■	■	■	■	■	
4c	■	■		■	■	■		
4d	■	■		■	■	■		
4e	■	■		■	■	■		
4f		■	■	■	■	■		
4g		■	■	■	■	■		■
4h								
4i	■	■	■	■	■	■		
4j	■	■	■	■	■	■		
4k	■	■	■	■	■	■		
4l							■	
4m			■	■				
4n	■	■	■	■		■		■
4o			■	■	■	■		
4p				■	■		■	
4q								
4r				■				
4s			■	■	■			

[a]Black boxes show, for each molecule, positive response to the tests. Column entries from left to right indicate the following: variations in cell cycle distribution (Cell cycle); induction of cell death (Death); induction of granulocytic differentiation (CD11c); variation of the acetylated state of proteins (Acetylation); expression of key and/or silenced proteins (Expression); in vitro activity against HDAC1/4 (HDACs); in vitro activity against SIRT1 (SIRT1); in vitro modulation of DNMT1 activity (DNMT1). The experimental details are reported in the Experimental Section and the numerical values in Figures 3−8.

with a 7 T actively shielded magnet. Ions were generated using an Apollo API electrospray ionization (ESI) source with a voltage between 1800 and 2200 V (to optimize ionization efficiency) applied to the needle and with a countervoltage of 450 V applied to the capillary. Samples were prepared by adding a spray solution of 70:29.9:0.1 (v/v/v) CH_3OH/water/formic acid to a solution of the sample at a v/v ratio of 1−5% to give the best signal-to-noise ratio.

Data acquisition and data processing were performed using the XMASS software, version 6.1.2 (Bruker Daltonics). FAB experiments were performed on a VG AutoSpec instrument, using 3-nitrobenzylalcohol or glycerol as matrices.

The purity of the compounds was established in most cases by elemental analysis and, for those that did not give suitable crystals, by HPLC and found to be greater than 95%.

General Procedure for the Reaction of Indoles with Ethylbromopyruvate-2-oxime. Oxime **7** (1.0 mmol) was dissolved in anhydrous dichloromethane (3 mL) with an excess of substrate (2.0 mmol). Anhydrous sodium carbonate (5.5 mmol) was then added, and the suspension was stirred for 24 h at room temperature. After filtration through silica gel, the solvent was removed and the residue was purified by column chromatography on silica gel as indicated.

General Procedure for the Protection of Oximes with TrCl. Trityl chloride (2.0 mmol) was added to a stirred suspension of the indole **9** (1.0 mmol) and Na_2CO_3 (2.0 mmol) in CH_2Cl_2 (10 mL) and THF (1.5 mL). The mixture was stirred at room temperature for 16 h, filtered through a pad of silica gel saturated with Et_3N, and the filtrate was concentrated. The residue was subjected to chromatography as indicated to afford **11**.

General Procedure for Hydrolysis of Esters. $LiOH{\cdot}H_2O$ (15 mmol) was added to a solution of the ester **11** (1.0 mmol) in a 1:1 THF/H_2O mixture (3.5 mL). After stirring for 16 h at room temperature, water was added and the solution was neutralized by addition of 10% HCl. Extraction with ethyl acetate and crystallization from hexane/$CHCl_3$ afforded the corresponding acid **12**.

General Procedure for the Coupling of Acids with Amines. To a solution of acid **12** (1.0 mmol) in dioxane (4 mL) was added EDC (1.9 mmol) and *N*-hydroxysuccinimide (1.7 mmol), and the resulting solution was stirred for 2 h at 25 °C. Then a solution of amine **13** (0.5 or 1.0 mmol) and Et_3N (5.5 mmol) in dioxane (4 mL) and MeOH (4 mL) was added. After the mixture had been stirred for 16 h at room temperature, water was added and the mixture extracted with ethyl acetate. The solvent was removed in vacuo, and the residue was subjected to column chromatography on silica gel as indicated. Some of those compounds **14** could not be fully characterized because of their instability upon attempted additional purification on silica gel.

General Procedure for the Cleavage of the Trityl Protecting Group. The corresponding indole (1.0 mmol) was dissolved in a 20:1 CH_2Cl_2/MeOH mixture (6 mL) and placed in a pressure flask, and anhydrous HCl (7.3 mmol of a 1.0 M solution in ether) was added. The solution was then stirred at 25 °C for 2h. The mixture was diluted with water and MeOH, washed with hexane, and the MeOH was evaporated in vacuo. EtOAc was then added, and the aqueous layer was extracted with EtOAc (3×). The combined organic extracts were dried over Na_2SO_4, filtered, and the solvent was evaporated in vacuo. The residue was subjected to column chromatography on silica gel (95:5 CH_2Cl_2/MeOH)..

dx.doi.org/10.1021/jm300618u | J. Med. Chem. 2012, 55, 9467−9491

(*E*)-Ethyl 3-(5-Bromo-1*H*-indol-3-yl)-2-(hydroxyimino)-propanoate (9a). Following the general procedure described for the reaction of indoles with ethyl bromopyruvate-2-oxime, indole **5a** (1.00 g, 5.10 mmol) gave, after purification by column chromatography (SiO_2, 35:65 EtOAc/hexane), oxime **9a** (0.50 g, 60%) as a white solid, mp 175−176 °C ($CHCl_3$/hexane), and oxazine **10a** (0.03 g, 4%) as a yellow solid,mp 161−162 °C ($CHCl_3$/hexane).

Data for (*E*)-Ethyl 3-(5-Bromo-1*H*-indol-3-yl)-2-(hydroxyimino)propanoate (9a). ^{1}H NMR (CD_3COCD_3, 400.13 MHz): δ 10.24 (br, 1H, NH), 7.92 (d, J = 1.7 Hz, 1H, H4′), 7.33 (d, J = 8.5 Hz, 1H, H7′), 7.27 (d, J = 2.3 Hz, 1H, H2′), 7.20 (dd, J = 8.5, 1.7 Hz, 1H, H6′), 4.19 (q, J = 7.1 Hz, 2H, $CO_2C\underline{H}_2CH_3$), 4.05 (s, 2H, 2H3), 1.22 (t, J = 7.1 Hz, 3H, $CO_2CH_2C\underline{H}_3$) ppm. ^{13}C NMR (CD_3COCD_3, 100.62 MHz): δ 165.6 (s), 152.9 (s), 136.9 (s), 131.1 (s), 127.4 (d), 125.7 (d), 123.3 (d), 114.9 (d), 113.5 (s), 111.0 (s), 62.6 (t), 21.6 (t), 15.3 (q) ppm. IR: ν 3500−3100 (br, N−H and O−H), 2983 (w, C−H), 1705 (s, C═O and C═N), 1426 (w), 1096 (w), 1014 (m), 864 (w) cm^{-1}. MS (FAB$^+$): m/z (%) 327 ([M + 1]$^+$ [^{81}Br], 61), 326 ([M]$^+$ [^{81}Br], 34), 325 ([M + 1]$^+$ [^{79}Br], 67), 324 ([M]$^+$ [^{79}Br], 26) 311 (62), 310 (35), 309 (84), 308 (25), 307 (26), 235 (22), 210 (99), 208 (100), 156 (24). HRMS (FAB$^+$) calcd for $C_{13}H_{13}{}^{81}BrN_2O_3$ and $C_{13}H_{13}{}^{79}BrN_2O_3$ ([M]$^+$), 326.0089 and 324.0110; found, 326.0100 and 324.0112. Anal. Calcd for $C_{13}H_{13}BrN_2O_3$: C, 48.02; H, 4.03; N, 8.62. Found: C, 48.02; H, 4.03; N, 8.65.

Data for (4a*R,9a*R**,*E*)-Ethyl 6-Bromo-4a-[3-ethoxy-2-(hydroxyimino)-3-oxopropyl]-4,4a,9,9a-tetrahydro[1,2]oxazino[6,5-*b*]-indole-3-carboxylate (10a).** ^{1}H NMR ($CDCl_3$, 400.13 MHz): δ 10.02 (br, 1H, NH), 7.10 (s, 2H, ArH), 6.42 (d, J = 8.5 Hz, 1H, ArH), 5.66 (s, 1H), 5.14 (s, 1H), 4.4−4.1 (m, 4H, 2 × $CO_2C\underline{H}_2CH_3$), 3.3−3.1 (m, 3H), 2.60 (d, J = 15.8 Hz, 1H, H4A), 1.3−1.2 (m, 6H, 2 × $CO_2CH_2C\underline{H}_3$) ppm. ^{13}C NMR ($CDCl_3$, 100.62 MHz): δ 163.6 (s), 162.0 (s), 159.3 (s), 148.9 (s), 147.3 (s), 131.7 (d), 131.3 (s), 126.5 (d), 110.9 (s), 110.4 (d), 94.8 (d), 62.4 (t), 62.3 (t), 50.6 (s), 32.9 (t), 27.8 (t), 13.9 (q, 2×) ppm. IR: ν 3500−3100 (br, N−H and O−H), 2986 (m, C−H), 1721 (s, C═O and C═N), 1606 (m), 1476 (m), 1435 (m), 1279 (s), 1167 (m), 1017 (m), 757 (s) cm^{-1}. HRMS (ESI$^+$) calcd for $C_{18}H_{20}{}^{81}BrN_3O_6Na$ and $C_{18}H_{20}{}^{79}BrN_3O_6Na$ ([M + Na]$^+$), 478.0407 and 476.0428; found, 478.0410 and 476.0428. Anal. Calcd for $C_{18}H_{20}BrN_3O_6$: C, 47.59; H, 4.44; N, 9.25. Found: C, 47.38; H, 4.44; N, 9.28.

(*E*)-Ethyl 3-(5-Bromo-1*H*-indol-3-yl)-2-(trityloxyimino)-propanoate (11a). In accordance with the general procedure described for the protection of oximes, indole **9a** (0.70 g, 2.10 mmol) afforded, after purification by column chromatography (SiO_2, 72:25:3 hexane/EtOAc/Et_3N), the protected oxime **11a** (0.90 g, 74%) as a white solid, mp 166−167 °C ($CHCl_3$/hexane). ^{1}H NMR (CD_3COCD_3, 400.13 MHz): δ 10.26 (br, 1H, NH), 7.90 (d, J = 1.4 Hz, 1H, H4′), 7.4−7.2 (m, 16H, ArH), 7.21 (dd, J = 8.6, 1.8 Hz, 1H, H6′), 7.18 (d, J = 2.0 Hz, 1H, H2′), 4.22 (s, 2H, 2H3), 4.11 (q, J = 7.1 Hz, 2H, $CO_2C\underline{H}_2CH_3$), 1.15 (t, J = 7.1 Hz, 3H, $CO_2CH_2C\underline{H}_3$) ppm. ^{13}C NMR (CD_3COCD_3, 100.62 MHz): δ 165.1 (s), 153.0 (s), 145.8 (s, 3×), 136.9 (s), 131.0 (d, 6×), 129.5 (d, 6×), 129.3 (d, 3×), 127.3 (d), 125.9 (d), 123.3 (d), 115.0 (d), 113.7 (s), 110.5 (s), 94.6 (s), 62.9 (t), 23.3 (t), 15.3 (q) ppm. IR: ν 3500−3300 (br, N−H), 3059 (w, C−H), 3028 (w, C−H), 2983 (w, C−H), 1716 (s, C═O and C═N), 1597 (w), 1450 (s), 1323 (m), 1195 (s), 754 (s) cm^{-1}. HRMS (ESI$^+$) calcd for $C_{32}H_{27}{}^{81}BrN_2O_3Na$ and $C_{32}H_{27}{}^{79}BrN_2O_3Na$ ([M + Na]$^+$), 591.1077 and 589.1097; found, 591.1063 and 589.1082. Anal. Calcd for $C_{32}H_{27}BrN_2O_3$: C, 67.73; H, 4.80; N, 4.94. Found: C, 67.82; H, 4.81; N, 4.98.

(*E*)-3-(5-Bromo-1*H*-indol-3-yl)-2-(trityloxyimino)propanoic Acid (12a). According to the general procedure described for the hydrolysis of esters, **11a** (0.70 g, 1.20 mmol) gave, after crystallization, acid **12a** (0.65 g, 99%) as a white solid, mp 171−172 °C (dec) (hexane/$CHCl_3$). ^{1}H NMR (CD_3COCD_3, 400.13 MHz): δ 10.23 (br, 1H, NH), 7.92 (d, J = 1.7 Hz, 1H, H4′), 7.4−7.2 (m, 16H, ArH), 7.19 (dd, J = 8.6, 1.7 Hz, 1H, H6′), 7.15 (s, 1H, H2′), 4.21 (s, 2H, 2H1) ppm. ^{13}C NMR (CD_3COCD_3, 100.62 MHz): δ 166.5 (s), 153.7 (s), 145.9 (s, 3×), 137.0 (s), 131.1 (s), 131.0 (d, 6×), 129.5 (d, 6×), 129.2 (d, 3×), 127.3 (d), 125.9 (d), 123.3 (d), 115.0 (d), 113.7 (s), 110.7 (s), 94.5 (s), 23.0 (t) ppm. IR: ν 3500−3200 (br, N−H and O−H), 3059 (w, C−H), 1756 (m, C═O), 1702 (m, C═N), 1597 (w), 1447 (s), 1216 (s), 972 (s), 757 (s), 700 (s) cm^{-1}. HRMS (ESI$^+$) calcd for $C_{30}H_{23}{}^{81}BrN_2O_3Na$ and $C_{30}H_{23}{}^{79}BrN_2O_3Na$ ([M + Na]$^+$), 563.0764 and 561.0784; found, 563.0755 and 561.0776. Anal. Calcd for $C_{30}H_{23}BrN_2O_3 \cdot {}^1/_2H_2O$: C, 65.70; H, 4.41; N, 5.11. Found: C, 65.57; H, 4.50; N, 4.99.

(2*E*,2′*E*)-*N*,*N*′-[2,2′-Disulfanediylbis(ethane-2,1-diyl)]bis[3-(5-bromo-1*H*-indol-3-yl)-2-(trityloxyimino)propanamide] (14a). Following the general procedure described for the coupling of acids with amines, **12a** (0.60 g, 1.11 mmol) afforded, after purification by column chromatography (SiO_2, gradient from 47:50:3 hexane/EtOAc/Et_3N to 100% EtOAc), disulfide **14a** (0.56 g, 84%) as a white solid, mp 172−173 °C (hexane/$CHCl_3$). ^{1}H NMR (CD_3COCD_3, 400.13 MHz) (data for monomer): δ 10.24 (br, 1H, NH), 7.96 (s, 1H, ArH), 7.4−7.1 (m, 17H, ArH), 6.97 (s, 1H, ArH), 4.20 (s, 2H, 2H3), 3.4−3.2 (m, 2H, 2H1″), 2.87 (s, 1H, CONH), 2.60 (t, J = 6.3 Hz, 2H, 2H2″) ppm. ^{13}C NMR (CD_3COCD_3, 100.62 MHz) (data for monomer): δ 164.4 (s), 154.5 (s), 145.8 (s, 3×), 136.9 (s), 131.1 (s), 130.8 (d, 6×), 129.6 (d, 6×), 129.2 (d, 3×), 127.5 (d), 125.8 (d), 123.5 (d), 114.9 (d), 113.7 (s), 110.7 (s), 94.3 (s), 39.9 (t), 39.1 (t), 21.8 (t) ppm. IR: ν 3500−3200 (br, N−H), 3059 (w, C−H), 3022 (w, C−H), 1669 (s, C═O and C═N), 1520 (s), 1448 (s), 1217 (m), 971 (m), 755 (s), 701 (s) cm^{-1}. HRMS (ESI$^+$) calcd for $C_{64}H_{54}{}^{81}Br_2N_6O_4S_2Na$, $C_{64}H_{54}{}^{79}Br^{81}BrN_6O_4S_2Na$, and $C_{64}H_{54}{}^{79}Br_2N_6O_4S_2Na$ ([M + Na]$^+$), 1219.1866, 1217.1886, and 1215.1907; found, 1219.1852, 1217.1855, and 1215.1877. Anal. Calcd for $C_{64}H_{54}Br_2N_6O_4S_2 \cdot 2H_2O$: C, 62.44; H, 4.75; N, 6.83; S, 5.21. Found: C, 62.50; H, 4.97; N, 6.32; S, 4.67.

(2*E*,2′*E*)-*N*,*N*′-[2,2′-Disulfanediylbis(ethane-2,1-diyl)bis(3-(5-bromo-1*H*-indol-3-yl)-2-(hydroxyimino)propanamide] (4a). In accordance with the general procedure described for the cleavage of the trityl group, **14a** (0.09 g, 0.08 mmol) gave, after purification by column chromatography (SiO_2, 95:5 CH_2Cl_2/MeOH), disulfide **4a** (0.04 g, 81%) as a yellowish solid, mp 179−180 °C (hexane/EtOAc). ^{1}H NMR (CD_3OD, 400.13 MHz) (data for monomer): δ 7.83 (d, J = 1.8 Hz, 1H, H4′), 7.15 (d, J = 8.5 Hz, 1H, H7′), 7.10 (dd, J = 8.5, 1.8 Hz, 1H, H6′), 7.09 (s, 1H, H1′), 3.97 (s, 2H, 2H3), 3.40 (t, J = 6.7 Hz, 2H, 2H1″), 2.65 (t, J = 6.7 Hz, 2H, 2H2″) ppm. ^{13}C NMR (CD_3OD, 100.62 MHz) (data for monomer): δ 166.2 (s), 153.6 (s), 136.3 (s), 130.4 (s), 126.5 (d), 124.9 (d), 122.6 (d), 113.7 (d), 112.9 (s), 110.2 (s), 39.6 (t), 38.4 (t), 19.7 (t) ppm. IR: ν 3500−3100 (br, N−H and OH), 3061 (w, C−H), 2925 (w, C−H), 1705 (m), 1662 (s, C═O and C═N), 1526 (s), 1448 (s), 1360 (m), 1226 (m), 793 (w) cm^{-1}. HRMS (ESI$^+$) calcd for $C_{26}H_{27}{}^{81}Br_2N_6O_4S_2$, $C_{26}H_{27}{}^{79}Br^{81}BrN_6O_4S_2$, and $C_{26}H_{27}{}^{79}Br_2N_6O_4S_2$ ([M + H]$^+$), 712.9855, 710.9876, and 708.9896; found, 712.9831, 710.9851, and 708.9879. Anal. Calcd for $C_{26}H_{26}Br_2N_6O_4S_2$: C, 43.95; H, 3.69; N, 11.83; S, 9.03. Found: C, 44.40; H, 3.94; N, 11.62; S, 9.21.

(2*E*,2′*E*)-*N*,*N*′-[2,2′-Disulfanediylbis(ethane-2,1-diyl)]bis[2-(hydroxyimino)-3-(1*H*-indol-3-yl)propanamide] (4b). In accordance with the general procedure for the cleavage of trityl groups, **14b** (0.08 g, 0.07 mmol) gave, after purification by column chromatography (SiO_2, 95:5 CH_2Cl_2/MeOH), disulfide **4b** (0.04 g, 78%) as a yellow oil. ^{1}H NMR (CD_3OD, 400.13 MHz) (data for monomer): δ 7.64 (d, J = 7.9 Hz, 1H, ArH), 7.21 (d, J = 8.1 Hz, 1H, ArH), 7.01 (s, 1H, H2′), 6.98 (t, J = 7.5 Hz, 1H, ArH), 6.91 (t, J = 7.4 Hz, 1H, ArH), 3.98 (s, 2H, 2H3), 3.36 (t, J = 6.7 Hz, 2H, 2H1″), 3.27 (br, 1H, CONH), 2.60 (t, J = 6.7 Hz, 2H, 2H2″) ppm. ^{13}C NMR (CD_3OD, 100.62 MHz) (data for monomer): δ 166.3 (s), 154.0 (s), 137.7 (s), 128.5 (s), 124.7 (d), 122.2 (d), 119.9 (d), 119.5 (d), 112.0 (d), 110.2 (s), 39.4 (t), 38.3 (t), 19.8 (t) ppm. IR: ν 3500−3000 (br, N−H and O−H), 3057 (w, C−H), 2925 (m, C−H), 2855 (w, C−H), 1702 (w, C═O), 1660 (s, C═N), 1527 (s), 1457 (s), 1423 (s), 1356 (m), 1227 (m), 1009 (m), 744 (s) cm^{-1}. HRMS (ESI$^+$) calcd for $C_{26}H_{28}N_6O_4S_2Na$ ([M + Na]$^+$), 575.1506; found, 575.1492.

(2*E*,2′*E*)-*N*,*N*′-[2,2′-Disulfanediylbis(ethane-2,1-diyl)]bis[3-(5-fluoro-1*H*-indol-3-yl)-2-(hydroxyimino)propanamide] (4c). In accordance with the general procedure for the cleavage of trityl groups, **14c** (0.30 g, 0.28 mmol) gave, after purification by column chromatography, disulfide **4c** (0.11 g, 38% in two steps) as a yellow oil. ^{1}H NMR (CD_3COCD_3, 400.13 MHz) (data for monomer): δ 10.13

dx.doi.org/10.1021/jm300618u | *J. Med. Chem.* 2012, 55, 9467−9491

(br, 1H, NH), 7.60 (t, J = 5.2 Hz, 1H, CONH), 7.50 (dd, $^3J_{H-F}$ = 10.2 Hz, J_{H-H} = 2.1 Hz, 1H, H4′), 7.32 (dd, J_{H-H} = 8.8 Hz, $^4J_{H-F}$ = 4.5 Hz, 1H, H7′), 7.27 (s, 1H, H2′), 6.85 (td, $^3J_{H-F}$ = J_{H-H} = 9.2 Hz, J_{H-H} = 2.3 Hz, 1H, H6′), 4.02 (s, 2H, 2H3), 3.53 (q, J = 6.5 Hz, 2H, NHC$\underline{H}_2$), 2.81 (t, J = 6.5 Hz, 2H, CH_2S) ppm. ^{13}C NMR (CD_3COCD_3, 100.62 MHz MHz) (data for monomer): δ 165.4 (s), 159.2 (s, J_{C-F} = 231.2 Hz), 154.7 (s), 134.8 (s), 129.7 (s, $^3J_{C-F}$ = 10.3 Hz), 128.1 (d), 113.8 (d, $^3J_{C-F}$ = 9.8 Hz), 111.6 (s, $^4J_{C-F}$ = 4.6 Hz), 111.0 (d, $^2J_{C-F}$ = 26.6 Hz), 105.6 (d, $^2J_{C-F}$ = 23.9 Hz), 40.1 (t), 39.3 (t), 20.5 (t) ppm. IR: ν 3500−3000 (br, N−H and O−H), 2925 (w, C−H), 1698 (m, C═O), 1658 (s, C═N), 1527 (s), 1482 (m), 1430 (s), 1356 (m), 1220 (s), 1011 (s), 854 (m), 791 (s), 713 (m) cm^{-1}. HRMS (ESI)$^+$ calcd for $C_{26}H_{27}F_2N_6O_4S_2$ ([M + H]$^+$), 589.1498, found 589.1470.

(2*E*,2′*E*)-*N*,*N*′-[2,2′-Disulfanediylbis(ethane-2,1-diyl)]bis[3-(5-chloro-1*H*-indol-3-yl)-2-(hydroxyimino)propanamide] (4d). In accordance with the general procedure for the cleavage of trityl groups, **14d** (0.13 g, 0.12 mmol) gave, after purification by column chromatography, disulfide **4d** (0.05 g, 30% in two steps) as a yellow oil. ^{1}H NMR (CD_3COCD_3, 400 MHz) (data for monomer): δ 11.06 (br, 1H, OH), 10.20 (br, 1H, NH), 7.81 (d, J = 1.8 Hz, 1H, H4′), 7.58 (t, J = 5.7 Hz, 1H, CONH), 7.34 (d, J = 8.6 Hz, 1H, H7′), 7.27 (s, 1H, H2′), 7.04 (dd, J = 8.6, 2.0 Hz, 1H, H6′), 4.03 (s, 2H, 2H3), 3.54 (q, J = 6.6 Hz, 2H, NHC$\underline{H}_2$), 2.83 (t, J = 6.6 Hz, 2H, CH_2S) ppm. ^{13}C NMR (CD_3COCD_3, 100.62 MHz) (data for monomer): δ 165.3 (s), 154.7 (s), 136.7 (s), 130.6 (s), 127.8 (d), 125.8 (s), 123.0 (d), 120.4 (d), 114.4 (d), 111.4 (s), 40.1 (t), 39.4 (t), 20.4 (t) ppm. IR: ν 3500−3000 (br, N−H and O−H), 3063 (w, C−H), 2920 (m, C−H), 1702 (s, C═O), 1658 (s, C═N), 1525 (s), 1461 (s), 1423 (s), 1359 (s), 1226 (s), 1011 (m), 980 (m), 900 (m), 794 (s) cm^{-1}. HRMS (ESI)$^+$ calcd for $C_{26}H_{27}{}^{37}Cl_2N_6O_4S_2$, $C_{26}H_{27}{}^{37}Cl^{35}ClN_6O_4S_2$, and $C_{26}H_{27}{}^{35}Cl_2N_6O_4S_2$ ([M + H]$^+$), 625.0808, 623.0845, and 621.0880; found, 625.0862, 623.0882, and 621.0907.

(2*E*,2′*E*)-*N*,*N*′-[2,2′-Disulfanediylbis(ethane-2,1-diyl)]bis[2-(hydroxyimino)-3-(5-iodo-1*H*-indol-3-yl)propanamide] (4e). In accordance with the general procedure for the cleavage of trityl groups, **14e** (0.15 g, 0.11 mmol) gave, after purification by column chromatography, disulfide **4e** (0.05 g, 13% in two steps) as a yellow oil. ^{1}H NMR (CD_3COCD_3, 400 MHz) (data for monomer): δ 10.23 (br, 1H, NH), 8.16 (br, 1H, H2′), 7.60 (t, J = 5.7 Hz, 1H, CONH), 7.33 (dd, J = 8.5, 1.5 Hz, 1H, H6′), 7.21 (d, J = 8.3 Hz, 1H, H7′), 7.20 (d, J = 1.2 Hz, 1H, H2′), 4.01 (s, 2H, 2H3), 3.53 (q, J = 6.6 Hz, 2H, NHC$\underline{H}_2$), 2.84 (t, J = 6.6 Hz, 2H, CH_2S) ppm. ^{13}C NMR (CD_3COCD_3, 100.62 MHz) (data for monomer): δ 165.3 (s), 154.7 (s), 137.3 (s), 132.1 (s), 131.1 (d), 130.0 (d), 127.2 (d), 115.4 (d), 111.0 (s), 83.6 (s), 40.2 (t), 39.4 (t), 20.4 (t) ppm. IR: ν 3500−3000 (br, N−H and O−H), 3064 (w, C−H), 2923 (w, C−H), 1690 (s, C═O), 1662 (s, C═N), 1529 (s), 1451 (s), 1253 (s), 1015 (m), 794 (m) cm^{-1}. HRMS (ESI)$^+$ calcd for $C_{26}H_{27}I_2N_6O_4S_2$ ([M + H]$^+$), 804.9619, found 804.9582.

(2*E*,2′*E*)-*N*,*N*′-[2,2′-Disulfanediylbis(ethane-2,1-diyl)]bis[2-(hydroxyimino)-3-(5-methoxy-1*H*-indol-3-yl)propanamide] (4f). In accordance with the general procedure for the cleavage of trityl groups, **14f** (0.04 g, 0.04 mmol) gave, after purification by column chromatography, disulfide **4f** (0.02 g, 4% in two steps) as a yellow oil. ^{1}H NMR (CD_3COCD_3, 400 MHz) (data for monomer): δ 9.86 (br, 1H, NH), 7.52 (t, J = 5.3 Hz, 1H, CONH), 7.32 (d, J = 2.1 Hz, 1H, H4′), 7.21 (d, J = 8.8 Hz, 1H, H7′), 7.13 (s, 1H, H2′), 6.71 (dd, J = 8.8, 2.3 Hz, 1H, H6′), 4.01 (s, 2H, 2H3), 3.78 (s, 3H, OCH_3), 3.52 (q, J = 6.5 Hz, 2H, NHC$\underline{H}_2$), 2.83 (t, J = 6.6 Hz, 2H, CH_2S) ppm. ^{13}C NMR (CD_3COCD_3, 100.62 MHz) (data for monomer): δ 165.4 (s), 155.6 (s), 155.1 (s), 133.4 (s), 129.9 (d), 126.5 (d), 113.5 (d), 113.2 (d), 111.1 (s), 102.8 (d), 56.7 (q), 40.1 (t), 39.4 (t), 20.5 (t) ppm. IR: ν 3500−3100 (br, N−H and O−H), 2429 (s, C−H), 2818 (w, C−H), 1658 (s, C═O and C═N), 1526 (s), 1484 (s), 1216 (s), 1051 (m), 739 (m) cm^{-1}. HRMS (ESI$^+$) calcd for $C_{28}H_{32}N_6NaO_6S_2$ ([M + H]$^+$), 635.1722, found 635.1717.

(2*E*,2′*E*)-*N*,*N*′-[2,2′-Disulfanediylbis(ethane-2,1-diyl)]bis[3-(5-(benzyloxy)-1*H*-indol-3-yl)-2-(hydroxyimino)propanamide] (4g). In accordance with the general procedure for the cleavage of trityl groups, **14g** (0.10 g, 0.08 mmol) gave, after purification by column chromatography, disulfide **4g** (0.02 g, 20% in two steps) as a yellow oil. ^{1}H NMR (CD_3COCD_3, 400.13 MHz) (data for monomer): δ 10.95 (s, 1H, OH), 9.83 (br, 1H, NH), 7.52 (d, J = 6.6 Hz, 1H), 7.51 (d, J = 7.4 Hz, 2H, ArH), 7.45 (d, J = 2.3 Hz, 1H, H4′), 7.38 (t, J = 7.4 Hz, 2H, ArH), 7.30 (t, J = 7.4 Hz, 1H, ArH), 7.22 (d, J = 8.7 Hz, 1H, H7′), 7.14 (d, J = 2.1 Hz, 1H, H2′), 6.80 (dd, J = 8.7, 2.4 Hz, 1H, H6′), 5.09 (s, 2H, CH_2Ph), 4.02 (s, 2H, 2H3), 3.52 (q, J = 6.6 Hz, 2H, NHC$\underline{H}_2$), 2.81 (t, J = 6.6 Hz, 2H, CH_2S) ppm. ^{13}C NMR (CD_3COCD_3, 100.62 MHz) (data of monomer): δ 165.4 (s), 155.1 (s), 154.7 (s), 140.2 (s), 133.7 (s), 130.2 (d, 2×), 129.9 (s), 129.5 (d, 2×), 129.4 (d), 126.7 (d), 113.8 (d), 113.6 (d), 111.2 (s), 104.5 (d), 72.1 (t), 40.1 (t), 39.4 (t), 20.6 (t) ppm. IR: ν 3500−3000 (br, N−H and O−H), 3058 (w, C−H), 2926 (s, C−H), 2864 (w, C−H), 1660 (s, C═O and C═N), 1527 (s), 1477 (s), 1456 (s), 1213 (s), 1016 (s), 796 (m), 753 (s), 703 (m) cm^{-1}. HRMS (ESI$^+$) calcd for $C_{40}H_{41}N_6O_6S_2$ ([M + H]$^+$), 765.2523, found 765.2498.

(2*E*,2′*E*)-*N*,*N*′-[2,2′-Disulfanediylbis(ethane-2,1-diyl)]bis[3-(4-bromo-1*H*-indol-3-yl)-2-(hydroxyimino)propanamide] (4h). In accordance with the general procedure for the cleavage of trityl groups, **14h** (0.09 g, 0.08 mmol) gave, after purification by column chromatography (SiO_2, 95:5 CH_2Cl_2/MeOH), disulfide **4h** (0.04 g, 81%) as a brown oil. ^{1}H NMR (CD_3COCD_3, 400.13 MHz) (data for monomer): δ 10.95 (br, 1H), 10.29 (br, 1H), 7.74 (s, 1H, ArH), 7.34 (dd, J = 7.9, 3.9 Hz, 1H, ArH), 7.19 (dd, J = 7.2, 3.9 Hz, 1H, ArH), 7.0−6.9 (m, 2H, ArH), 4.43 (s, 2H, 2H3), 3.7−3.5 (m, 2H, 2H1″), 3.0−2.8 (m, 2H, 2H2″) ppm. ^{13}C NMR (CD_3COCD_3, 100.62 MHz) (data for monomer): δ 165.5 (s), 155.1 (s), 140.0 (s), 127.1 (s), 125.7 (d), 124.9 (d), 124.1 (d), 115.4 (s), 112.9 (d), 112.1 (s), 40.2 (t), 39.6 (t), 22.9 (t) ppm. IR: ν 3500−3100 (br, N−H and O−H), 3020 (m, C−H), 2927 (w, C−H), 1709 (m, C═O), 1663 (s, C═N), 1528 (s), 1426 (s), 1361 (m), 1218 (s), 760 (s) cm^{-1}. HRMS (ESI$^+$) calcd for $C_{26}H_{27}{}^{81}Br_2N_6O_4S_2$, $C_{26}H_{27}{}^{79}Br^{81}BrN_6O_4S_2$, and $C_{26}H_{27}{}^{79}Br_2N_6O_4S_2$ ([M + H]$^+$), 712.9855, 710.9876, and 708.9896; found, 712.9845, 710.9864, and 708.9884.

(2*E*,2′*E*)-*N*,*N*′-[2,2′-Disulfanediylbis(ethane-2,1-diyl)]bis[3-(6-bromo-1*H*-indol-3-yl)-2-(hydroxyimino)propanamide] (4i). In accordance with the general procedure for the cleavage of trityl groups, **14i** (0.10 g, 0.08 mmol) gave, after purification by column chromatography (SiO_2, 95:5 CH_2Cl_2/MeOH), disulfide **4i** (0.03 g, 54%) as a brown oil. ^{1}H NMR (CD_3COCD_3, 400.13 MHz) (data for monomer): δ 11.02 (br s, 1H), 10.18 (br s, 1H), 7.73 (d, J = 8.5 Hz, 1H, H4′), 7.55 (d, J = 1.8 Hz, 1H, H7′), 7.23 (s, 1H, H2′), 7.14 (dd, J = 8.5, 1.8 Hz, 1H, H5′), 4.05 (s, 2H, 2H3), 3.55 (q, J = 6.5 Hz, 2H, 2H1″), 2.85 (t, J = 6.7 Hz, 2H, 2H2″) ppm. ^{13}C NMR (CD_3COCD_3, 100.62 MHz) (data for monomer): δ 165.3 (s), 154.7 (s), 139.1 (s), 128.5 (s), 127.0 (d), 123.4 (d), 122.6 (d), 116.2 (s), 115.8 (d), 111.8 (s), 40.1 (t), 39.4 (t), 20.3 (t) ppm. IR: ν 3500−3100 (br, N−H and OH), 3065 (w, C−H), 2925 (w, C−H), 1703 (s, C═O), 1661 (s, C═N), 1528 (s), 1454 (s), 1361 (m), 1226 (m), 1048 (m), 807 (m) cm^{-1}. HRMS (ESI$^+$) calcd for $C_{26}H_{27}{}^{81}Br_2N_6O_4S_2$, $C_{26}H_{27}{}^{79}Br^{81}BrN_6O_4S_2$, and $C_{26}H_{27}{}^{79}Br_2N_6O_4S_2$ ([M + H]$^+$), 712.9855, 710.9876, and 708.9896; found, 712.9852, 710.9870, and 708.9890.

(2*E*,2′*E*)-*N*,*N*′-[2,2′-Disulfanediylbis(ethane-2,1-diyl)]bis[3-(7-bromo-1*H*-indol-3-yl)-2-(hydroxyimino)propanamide] (4j). In accordance with the general procedure for the cleavage of trityl groups, **14j** (0.07 g, 0.06 mmol) gave, after purification by column chromatography (SiO_2, 95:5 CH_2Cl_2/MeOH), disulfide **4j** (0.02 g, 60%) as a brown oil. ^{1}H NMR (CD_3COCD_3, 400.13 MHz) (data for monomer): δ 10.92 (br, 1H), 10.08 (br, 1H), 7.70 (d, J = 7.8 Hz, 1H, ArH), 7.47 (t, J = 5.7 Hz, 1H, CONH), 7.19 (s, 1H, ArH), 7.18 (d, J = 7.8 Hz, 1H, ArH), 6.85 (t, J = 7.8 Hz, 1H, H5′), 3.96 (s, 2H, 2H3), 3.45 (q, J = 6.5 Hz, 2H, 2H1″), 2.74 (t, J = 6.8 Hz, 2H, 2H2″) ppm. ^{13}C NMR (CD_3COCD_3, 100.62 MHz) (data for monomer): δ 165.3 (s), 154.7 (s), 136.5 (s), 131.1 (s), 127.1 (d), 125.6 (d), 121.8 (d), 120.6 (d), 113.0 (s), 105.9 (s), 40.1 (t), 39.5 (t), 20.6 (t) ppm. IR: ν 3500−3100 (br, N−H and OH), 3063 (w, C−H), 2933 (m, C−H), 2860 (w, C−H), 1661 (s, C═O and C═N), 1528 (s), 1433 (s), 1340 (m), 1203 (m), 1015 (m), 837 (m), 787 (m) cm^{-1}. HRMS (ESI$^+$) calcd for $C_{26}H_{27}{}^{81}Br_2N_6O_4S_2$, $C_{26}H_{27}{}^{79}Br^{81}BrN_6O_4S_2$, and $C_{26}H_{27}{}^{79}Br_2N_6O_4S_2$ ([M + H]$^+$), 712.9855, 710.9876, and 708.9896; found, 712.9839, 710.9860, and 708.9882.

dx.doi.org/10.1021/jm300618u | J. Med. Chem. 2012, 55, 9467−9491

(2*E*,2′*E*)-*N*,*N*′-[2,2′-Disulfanediylbis(ethane-2,1-diyl)]bis[3-(5-bromo-1-methyl-1*H*-indol-3-yl)-2-(hydroxyimino)-propanamide] (4k). In accordance with the general procedure described for the cleavage of trityl groups, **14k** (0.12 g, 0.10 mmol) gave, after purification by column chromatography (SiO_2, 95:5 CH_2Cl_2/MeOH), disulfide **4k** (0.07 g, 91%) as a white solid. ^{1}H NMR (CD_3COCD_3, 400.13 MHz) (data for monomer): δ 11.04 (s, 1H, NOH), 7.94 (d, J = 1.7 Hz, 1H, H4′), 7.55 (t, J = 5.3 Hz, 1H, CONH), 7.26 (d, J = 8.7 Hz, 1H, H6′), 7.21 (dd, J = 8.7, 1.7 Hz, 1H, H7′), 7.12 (s, 1H, H2′), 3.98 (s, 2H, 2H3), 3.53 (q, J = 6.6 Hz, 2H, 2H1″), 2.84 (s, 3H, NCH_3), 2.84 (t, J = 6.6 Hz, 2H, 2H2″) ppm. ^{13}C NMR (CD_3COCD_3, 100.61 MHz) (data for monomer): δ 165.2 (s), 154.6 (s), 137.4 (s), 131.9 (d), 131.5 (s), 125.5 (d), 123.8 (d), 113.5 (s), 112.9 (d), 110.4 (s), 40.1 (t), 39.4 (t), 33.8 (q), 20.2 (t) ppm. IR: ν 3500−3100 (br, O−H), 2924 (w, C−H), 1658 (s, C═N and C═O), 1527 (s), 1475 (s), 1422 (m), 1218 (s), 772 (s) cm^{-1}. HRMS (ESI$^+$) calcd for $C_{28}H_{30}{}^{81}Br_2N_6O_4S_2Na$, $C_{28}H_{30}{}^{81}Br^{79}BrN_6O_4S_2Na$, and $C_{28}H_{30}{}^{79}Br_2N_6O_4S_2Na$ ([M + Na]$^+$) 762.9988, 761.0008, and 759.0029; found, 762.9994, 761.0016, and 759.0042.

(2*E*,2′*E*)-*N*,*N*′-[2,2′-Disulfanediylbis(ethane-2,1-diyl)]bis[3-(5-bromo-1-[4-bromobenzyl]-1*H*-indol-3-yl)-2-(hydroxyimino)-propanamide] (4l). In accordance with the general procedure described for the cleavage of trityl groups, **14l** (0.14 g, 0.10 mmol) gave, after purification by column chromatography (SiO_2, 95:5 CH_2Cl_2/MeOH), disulfide **4l** (0.06 g, 59%) as a white foam. ^{1}H NMR (CD_3COCD_3, 400.13 MHz) (data for monomer): δ 7.97 (d, J = 1.8 Hz, 1H, H4′), 7.59 (t, J = 5.9 Hz, 1H, CONH), 7.45 (d, J = 8.5 Hz, 2H, ArH), 7.30 (s, 1H, H2′), 7.26 (d, J = 8.7 Hz, 1H, H7′), 7.17 (dd, J = 8.7, 1.9 Hz, 1H, H6′), 7.08 (d, J = 8.5 Hz, 2H, ArH), 5.34 (s, 2H, NCH_2Ar), 4.01 (s, 2H, 2H3), 3.53 (q, J = 6.6 Hz, 2H, 2H1″), 2.87 (s, 1H, NOH), 2.82 (t, J = 6.6 Hz, 2H, 2H2″) ppm. ^{13}C NMR (CD_3COCD_3, 100.61 MHz) (data for monomer): δ 165.2 (s), 154.4 (s), 139.4 (s), 136.8 (s), 133.5 (d, 2×), 131.9 (s), 131.4 (d), 130.8 (d, 2×), 125.8 (d), 124.0 (d), 122.7 (s), 113.9 (s), 113.5 (d), 111.3 (s), 50.6 (t), 40.1 (t), 39.3 (t), 20.2 (t) ppm. IR: ν 3500−3100 (br, O−H), 2922 (w, C−H), 1656 (s, C═N and C═O), 1525 (s), 1463 (m), 1010 (s), 786 (s), 717 (s) cm^{-1}. HRMS (ESI$^+$) calcd for $C_{40}H_{36}{}^{81}Br_4N_6O_4S_2Na$, $C_{40}H_{36}{}^{81}Br_2{}^{79}Br_2N_6O_4S_2Na$, and $C_{40}H_{36}{}^{79}Br_4N_6O_4S_2Na$ ([M + Na]$^+$) 1072.8813, 1070.8829, and 1068.8849; found, 1072.8812, 1070.8828, and 1068.8846.

(2*E*,2′*E*)-*N*,*N*′-[3,3′-Disulfanediylbis(propane-3,1-diyl)]bis[3-(5-bromo-1*H*-indol-3-yl)-2-(hydroxyimino)propanamide] (4m). In accordance with the general procedure described for the cleavage of the trityl group, **14m** (0.07 g, 0.05 mmol) gave, after purification by column chromatography (SiO_2, 95:5 CH_2Cl_2/MeOH), disulfide **4m** (0.01 g, 19% two steps) as a yellow oil. ^{1}H NMR (CD_3COCD_3, 400.13 MHz) (data for monomer): δ 10.28 (br, 1H, OH), 7.96 (s, J = 1.8 Hz, 1H, H4′), 7.51 (t, J = 4.9 Hz, 1H, NH), 7.31 (d, J = 8.6 Hz, 1H, H7′), 7.25 (s, 1H, H2′), 7.16 (dd, J = 8.6, 1.8 Hz, 1H, H6′), 4.03 (s, 2H, 2H3), 3.34 (q, J = 7.0 Hz, 2H, 2H1″), 2.63 (t, J = 7.0 Hz, 2H, 2H3″), 1.85 (quint, J = 7.0 Hz, 2H, 2H2″) ppm. ^{13}C NMR (CD_3COCD_3, 100.62 MHz) (data for monomer): δ 165.4 (s), 155.0 (s), 137.0 (s), 131.3 (s), 127.6 (d), 125.6 (d), 123.6 (d), 114.9 (d), 113.5 (s), 111.4 (s), 39.6 (t), 37.5 (t), 31.1 (t), 20.4 (t) ppm. IR: ν 3500−3100 (br, N−H and O−H), 3060 (w, C−H), 2927 (w, C−H), 1701 (m, C═O), 1656 (s, C═N), 1626 (m, C═N), 1530 (s), 1446 (s), 1423 (s), 1363 (m), 1207 (m), 1094 (w), 1039 (w), 987 (m), 881 (s), 792 (s) cm^{-1}. HRMS (ESI$^+$) calcd for $C_{28}H_{30}{}^{81}Br_2N_6O_4S_2$, $C_{28}H_{30}{}^{81}Br^{79}BrN_6O_4S_2$, and $C_{28}H_{30}{}^{79}Br_2N_6O_4S_2$ ([M + Na]$^+$) 762.9992, 761.0010, 759.0029; found, 762.9985, 761.0031, and 759.0007.

(2*E*,2′*E*)-*N*,*N*′-[4,4′-Disulfanediylbis(butane-4,1-diyl)]bis[3-(5-bromo-1*H*-indol-3-yl)-2-(hydroxyimino)propanamide] (4n). In accordance with the general procedure described for cleavage of the trityl group, **14n** (0.09 g, 0.08 mmol) gave, after purification by column chromatography (SiO_2, 95:5 CH_2Cl_2/MeOH), disulfide **4n** (0.03 g, 42% two steps) as a yellow oil. ^{1}H NMR (CD_3COCD_3, 400.13 MHz) (data for monomer): δ 10.22 (br, 1H, OH), 7.93 (d, J = 1.8 Hz, 1H, H4′), 7.40 (br, 1H, NH), 7.27 (d, J = 8.6 Hz, 1H, H7′), 7.21 (d, J = 1.3 Hz, 1H, H2′), 7.11 (dd, J = 8.6, 1.8 Hz, 1H, H6′), 4.00 (s, 2H, 2H3), 3.23 (q, J = 6.4 Hz, 2H, 2H1″), 2.59 (t, J = 6.4 Hz, 2H, 2H4″), 1.6−1.5 (m, 4H, 2H2″ + 2H3″) ppm. ^{13}C NMR (CD_3COCD_3, 100.62 MHz) (data for monomer): δ 165.3 (s), 155.0 (s), 136.9 (s), 131.3 (s), 127.7 (d), 125.6 (d), 123.6 (d), 114.8 (d), 113.5 (s), 111.4 (s), 40.2 (t), 39.9 (t), 30.1 (t), 28.1 (t), 20.4 (t) ppm. IR: ν 3500−3100 (br, N−H and O−H), 3058 (w, C−H), 2930 (w, C−H), 1702 (m, C═O), 1656 (s, C═N), 1626 (m, C═N), 1530 (s), 1448 (s), 1423 (s), 1362 (m), 1226 (m), 1205 (m), 993 (s), 881 (s), 792 (s) cm^{-1}. HRMS (ESI$^+$) calcd for $C_{30}H_{34}{}^{81}Br_2N_6O_4S_2$, $C_{30}H_{34}{}^{81}Br^{79}BrN_6O_4S_2$, and $C_{30}H_{34}{}^{79}Br_2N_6O_4S_2$ ([M + H]$^+$) 791.0306, 789.0323, and 787.0342; found, 791.0255, 789.0318, and 787.0346.

(2*E*,2′*E*)-*N*,*N*′-[5,5′-Disulfanediylbis(pentane-5,1-diyl)]bis[3-(5-bromo-1*H*-indol-3-yl)-2-(hydroxyimino)propanamide] (4o). In accordance with the general procedure described for cleavage of the trityl group, **14o** (0.08 g, 0.07 mmol) gave, after purification by column chromatography (SiO_2, 95:5 CH_2Cl_2/MeOH), disulfide **4o** (0.03 g, 38% two steps) as a yellow oil. ^{1}H NMR (CD_3COCD_3, 400.13 MHz) (data for monomer): δ 10.27 (br, 1H, OH), 7.97 (s, 1H, H4′), 7.38 (t, J = 5.4 Hz, 1H, NH), 7.31 (d, J = 8.6 Hz, 1H, H7′), 7.25 (s, 1H, H2′), 7.17 (dd, J = 8.6, 1.6 Hz, 1H, H6′), 4.03 (s, 2H, 2H3), 3.24 (q, J = 6.6 Hz, 2H, 2H1″), 2.63 (t, J = 7.2 Hz, 2H, 2H5″), 1.63 (quint, J = 7.2 Hz, 2H, −CH_2), 1.50 (quint, J = 7.2 Hz, 2H, −CH_2), 1.34 (quint, J = 7.2 Hz, 2H, −CH_2) ppm. ^{13}C NMR (CD_3COCD_3, 100.62 MHz) (data for monomer): δ 165.2 (s), 155.0 (s), 136.9 (s), 131.3 (s), 127.7 (d), 125.6 (d), 123.6 (d), 114.8 (d), 113.5 (s), 111.4 (s), 40.6 (t), 40.1 (t), 30.9 (t), 30.4 (t), 27.3 (t), 20.4 (t) ppm. IR: ν 3500−3100 (br, N−H and O−H), 2929 (w, C−H), 2858 (w, C−H), 1703 (s, C═O), 1656 (s, C═N), 1627 (m, C═N), 1531 (s), 1456 (s), 1423 (s), 1362 (s), 1227 (s), 1092 (m), 1040 (m), 992 (s), 881 (s), 792 (s) cm^{-1}. HRMS (ESI$^+$) calcd for $C_{32}H_{39}{}^{81}Br_2N_6O_4S_2$, $C_{32}H_{39}{}^{81}Br^{79}BrN_6O_4S_2$, and $C_{32}H_{39}{}^{79}Br_2N_6O_4S_2$ ([M + H]$^+$) 797.0801, 795.0817, and 793.0835; found, 797.0746, 795.0812, and 793.0800.

(2*E*,2′*E*)-*N*,*N*′-(Hexane-1,6-diyl)bis[3-(5-bromo-1*H*-indol-3-yl)-2-(hydroxyimino)propanamide] (4p). In accordance with the general procedure described for the cleavage of trityl groups, **14p** (0.10 g, 0.09 mmol) gave, after purification by column chromatography (SiO_2, 97:3 CH_2Cl_2/MeOH), disulfide **4p** (0.06 g, 98%) as a yellow solid, mp 240−214 °C (dec) (MeOH/EtOAc). ^{1}H NMR (CD_3COCD_3, 400.13 MHz) (data for monomer): δ 10.96 (br s, 1H), 10.25 (br, 1H), 7.95 (br, 1H, ArH), 7.29 (dd, J = 8.6, 1.9 Hz, 1H, H6′), 7.24 (br, 1H, ArH), 7.16 (d, J = 8.6 Hz, 1H, H7′), 4.04 (s, 2H, 2H3), 3.3−3.2 (m, 2H, 2H1″), 1.3−1.2 (m, 2H), 1.2−1.1 (m, 2H) ppm. ^{13}C NMR (DMSO-d_6, 100.62 MHz): δ 163.3 (s), 152.5 (s), 134.5 (s), 128.8 (s), 125.5 (d), 123.2 (d), 121.0 (d), 113.2 (d), 110.9 (s), 108.7 (s), 38.5 (t), 28.9 (t), 25.9 (t), 18.8 (t) ppm. IR: ν 3500−3000 (br, N−H and O−H), 2930 (m, C−H), 2858 (w, C−H), 1668 (s, C═O and C═N), 1539 (m), 1456 (m), 1206 (s), 1143 (m), 799 (w) cm^{-1}. HRMS (ESI$^+$) calcd for $C_{28}H_{30}{}^{81}Br_2N_6O_4Na$, $C_{28}H_{30}{}^{79}Br^{81}BrN_6O_4Na$, and $C_{28}H_{30}{}^{79}Br_2N_6O_4Na$ ([M + Na]$^+$), 699.0552, 697.0573, and 695.0593; found, 699.0556, 697.0568, and 695.0584.

(*E*)-3-(5-Bromo-1*H*-indol-3-yl)-2-(hydroxyimino)-*N*-(2-methoxyethyl)propanamide (4q). In accordance with the general procedure described for the cleavage of trityl groups, **14q** (0.05 g, 0.09 mmol) gave, after purification by column chromatography (SiO_2, 97:3 CH_2Cl_2/MeOH), disulfide **4q** (0.02 g, 71%) as a colorless oil. ^{1}H NMR (CD_3OD, 400.13 MHz): δ 7.85 (d, J = 1.8 Hz, 1H, H4′), 7.20 (d, J = 8.6 Hz, 1H, H7′), 7.13 (dd, J = 8.6, 1.8 Hz, 1H, H6′), 7.11 (s, 1H, H2′), 3.98 (s, 2H, 2H3), 3.4−3.3 (m, 4H, 2H1″+ 2H2″), 3.27 (s, 3H, OCH_3) ppm. ^{13}C NMR (CD_3OD, 100.62 MHz): δ 166.2 (s), 153.6 (s), 136.4 (s), 130.4 (s), 126.5 (d), 124.9 (d), 122.7 (d), 113.7 (d), 112.9 (s), 110.3 (s), 71.9 (t), 58.9 (q), 40.0 (t), 19.7 (t) ppm. IR: ν 3500−3100 (br, N−H and O−H), 3057 (w, C−H), 2928 (w, C−H), 2877 (w, C−H), 1659 (s, C═O and C═N), 1533 (s), 1453 (m), 1200 (m), 1097 (m), 994 (m), 876 (m) cm^{-1}. MS (FAB$^+$): m/z (%) 357 ([M + 1]$^+$ [^{81}Br], 19), 356 ([M]$^+$ [^{81}Br], 90), 355 ([M + 1]$^+$ [^{79}Br], 33), 354 ([M]$^+$ [^{79}Br], 100), 338 (24), 233 (31), 210 (24), 208 (24). HRMS (FAB$^+$) calcd for $C_{14}H_{17}{}^{81}BrN_3O_3$ and $C_{14}H_{19}{}^{79}BrN_3O_3$ ([M + 1]$^+$), 356.0433 and 354.0453; found, 356.0442 and 354.0461.

(*E*)-3-(5-Bromo-1*H*-indol-3-yl)-*N*-(2-hydroxyethyl)-2-(hydroxyimino)propanamide (4r). A solution of **14r** (0.06 g, 0.09

dx.doi.org/10.1021/jm300618u | *J. Med. Chem.* 2012, 55, 9467−9491

mmol) in a 6:3:1 THF/HCO_2H/H_2O mixture was stirred for 19 h. Water was added, and the reaction mixture was extracted with EtOAc. The organic extracts were washed with brine and dried over Na_2SO_4. The solvent was removed in vacuo to yield a yellow oil. The residue was dissolved in a 20:1 CH_2Cl_2/MeOH mixture (0.6 mL), placed in a Schlenk flask, and anhydrous HCl (0.63 mmol of a 1.0 M ether solution) was added. The solution was then stirred at 25 °C for 1 h. The mixture was diluted with 1:1 MeOH/H_2O mixture and washed with hexane. The MeOH was removed in vacuo, and the aqueous layer was extracted with EtOAc. The combined organic extracts were dried over Na_2SO_4 and filtered, and the solvent was removed in vacuo. The residue was subjected to column chromatography (SiO_2, 95:5 CH_2Cl_2/MeOH) to afford amide **4r** (0.02 g, 59%) as a colorless oil. ^{1}H NMR (CD_3COCD_3, 400.13 MHz): δ 11.02 (s, 1H), 10.17 (br, 1H), 7.79 (d, J = 7.9 Hz, 1H, ArH), 7.57 (t, J = 5.3 Hz, 1H, CONH), 7.28 (s, 1H, ArH), 7.27 (d, J = 7.4 Hz, 1H, ArH), 6.95 (t, J = 7.8 Hz, 1H, ArH), 4.05 (s, 2H), 3.54 (q, J = 6.5 Hz, 2H, 2H2″), 2.84 (t, J = 6.7 Hz, 2H, 2H1″) ppm. ^{13}C NMR (CD_3COCD_3, 100.62 MHz): δ 165.3 (s), 154.7 (s), 136.9 (s), 131.3 (s), 127.7 (d), 125.6 (d), 123.6 (d), 114.8 (d), 113.4 (s), 111.4 (s), 62.6 (t), 43.6 (t), 20.2 (t) ppm. IR: ν 3500−3100 (br, N−H and O−H), 3069 (w, C−H), 2931 (w, C−H), 2884 (w, C−H), 1702 (m, C═O or C═N), 1657 (s, C═O or C═N), 1534 (s), 1459 (s), 1227 (m), 1064 (m), 1041 (m), 883 (w), 794 (m) cm^{-1}. MS (FAB$^+$): m/z (%) 342 ([M + 1]$^+$ [^{81}Br], 87), 341 ([M]$^+$ [^{81}Br], 55), 340 ([M + 1]$^+$ [^{79}Br], 100), 339 ([M]$^+$ [^{79}Br], 40), 257 (23), 255 (23), 237 (30), 236 (38), 235 (36), 234 (35), 210 (44), 208 (46), 173 (41), 159 (25), 157 (24), 156 (33), 155 (30), 154 (33). HRMS (FAB$^+$) calcd for $C_{13}H_{14}{}^{81}BrN_3O_3$ and $C_{13}H_{14}{}^{79}BrN_3O_3$ ([M]$^+$), 341.0198 and 339.0219; found, 341.0214 and 339.0218.

(*E*)-3-(5-Bromo-1*H*-indol-3-yl)-2-(hydroxyimino)-*N*-[2-(methylthio)ethyl]propanamide (4s). $NaBH_4$ (2 mg, 0.06 mmol) was added to a solution of **4a** (0.01 g, 0.01 mmol) and NaOH (2 mg, 0.05 mmol) in dry MeOH (0.1 mL) at room temperature. The reaction mixture was stirred for 0.5 h, and then MeI (0.01 mL, 0.11 mmol) was added. After 16 h, the methanol was evaporated and the residue dissolved in CH_2Cl_2, washed with water, and dried with Na_2SO_4. The solvent was removed in vacuo and the residue was purified by column chromatography (SiO_2, 97:3 CH_2Cl_2/MeOH) to afford 8 mg (80%) of **4s** as a yellow oil. ^{1}H NMR (CD_3COCD_3, 400.13 MHz): δ 11.00 (br, 1H), 10.22 (br, 1H), 7.97 (d, J = 1.8 Hz, 1H, H4′), 7.48 (br, 1H, CONH), 7.31 (d, J = 8.6 Hz, 1H, H7′), 7.25 (d, J = 2.2 Hz, 1H, H2′), 7.17 (dd, J = 8.6, 1.8 Hz, 1H, H6′), 4.02 (s, 2H, 2H3), 3.45 (q, J = 6.4 Hz, 2H, 2H1″), 2.61 (t, J = 7.0 Hz, 2H, 2H2″), 2.06 (s, 3H, SCH_3) ppm. ^{13}C NMR (CD_3COCD_3, 100.62 MHz): δ 165.0 (s), 154.7 (s), 136.9 (s), 131.3 (s), 127.7 (d), 125.5 (d), 123.6 (d), 114.8 (d), 113.4 (s), 111.4 (s), 39.9 (t), 34.9 (t), 20.3 (t), 15.9 (q) ppm. IR: ν 3500−3100 (br, N−H and O−H), 3064 (w, C−H), 2921 (m, C−H), 1661 (s, C═O and C═N), 1529 (s), 1453 (s), 1225 (m), 1036 (m), 998 (m), 793 (m) cm^{-1}. MS (FAB$^+$): m/z (%) 372 ([M + 1]$^+$ [^{81}Br], 92), 371 ([M]$^+$ [^{81}Br], 62), 370 ([M + 1]$^+$ [^{79}Br], 100), 369 ([M]$^+$ [^{79}Br], 43), 322 (39), 236 (31), 235 (23), 234 (30), 210 (33), 208 (34), 165 (29), 161 (30), 159 (32), 155 (45), 154 (79). HRMS (FAB$^+$) calcd for $C_{14}H_{16}{}^{81}BrN_3O_2S$ and $C_{14}H_{16}{}^{79}BrN_3O_2S$ ([M]$^+$), 371.0126 and 369.0147; found, 371.0125 and 369.0150.

(*E*)-Ethyl 3-(5-Bromo-1*H*-indol-3-yl)-2-(methoxyimino)-propanoate (15a). Silver(I) oxide (0.04 g, 0.17 mmol) and iodomethane (0.15 mL, 2.40 mmol) were added to a solution of ester **9a** (0.05 g, 0.15 mmol) in acetone (0.5 mL). After being stirred at room temperature for 14 h, the solution was filtered through a pad of Celite and the solvent was evaporated. The residue was purified by column chromatography (SiO_2, 75:25 hexane/EtOAc) to afford indole **15a** (0.02 g, 42%) as a colorless oil. ^{1}H NMR (CD_3COCD_3, 400.13 MHz): δ 10.28 (br, 1H, NH), 7.81 (d, J = 1.9 Hz, 1H, H4′), 7.34 (d, J = 8.6 Hz, 1H, H7′), 7.23 (d, J = 2.4 Hz, 1H, H2′), 7.20 (dd, J = 8.6, 1.9 Hz, 1H, H6′), 4.20 (q, J = 7.1 Hz, 2H, $CO_2C\underline{H}_2CH_3$), 4.08 (s, 3H, $NOCH_3$), 3.98 (s, 2H, 2H3), 1.24 (t, J = 7.1 Hz, 3H, $CO_2CH_2C\underline{H}_3$) ppm. ^{13}C NMR (CD_3COCD_3, 100.62 MHz): δ 165.1 (s), 152.7 (s), 137.0 (s), 131.0 (s), 127.5 (d), 125.8 (d), 123.2 (d), 115.0 (d), 113.6 (s), 110.6 (s), 64.3 (q), 63.0 (t), 22.4 (t), 15.4 (q) ppm. IR: ν 3500−3100 (br, NH), 2980 (w, C−H), 2938 (w, C−H), 1719 (s, C═O and C═N), 1458 (m), 1323 (m), 1205 (m), 1116 (m), 1046 (s), 793 (m) cm^{-1}. MS (FAB$^+$): m/z (%) 341 ([M + 1]$^+$ [^{81}Br], 92), 340 ([M]$^+$ [^{81}Br], 96), 339 ([M + 1]$^+$ [^{79}Br], 100), 338 ([M]$^+$ [^{79}Br], 84), 238 (17), 236 (28), 235 (29), 233 (26), 210 (82), 209 (16), 208 (81). HRMS (FAB$^+$) calcd for $C_{14}H_{15}{}^{81}BrN_2O_3$ and $C_{14}H_{15}{}^{79}BrN_2O_3$ ([M]$^+$), 340.0246 and 338.0266; found, 340.0277 and 338.0277.

(*E*)-Ethyl 2-(Benzyloxyimino)-3-(5-bromo-1*H*-indol-3-yl)-propanoate (15b). To a solution of oxime **9a** (0.10 g, 0.31 mmol) and potassium *tert*-butoxide (0.04 g, 0.38 mmol) in 1,2-dimethoxyethane (DME) (6 mL) was added a solution of benzyl bromide (0.05 mL, 0.43 mmol) in DME (2 mL). The mixture was stirred for 15 h at room temperature, and the solvent was removed under reduced pressure. A solution of the residue in CH_2Cl_2 was washed successively with 10% HCl and brine and subsequently dried over Na_2SO_4. The residue was subjected to column chromatography (SiO_2, 70:30 hexane/EtOAc) to give the *O*-benzyloxime **15b** (0.09 g, 72%) as a yellow oil. ^{1}H NMR ($CDCl_3$, 400.13 MHz): δ 8.07 (br, 1H, NH), 7.83 (s, 1H, ArH), 7.5−7.3 (m, 5H, ArH), 7.3−7.2 (m, 1H, ArH), 7.17 (d, J = 8.5 Hz, 1H, ArH), 7.02 (s, 1H, ArH), 5.36 (s, 2H, OCH_2Ph), 4.28 (q, J = 7.0 Hz, 2H, $CO_2C\underline{H}_2CH_3$), 4.01 (s, 2H, 2H3), 1.31 (t, J = 7.1 Hz, 3H, $CO_2CH_2C\underline{H}_3$) ppm. ^{13}C NMR ($CDCl_3$, 100.62 MHz): δ 163.4 (s), 151.0 (s), 136.2 (s), 134.4 (s), 128.9 (s), 128.7 (d, 2×), 128.6 (d, 2×), 128.3 (d), 124.8 (d), 124.6 (d), 121.9 (d), 112.8 (s), 112.4 (d), 109.5 (s), 77.9 (t), 61.9 (t), 21.1 (t), 14.1 (q) ppm. IR: ν 3500−3100 (br, N−H), 3031 (w, C−H), 2982 (w, C−H), 2935 (w, C−H), 1718 (s, C═O and C═N), 1454 (s), 1323 (m), 1199 (s), 1012 (s), 772 (s) cm^{-1}. MS (FAB$^+$): m/z (%) 417 ([M + 1]$^+$ [^{81}Br], 95), 416 ([M]$^+$ [^{81}Br], 90), 415 ([M + 1]$^+$ [^{79}Br], 100), 414 ([M]$^+$ [^{79}Br], 72), 325 (24), 323 (24), 309 (26), 307 (34), 210 (46), 208 (46), 155 (23), 154 (63). HRMS (FAB$^+$) calcd for $C_{20}H_{19}{}^{81}BrN_2O_3$ and $C_{20}H_{19}{}^{79}BrN_2O_3$ ([M]$^+$), 416.0559 and 414.0579; found, 416.0569 and 414.0575.

(*E*)-3-(5-Bromo-1*H*-indol-3-yl)-2-(methoxyimino)propanoic Acid (16a). According the general procedure described for the hydrolysis of esters, indole **15a** (0.15 g, 0.44 mmol) gave, after crystallization, acid **16a** (0.11 g, 84%) as a yellow solid, mp 154−155 °C (hexane/CH_2Cl_2/MeOH). ^{1}H NMR (CD_3COCD_3, 400.13 MHz): δ 10.28 (br, 1H, NH), 7.84 (d, J = 1.9 Hz, 1H, H4′), 7.34 (d, J = 8.6 Hz, 1H, H7′), 7.23 (d, J = 1.9 Hz, 1H, H2′), 7.20 (dd, J = 8.6, 1.9 Hz, 1H, H6′), 4.08 (s, 3H, $NOC\underline{H}_3$), 3.97 (s, 2H, 2H3) ppm. ^{13}C NMR (CD_3COCD_3, 100.62 MHz): δ 165.6 (s), 152.5 (s), 137.0 (s), 131.1 (s), 127.5 (d), 125.8 (d), 123.3 (d), 115.0 (d), 113.6 (s), 110.6 (s), 64.4 (q), 22.0 (t) ppm. IR: ν 3500−3100 (br, OH) 3410 (s, NH), 2985 (w, C−H), 2933 (w, C−H), 1711 (s, C═O and C═N), 1429 (m), 1211 (w), 1044 (s), 785 (m). MS (FAB$^+$): m/z (%) 313 ([M + 1]$^+$ [^{81}Br], 61), 312 ([M]$^+$ [^{81}Br], 59), 311 ([M + 1]$^+$ [^{79}Br], 62), 310 ([M]$^+$ [^{79}Br], 51), 281 (24), 210 (100), 208 (99), 185 (22), 156 (21). HRMS (FAB$^+$) calcd for $C_{12}H_{11}{}^{81}BrN_2O_3$ and $C_{12}H_{11}{}^{79}BrN_2O_3$ ([M]$^+$), 311.9933 and 309.9953; found, 311.9957 and 309.9966.

(*E*)-2-(Benzyloxyimino)-3-(5-bromo-1*H*-indol-3-yl)propanoic Acid (16b). According to the general procedure described for the hydrolysis of esters, indole **15b** (0.07 g, 0.17 mmol) gave, after crystallization, acid (0.65 g, 99%) as a white solid. ^{1}H NMR (CD_3COCD_3, 400.13 MHz): δ 10.26 (br, 1H), 7.90 (s, 1H), 7.45 (d, J = 7.0 Hz, 2H), 7.4−7.3 (m, 5H), 7.24 (s, 1H), 7.22 (d, J = 8.6 Hz, 1H), 5.35 (s, 2H, OCH_2Ph), 4.06 (s, 2H, 2H3) ppm. ^{13}C NMR (CD_3COCD_3, 100.62 MHz): δ 165.5 (s), 152.7 (s), 138.6 (s), 136.8 (s), 130.9 (s), 130.2 (d, 2×), 130.1 (d, 2×), 129.9 (d), 127.5 (d), 125.7 (d), 123.1 (d), 114.9 (d), 113.6 (s), 110.3 (s), 79.1 (t), 22.1 (t) ppm.

(2*E*,2′*E*)-*N*,*N*′-[2,2′-Disulfanediylbis(ethane-2,1-diyl)]bis[3-(5-bromo-1*H*-indol-3-yl)-2-(methoxyimino)propanamide] (17a). Following the general procedure described for the coupling of acids with amines, acid **16a** (0.11 g, 0.35 mmol) afforded, after purification by column chromatography (SiO_2, 95:5 CH_2Cl_2/MeOH), disulfide **17a** (0.10 g, 77%) as a colorless oil. ^{1}H NMR (CD_3COCD_3, 400.13 MHz) (data for monomer): δ 10.22 (br, 1H, NH), 7.87 (d, J = 1.8 Hz, 1H, H4″), 7.68 (t, J = 5.2 Hz, 1H, CONH), 7.31 (d, J = 8.6 Hz, 1H, H7″), 7.21 (d, J = 2.1 Hz, 1H, H2″), 7.17 (dd, J = 8.6, 1.8 Hz, 1H, H6″), 3.98 (s, 3H, $NOCH_3$), 3.97 (s, 2H, 2H3′), 3.55 (q, J = 6.8 Hz, 2H, 2H1), 2.85 (t, J = 6.8 Hz, 2H, 2H2) ppm. ^{13}C NMR (CD_3COCD_3, 100.62 MHz) (data for monomer): δ 164.6 (s), 154.4 (s), 137.0 (s), 131.2 (s),

dx.doi.org/10.1021/jm300618u | J. Med. Chem. 2012, 55, 9467−9491

127.6 (d), 125.7 (d), 123.5 (d), 114.9 (d), 113.5 (s), 110.9 (s), 64.0 (q), 40.4 (t), 39.3 (t), 21.1 (t) ppm. IR: ν 3500−3100 (br, NH), 3008 (w, C−H), 2976 (w, C−H), 2936 (w, C−H), 1664 (s, C═O and C═N), 1523 (s), 1458 (m), 1218 (m), 1047 (s), 760 (s) cm^{-1}. MS (FAB^+): m/z (%) 741 ($[M + 1]^+$ $[^{81}Br]$, 42), 740 ($[M]^+$ $[^{81}Br]$, 42), 739 ($[M + 1]^+$ $[^{81}Br]$ $[^{79}Br]$, 71), 738 ($[M + 2]^+$ $[^{79}Br]$, 40), 737 ($[M + 1]^+$ $[^{79}Br]$, 39), 708 (12), 707 (19), 664 (42), 663 (100), 662 (60), 648 (28), 647 (57). HRMS (FAB^+) calcd for $C_{28}H_{31}{}^{81}Br_2N_6O_4S_2$, $C_{28}H_{31}{}^{81}Br^{79}BrN_6O_4S_2$, and $C_{28}H_{31}{}^{79}Br_2N_6O_4S_2$ ($[M + 1]^+$), 741.0174, 739.0194, and 737.0215; found, 741.0184, 739.0203, and 737.0237.

(2*E*,2′*E*)-*N*,*N*′-[2,2′-Disulfanediylbis(ethane-2,1-diyl)]bis[2-(benzyloxyimino)-3-(5-bromo-1*H*-indol-3-yl)propanamide] (17b). Following the general procedure described for the coupling of acids with amines, indole **16b** (0.18 g, 0.46 mmol) gave, after purification by column chromatography (SiO_2, 50:50 hexane/EtOAc), disulfide **17b** (0.16 g, 80%) as a yellow oil. ^1H NMR (CD_3COCD_3, 400.13 MHz) (data for monomer): δ 10.23 (br, 1H, NH), 7.88 (d, J = 1.6 Hz, 1H, H4′), 7.71 (t, J = 5.4 Hz, 1H, CONH), 7.4−7.3 (m, 6H, ArH), 7.19 (d, J = 2.2 Hz, 1H, H2′), 7.17 (dd, J = 8.6, 1.9 Hz, 1H, H6′), 5.23 (s, 2H, OCH_2Ph), 4.01 (s, 2H, 2H3), 3.54 (t, J = 6.5 Hz, 2H, 2H1″), 2.9−2.8 (m, 2H, 2H2″) ppm. ^{13}C NMR (CD_3COCD_3, 100.62 MHz) (data for monomer): δ 164.6 (s), 154.8 (s), 139.0 (s), 136.9 (s), 131.2 (s), 130.3 (d, 2×), 130.2 (d, 2×), 129.9 (d), 127.7 (d), 125.7 (d), 123.5 (d), 114.9 (d), 113.6 (s), 110.7 (s), 78.8 (t), 40.4 (t), 39.3 (t), 21.3 (t) ppm. IR: ν 3500−3100 (br, N−H), 3032 (w, C−H), 2930 (w, C−H), 1666 (s, C═O and C═N), 1521 (s), 1455 (s), 1362 (m), 1226 (m), 1207 (m), 1013 (s), 793 (m) cm^{-1}. HRMS (ESI^+) calcd for $C_{40}H_{38}{}^{81}Br_2N_6O_4S_2$, $C_{40}H_{38}{}^{79}Br^{81}BrN_6O_4S_2$, and $C_{40}H_{38}{}^{79}Br_2N_6O_4S_2$ ($[M]^+$), 893.0794, 891.0815, and 889.0835; found, 893.0811, 891.0836, and 889.0841.

Methyl 3-(5-Bromo-1*H*-indol-3-yl)propanoate (18a). Methyl acrylate (0.88 g, 10.20 mmol) and $ZrCl_4$ (0.15 mL, 2.40 mmol) were added to a solution of 5-bromo-1*H*-indole **5a** (1.00 g, 5.10 mmol) in CH_2Cl_2 (0.5 mL). After the mixture was stirred at room temperature for 5 h, water was added and the solution was extracted with EtOAc (3×). The combined organic extracts were dried over Na_2SO_4, filtered, evaporated and the residue was purified by column chromatography (SiO_2, 70:30 hexane/EtOAc) to afford 0.83 g (58%) of ester **18a** as a white solid and 0.07 g (7%) of starting 5-bromo-1*H*-indole. ^1H NMR (CD_3COCD_3, 400.13 MHz): δ 10.18 (br, 1H, NH), 7.75 (d, J = 2.0 Hz, 1H, H4′), 7.35 (d, J = 8.4 Hz, 1H, H7′), 7.21 (s, 1H, H2′), 7.20 (dd, J = 8.4, 2.0 Hz, H6′), 3.61 (s, 3H, CO_2CH_3), 3.04 (t, J = 7.5 Hz, 2H), 2.69 (t, J = 7.5 Hz, 2H) ppm. ^{13}C NMR (CD_3COCD_3, 100.62 MHz): δ 174.8 (s), 137.3 (s), 131.1 (s), 125.7 (d), 125.6 (s), 122.7 (d), 115.8 (s), 115.0 (d), 113.4 (s), 52.6 (q), 39.3 (t), 22.0 (t) ppm. IR: ν 3335 (s, NH), 2950 (w, C−H), 2917 (w, C−H), 2855 (w, C−H) 1712 (s, C═O), 1438 (m), 1382 (m), 1302 (m), 1193 (s), 1170 (s), 981 (m), 882 (m), 791 (s) cm^{-1}. MS (FAB^+): m/z (%) 284 ($[M + 1]^+$ $[^{81}Br]$, 37), 283 ($[M]^+$ $[^{81}Br]$, 94), 282 ($[M + 1]^+$ $[^{79}Br]$, 52), 281 ($[M]^+$ $[^{79}Br]$, 100), 280 (14), 224 (13), 223 (12), 222 (12), 221 (12), 211 (11), 210 (82), 209 (13), 208 (86), 207 (12), 203 (13). HRMS (FAB^+) calcd for $C_{12}H_{12}{}^{81}BrNO_2$ and $C_{12}H_{12}{}^{79}BrNO_2$ ($[M]^+$), 283.0031 and 281.0051; found, 283.0024 and 281.0056.

Methyl 3-(5-Bromo-1-methyl-1*H*-indol-3-yl)propanoate (18b). Following the general procedure, indole **5k** (0.50 g, 2.39 mmol) afforded, after purification by column chromatography (SiO_2, 85:15 hexane/EtOAc), ester **18b** (0.56 g, 79%) as a colorless oil. ^1H NMR (CD_3COCD_3, 400.13 MHz): δ 7.74 (s, 1H, ArH), 7.26 (s, 2H, ArH), 7.06 (s, 1H, ArH), 3.73 (s, 3H, OCH_3), 3.61 (s, 3H, NCH_3), 3.01 (t, J = 7.5 Hz, 2H, CH_2), 2.66 (t, J = 7.5 Hz, 2H, CH_2) ppm. ^{13}C NMR (CD_3COCD_3, 100.61 MHz): δ 174.1 (s), 137.6 (s), 131.2 (s), 130.0 (d), 125.6 (d), 122.8 (d), 114.8 (s), 113.4 (s), 113.0 (d), 52.6 (q), 36.3 (t), 33.8 (q), 21.8 (t) ppm. IR: ν 2949 (w, C−H), 1732 (s, C═O), 1476 (s), 1425 (w), 1422 (w), 1245 (m), 1198 (m), 1155 (s), 1047 (w), 790 (s) cm^{-1}. MS (ESI^+): m/z (%) 298 ($[M + H]^+$ $[^{81}Br]$, 98), 297 ($[M]^+$ $[^{81}Br]$ $[^{79}Br]$, 25), 296 ($[M + H]^+$ $[^{79}Br]$, 100), 223 (31), 221 (30). HRMS (ESI^+) calcd for $C_{13}H_{15}{}^{81}BrNO_2$, $C_{13}H_{15}{}^{79}BrNO_2$ ($[M + H]^+$) 298.0261, 296.0281; found, 298.0254 and 296.0273.

3-(5-Bromo-1*H*-indol-3-yl)propanoic Acid (19a). According to the general procedure described for the hydrolysis of esters, **18a** (0.06 g, 0.20 mmol) gave, after crystallization, acid **19a** (0.05 g, 98%) as a white solid, mp 86−87 °C (hexane/CH_2Cl_2/MeOH). ^1H NMR (CD_3OD, 400.13 MHz): δ 7.66 (d, J = 1.7 Hz, 1H, H4′), 7.24 (d, J = 8.6 Hz, 1H, H7′), 7.16 (dd, J = 8.6, 1.7 Hz, 1H, H7′), 7.08 (s, 1H, H2′), 3.00 (t, J = 7.5 Hz, 2H, CH_2), 2.65 (t, J = 7.5 Hz, 2H, CH_2) ppm. ^{13}C NMR (CD_3OD, 100.62 MHz): δ 177.4 (s), 136.7 (s), 130.3 (s), 125.0 (d), 124.6 (d), 121.8 (d), 114.8 (s), 113.9 (d), 112.7 (s), 36.0 (t), 21.7 (t) ppm. IR: ν 3500−3100 (br, OH and NH), 2923 (w, C−H), 2851 (w, C−H), 1706 (s, C═O), 1623 (s), 1566 (m), 1541 (m), 1450 (s), 1212 (m), 822 (s), 801 (s), 785 (s), 680 (s) cm^{-1}. MS (FAB^+): m/z (%) 270 ($[M + 1]^+$ $[^{81}Br]$, 61), 269 ($[M]^+$ $[^{81}Br]$, 100), 268 ($[M + 1]^+$ $[^{79}Br]$, 70), 267 ($[M]^+$ $[^{79}Br]$, 92), 210 (34), 208 (34). HRMS (FAB^+) calcd for $C_{11}H_{11}{}^{81}BrNO_2$ and $C_{11}H_{11}{}^{79}BrNO_2$ ($[M + 1]^+$), 268.9874 and 266.9895; found, 268.9872 and 266.9886.

3-(5-Bromo-1-methyl-1*H*-indol-3-yl)propanoic Acid (19b). According to the general procedure described for the hydrolysis of esters, **18b** (0.20 g, 0.68 mmol) gave, after crystallization, **19b** (0.18 g, 95%) as a brown solid, mp 157−160 °C (hexane/$CHCl_3$). ^1H NMR (CD_3OD, 400.13 MHz): δ 7.65 (s, 1H, ArH), 7.20 (d, J = 8.6 Hz, 1H, ArH), 7.18 (d, J = 8.6 Hz, 1H, ArH), 6.97 (s, 1H, ArH), 3.69 (s, 3H, NCH_3), 2.98 (t, J = 7.4 Hz, 2H, CH_2), 2.62 (t, J = 7.4 Hz, 2H, CH_2) ppm. ^{13}C NMR (CD_3OD, 100.61 MHz): δ 177.0 (s), 137.3 (s), 130.8 (s), 129.1 (d), 125.2 (d), 122.1 (d), 114.5 (s), 113.0 (s), 111.9 (d), 36.0 (t), 32.8 (q), 21.4 (t) ppm. IR: ν 3500−2500 (br, O−H), 1700 (s, C═O), 1481 (m), 1433 (m), 1402 (m), 1368 (w), 1310 (s), 1201 (s), 907 (m), 788 (s) cm^{-1}. MS (EI^+): m/z (%) 284 ($[M + 1]^+$ $[^{81}Br]$, 3), 283 ($[M]^+$ $[^{81}Br]$, 24), 281 ($[M]^+$ $[^{79}Br]$, 20), 225 ($[M - CH_3 - CO_2 + 1]^+$ $[^{81}Br]^+$, 10), 224 ($[M - CH_3 - CO_2]^+$ $[^{81}Br]^+$,100), 223 ($[M - CH_3 - CO_2 + 1]^+$ $[^{79}Br]^+$, 12), 222 ($[M - CH_3 - CO_2]^+$ $[^{79}Br]^+$,99), 203 ($[M - Br + 1]^+$, 16), 157 (17), 144 (57), 143 (44), 142 (10). HRMS (EI^+) calcd for $C_{12}H_{12}{}^{81}BrNO_2$, $C_{12}H_{12}{}^{79}BrNO_2$ $[M]^+$, 283.0031 and 281.0051; found, 283.0028 and 281.0048. Anal. Calcd for $C_{12}H_{12}BrNO_2$: C, 51.09; H, 4.29; N, 4.96. Found: C, 50.92; H, 4.29; N, 4.96.

***N*,*N*′-[2,2′-Disulfanediylbis(ethane-2,1-diyl)]bis[3-(5-bromo-1*H*-indol-3-yl)propanamide] (20a).** Following the general procedure described for the coupling of acids with amines, **19a** (0.05 g, 0.20 mmol) afforded, after purification by column chromatography (SiO_2, 95:5 CH_2Cl_2/MeOH), disulfide **20a** (0.04 g, 65%) as a colorless oil. ^1H NMR (CD_3COCD_3, 400.13 MHz) (data for monomer): δ 10.19 (br, 1H, NH), 7.73 (s, 1H, H4″), 7.47 (br, 1H, CONH), 7.32 (d, J = 8.6 Hz, 1H, H7″), 7.18 (d, J = 2.1 Hz, 1H), 7.17 (d, J = 2.1 Hz, 1H), 3.43 (t, J = 6.6 Hz, 2H, CH_2), 3.04 (t, J = 7.4 Hz, 2H, CH_2), 2.73 (t, J = 6.6 Hz, 2H, CH_2), 2.56 (t, J = 7.4 Hz, 2H, CH_2) ppm. ^{13}C NMR (CD_3COCD_3, 100.62 MHz) (data for monomer): δ 174.1 (s), 137.2 (s), 131.2 (s), 125.7 (d), 125.5 (d), 122.8 (d), 116.2 (s), 114.8 (d), 113.2 (s), 40.1 (t), 39.5 (t), 38.5 (t), 22.7 (t) ppm. IR: ν 3500−3100 (br, NH), 2920 (m, C−H), 1623 (s, C═O), 1539 (s), 1453 (s), 1212 (m), 1098 (m), 881 (m), 794 (s), 753 (s) cm^{-1}. MS (FAB^+): m/z (%) 655 ($[M]^+$ $[^{81}Br]$, 59), 654 ($[M + 2]^+$ $[^{81}Br]$ $[^{79}Br]$, 40), 653 ($[M]^+$ $[^{81}Br]$ $[^{79}Br]$, 100), 652 ($[M + 2]^+$ $[^{79}Br]$, 31), 651 ($[M + 1]^+$ $[^{79}Br]$, 54), 327 (88), 325 (77). HRMS (FAB^+) calcd for $C_{26}H_{29}{}^{81}Br_2N_4O_2S_2$, $C_{26}H_{29}{}^{81}Br^{79}BrN_4O_2S_2$, and $C_{26}H_{29}{}^{79}Br_2N_4O_2S_2$ ($[M + 1]^+$), 655.0058, 653.0078, and 651.0099; found, 655.0072, 653.0081, and 651.0084.

***N*,*N*′-[2,2′-Disulfanediylbis(ethane-2,1-diyl)]bis[3-(5-bromo-1-methyl-1*H*-indol-3-yl)propanamide] (20b).** Following the general procedure described for the coupling of acids with amines, **19b** (0.06 g, 0.21 mmol) afforded, after purification by column chromatography (SiO_2, 95:5 CH_2Cl_2/MeOH), disulfide **20b** (0.05 g, 42%) as a white foam. ^1H NMR (CD_3COCD_3, 400.13 MHz) (data for monomer): δ 7.71 (d, J = 1.7 Hz, 1H, H4″), 7.48 (br, CONH), 7.28 (d, J = 8.6 Hz, 1H, H7″), 7.22 (dd, J = 8.6, 1.7 Hz, 1H, H6″), 7.04 (s, 1H, H2″), 3.73 (s, 3H, NCH_3), 3.42 (q, J = 6.6 Hz, 2H, CH_2), 3.00 (t, J = 7.4 Hz, 2H, CH_2), 2.73 (t, J = 6.6 Hz, 2H, CH_2), 2.54 (t, J = 7.4 Hz, 2H, CH_2) ppm. ^{13}C NMR (CD_3COCD_3, 100.62 MHz) (data for monomer): δ 174.1 (s), 137.8 (s), 131.5 (s), 130.2 (d), 125.5 (d), 123.1 (d), 115.5 (s), 113.3 (s), 113.0 (d), 40.1 (t), 39.6 (t), 38.7 (t),

dx.doi.org/10.1021/jm300618u | *J. Med. Chem.* 2012, 55, 9467−9491

33.8 (q), 22.7 (t) ppm. IR: ν 3300 (m, NH), 2918 (w, C−H), 1634 (s, C═O), 1549 (s), 1478 (m), 1266 (w), 810 (w) cm^{-1}. MS (FAB^+): *m*/*z* (%) 683 ($[M + 1]^+$ [^{81}Br], 38), 679 ($[M + 1]^+$ [^{79}Br], 38), 561 (15), 559 (15), 342 (18), 341 (22), 340 (21), 225 (14), 224 (97), 222 (100). HRMS (FAB^+) calcd for $C_{28}H_{33}{}^{81}Br_2N_4O_2S_2$ ($[M + 1]^+$), $C_{28}H_{33}{}^{79}Br_2N_4O_2S_2$ ($[M + 1]^+$), 683.0371 and 679.0412; found, 683.0400 and 679.0394.

Biology. Cell Culture. U937 (human leukemic monocyte lymphoma cell line, ATCC) were grown in RPMI 1640 medium (Euroclone) supplemented with 10% heat-inactivated FBS (Euroclone), 1% glutamin (Lonza), 1% penicillin/streptomycin (Euroclone), and 0.1% gentamycin (Lonza) at 37 °C in air and 5% CO_2. MCF7 (human breast cancer cell line, ATCC) were cultured in Dulbecco's modified Eagle's medium (DMEM, Euroclone) supplemented with 10% FCS (Sigma), 50 mg/mL penicillin−streptomycin (Gibco), and 2 mM glutamine (Gibco). Cell lines were maintained at 37 °C in a humidified atmosphere of 95% air, 5% CO_2 as previously reported.

Ligands and Materials. SAHA (Alexis), MS-275 (a kind gift of Schering AG), SGI1027, and indole-derived psammaplin A analogues were dissolved in DMSO (Sigma-Aldrich) and used at 5 or 0.5 μM. RG108 was dissolved in ethanol and used at 5 μM. ALX (Alexis) was dissolved in DMSO and used at a final concentration of 1 μM.

Cell Cycle Analysis. 2.5×10^5 U937 cells were collected by centrifugation after 24 h of stimulation with reference or testing compounds at 5 μM. The cells were resuspended in 500 μL of hypotonic buffer (0.1% NP-40, 0.1% sodium citrate, 50 μg/mL PI, RNase A) and incubated in the dark for 30 min. The analysis was performed by FACS-Calibur (Becton Dickinson) using the Cell Quest Pro software (Becton Dickinson) and ModFit LT, version 3, software (Verity). The experiment was performed in triplicate.

Granulocytic Differentiation Analysis. 2.5×10^5 U937 cells were collected by centrifugation after 30 h of stimulation with reference compound MS-275 at 5 μM or indole derivatives at 5 μM. The cells were washed with PBS and incubated in the dark at 4 °C for 30 min with 10 μL of PE-conjugated anti-CD11c surface antigen antibody or with 10 μL of PE-conjugated IgG in order to define the background signal. At the end of the incubation the samples were washed again and resuspended in 500 μL of PBS containing 0.25 μg/mL PI. The analysis was performed by FACS-Calibur (Becton Dickinson) using the Cell Quest Pro software (Becton Dickinson). The experiment was performed in triplicate, and PI positive cells were excluded from the analysis.

Histone Extraction. After stimulation with compounds, the cells were collected by centrifugation and washed two times with PBS. Then the samples were resuspended in Triton extraction buffer (PBS containing 0.5% Triton X-100 (v/v), 2 mM PMSF, 0.02% (w/v) NaN_3), and the lysis was performed for 10 min at 4 °C. Next, the samples were centrifuged at 2000 rpm for 10 min at 4 °C, and the pellets were washed in TEB (half the volume). After a new centrifugation under the same conditions, the samples were resuspended in 0.2 N HCl and the acid histone extraction was carried out overnight at 4 °C. The supernatant was recovered by centrifugation and the protein content was ensured by BCA protein assay (Pierce).

Total Protein Extraction. U937 cells were harvested and washed once with cold PBS and lysed in a lysis buffer containing 50 mM Tris-HCl, pH 7.4, 150 mM NaCl, 1% NP40, 10 mM NaF, 1 mM PMSF (phenylmethylsulfonyl fluoride) and protease inhibitor cocktail (Roche). The lysates were centrifuged at 14 000 rpm × 30 min at 4 °C. Protein concentrations were estimated by Bradford assay (Bio-Rad).

Western Blot Analyses. The 50 mg of total protein and 10 mg of histone extract were denaturated by boiling samples in buffer (0.25 M Tris-HCl, pH 6.8, 8% SDS, 40% glycerol, 5% 2-mercaptoethanol, 0.05% bromophenol blue) for 3 min before electrophoresis. Proteins were subjected to SDS−PAGE (8%−10%−15% polyacrylamide) in Tris−glycine−SDS (25 mM Tris, 192 mM glycine, 0.1% SDS). After electrophoresis, proteins were transferred to nitrocellulose membranes (Schleicher-Schuell, Germany) in a buffer containing Tris-glycine (25 mM Tris, 192 mM glycine) (Bio-Rad, Italy) and 20% MeOH. The complete transfer was assessed using Ponceau Red (Sigma Aldrich, U.S.) staining. After blocking with 5% nonfat dry milk in TBS 1×/Tween 0.1% (10 mM Tris-HCl, pH 8.0, 150 mM NaCl, 0.1% Tween-20), the membrane was incubated with the primary antibody overnight at 4 °C. After washing with TBS 1×/Tween 0.1%, membranes were incubated with the horseradish peroxidase conjugated secondary antibody (1:5000) for 60 min at room temperature, and the reaction was detected with a chemoluminescence detection system (Amersham Biosciences, U.K.). The antibodies used were p21 (BD), p16 (Santa Cruz), acetyltubulin (Sigma), H3ac (Diagenode), H3K9ac (Abcam), DNMT1 (Abcam), p53K382ac (Abcam), and H3K56ac. Total ERKs (Santa Cruz) were used to normalize for equal loading of total protein extraction. H4 (Cell Signalling) or Ponceau red staining was used to normalize for equal loading of histone extracts.

HDACs Fluorimetric Assay. HDACs assays were performed in the presence of 3 mM HDAC buffer (16.7 mM Tris-HCl, pH 8, 45.7 mM NaCl, 0.9 mM KCl, 0.3 mM $MgCl_2$) and 5 μg of BSA. For these experiments 0.25 μg of HDAC1 (BPS Bioscience) or 2.5 ng of HDAC4 (BPS Bioscience) was added to the reaction mix, and after a preincubation of 15 min at 37 °C was also added to the specific substrate at 5 μM. The reaction was carried out for 2 h at 37 °C in gentle shaking, and in the end fluorescence was quantified with a TECAN Infinite M200 station.

DNMT1 Assay. DNMT1 Immunoprecipitation. The U937 cells were lysed in TAP buffer, pH 7−7.5 (50 mM Tris, pH 7.0, 180 mM NaCl, 0.15% NP40 v/v, 10% glycerol v/v, 1.5 mM $MgCl_2$, 1 mM $NaMnO_4$, 0.5 mM NaF, 1 mM DTT, 0.2 mM PMSF, and protease inhibitor cocktail) for 10 min in ice and centrifuged at 13 000 rpm for 30 min. An amount of 650 μg of extracts was diluted in TAP buffer up to 1 mL and precleared by incubating with 20 μL of A/G plus agarose (Santa Cruz) for 1 h on a rocking table at 4 °C. The supernatant was transferred to a new tube. Then 3.25 μg of antibody against DNMT1 (Abcam) was added and IP was allowed to proceed overnight at 4 °C on a rocking table. As negative control, the same amount of protein extracts was immunoprecipitated with purified rabbit IgG (Santa Cruz). The following day 50 μL of A/G and agarose were added, and incubation was continued for 2 h. The beads were recovered by brief centrifugation and washed with cold TAP buffer several times. At this point the resin was resuspended in 10 μL of DNMT buffer (5 mM EDTA, 0.2 mM DTT, 26 mM NaCl, 20 mM Tris HCl, pH 7.4) in order to proceed with the radioactive assay.

DNMT1 Radioactive Assay. DNMT1 assays were performed in the presence of the analogues at 5 μM plus a reaction mixture composed of 10 μL of DNMT1-bound resin, 5 μCi *S*-adenosyl-L-[methyl-^{3}H]methionine (radioactive methyl donor, 12−18 Ci/mmol), 0.1 μg of poly dI-dC (methyl acceptor), and DNMT buffer. The reaction was carried out for 2 h at 37 °C with gentle stirring, and the experiment was performed in duplicate. Subsequently each sample was spread on Whatman DE-81 paper (in quadruplicate) and the papers were washed three times with 5% Na_2HPO_4 and once with distilled water. The papers were then transferred to the scintillation vials containing 5 mL of scintillation fluid (Perkin-Elmer) in order to read the DPM values.

SIRT Assay. Dilution of the enzyme (no. BML-SE239) from 5 to 0.2 U/μL in SIRT1 assay buffer (no. KI-286: 50 mM Tris-HCl, pH 8, 137 mM NaCl, 2.7 mM KCl, 1 mM $MgCl_2$, BSA 1 mg/mL) was followed by the preparation of a combined 2× solution by diluting the Fluor de Lys (substrate KI-177, 50 mM stock solution) and NAD^+ (no. KI-282, 10 mM stock solution) to 500 μM and 1 mM, respectively, in SIRT1 assay buffer. The plate was prepared as shown in Table 3.

The reaction was carried out for 1.5 h at 37 °C in gentle shaking table. Then 50 μL/well developer solution (39 μL of trypsin buffer

Table 3

well	assay buffer	SIRT1 (0.2 U/μL)	2× solution	compd
control	20 μL	5 μL	25 μL	
+ inhibitor	15 μL	5 μL	25 μL	5 μL
blank	25 μL	25 μL		

dx.doi.org/10.1021/jm300618u | J. Med. Chem. 2012, 55, 9467−9491

(Tris-HCl, pH 8, 50 mM, NaCl 100 mM), 3 μL of nicotinamide (diluted at 50 mM in assay buffer from a 120 mM stock solution in DMSO), and 8 μL of trypsin (6 mg/mL)) was added. After incubation for 30 min, the fluorescence was quantified with a TECAN Infinity 200 station at 360 nm excitation, 460 nm emission.

Molecular Modeling. (a) Quantum Mechanics Calculations. The geometry of **4a**-derived thiol **21** was optimized using the ab initio quantum chemistry program Gaussian 03[114] and the HF/3-21G* basis set. A set of atom-centered RHF 6-31G*//3-21G* charges was then obtained by using the RESP methodology[115] as implemented in the AMBER suite of programs. Covalent and nonbonded parameters for the inhibitor atoms were assigned, by analogy or through interpolation, from those already present in the AMBER force field[116] (parm99) or consistently derived, as explained in more detail elsewhere.[117]

(b) Molecular Docking. The genetic algorithm[118] implemented in AutoDock[119] and the HDAC8 (PDB code 1t64)[101] as the target protein upon removal of trichostatin A was used to generate different HDAC-Zn-bound **4a**-derived thiol **21** conformers by randomly changing torsion angles and overall orientation of the molecule. A volume for exploration was defined in the shape of a three-dimensional cubic grid with a spacing of 0.3 Å that enclosed the residues that are known to make up the inhibitor's binding pocket. At each grid point, the receptor's atomic affinity potentials for carbon, oxygen, nitrogen, sulfur, bromine, and hydrogen atoms present in the ligand were precalculated for rapid intra- and intermolecular energy evaluation of the docking solution.

To obtain additional validation of the proposed binding mode for the ligands, the program GRID (http://www.moldiscovery.com/)[120] was also used to search for sites on the enzyme that could be complementary to the functional groups present in this inhibitor. For the GRID calculations, a 18 Å × 21 Å × 21 Å lattice of points spaced at 0.5 Å was established at the binding site. The probes used were C1═ (aromatic carbon), N1 (neutral flat NH, eg amide), N:# (sp nitrogen with lone pair), O (sp^2 carbonyl oxygen), and Br (bromine). The dielectric constants chosen were 4.0 for the macromolecule and 80.0 for the bulk water.

(c) Molecular Dynamics Simulations. Ternary complexes (HDAC8−Zn^{2+}−thiol **21**) representative of the most populated solutions were then refined using the second generation AMBER force field and 3000 steps of steepest descent energy minimization and 6000 steps of conjugate gradient of only the side chain of the protein and those atoms belonging to the bound ligand. This procedure allowed readjustment of covalent bonds and van der Waals contacts without changing the overall conformation of the complex. The HDAC−**21** complex was then neutralized by addition of eight sodium ions[121] that were placed in electrostatically favored positions and immersed in rectangular boxes each containing about 450 TIP3P water molecules[122] that extended 8 Å away from any solute atom. The cutoff distance for the nonbonded interactions was 9 Å, and periodic boundary conditions were applied. Electrostatic interactions were represented using the smooth particle mesh Ewald method with a grid spacing of ∼1 Å. Unrestrained molecular dynamics (MD) simulations at 300 K and 1 atm were then run for 6 ns using the SANDER module in AMBER 8.[123] The coupling constants for the temperature and pressure baths were 1.0 and 0.2 ps, respectively. SHAKE[124] was applied to all bonds involving hydrogens, and an integration step of 2 fs was used throughout. The nonbonded pair list was updated every 10 steps. The simulation protocol involved a series of progressive energy minimizations followed by a 20 ps heating phase and a 70 ps equilibration period before data collection. System coordinates were saved every 2 ps for further analysis.

(d) Analysis of the Molecular Dynamics Trajectories. Three-dimensional structures and trajectories were visually inspected using the computer graphics program InsightII. Root-mean-square (rms) deviations from both the initial and the average structures, interatomic distances, and snapshot geometries were obtained using the PTRAJ module in AMBER. Intermolecular van der Waals energies for individual residues were calculated with the ANAL module, whereas the solvent-corrected residue-based electrostatic interaction energies were calculated with DelPhi, following the procedure described.[124]

All calculations were performed on the SGI R14000 Origin 3800 at CIEMAT (Madrid, Spain), on the SGI 1.5 GHz Itanium2 at CESGA (Santiago de Compostela, Spain), and locally on SGI R12000 Octane workstations.

■ ASSOCIATED CONTENT

Ⓢ Supporting Information

Experimental procedures, molecular modeling, crystalographic data for compounds **9b** and **10b**, and NMR spectra. This material is available free of charge via the Internet at http://pubs.acs.org.

■ AUTHOR INFORMATION

Corresponding Author

*For L.A.: phone, 39-081-5667569; e-mail, lucia.altucci@unina2.it. For Á.R.d.L.: phone, 34-986-812316; e-mail, qolera@uvigo.es.

Author Contributions

#These authors contributed equally to this work.

Notes

The authors declare the following competing financial interest(s): H. G. Stunnenberg, Á. R. de Lera, H. Gronemeyer, and L. Altucci are inventors for the patent WO2008/125988 entitled "Novel Derivatives of Psammaplin A, a Method for Their Synthesis and Their Use for the Prevention or Treatment of Cancer".

■ ACKNOWLEDGMENTS

This work was supported by the European Union Grant LSHC-CT-2005-518417 "Epitron"; the Italian IHEC (Flag Project EPIGEN); the Italian Association for Cancer Research (Contract No. 11812); the Italian Ministry of University and Research (Grants PRIN_2009PX2T2E_004, PON002782, PON0101227); La Ligue Contre le Cancer (HG, équipe labellisée); Association pour la Recherche sur le Cancer (ARC to H.G.); Grant ANR-07-EMPB-012-01 "EPI_DRUG"; MINECO (Grant SAF2010-17935 FEDER to Á.R.d.L.); and Xunta de Galicia (Consolidación, INBIOMED, to Á.R.d.L.). Mayra Stuhldreier was an Erasmus student from Georg-August Universität Göttingen, Germany.

■ DEDICATION

This paper is dedicated to the memory of Annamaria Scognamiglio.

■ ABBREVIATIONS USED

AML, acute myeloid leukemia; APL, acute promyelocytic leukemia; CTCL, cutaneous T cell lymphoma; DNMT, DNA methyltransferase; DNMTis, DNA methyltransferase inhibitors; HAT, histone acetyltransferase; HDAC, histone deacetylase; HDACis, histone deacetylase inhibitors; HDM, histone demethylase; HMT, histone methyltransferase; MDS, myelodysplastic syndrome; NAD, nicotine adenine dinucleotide; SAH, *S*-adenosyl homocysteine (AdoHcy); SAHA, suberoylanilide hydroxamic acid; SAM, *S*-adenosylmethionine (AdoMet); SAR, structure−activity relationship

■ REFERENCES

(1) Wolffe, A. P. *Chromatin: Structure and Function*; Academic Press: London, 1992.

(2) Kouzarides, T. Chromatin modifications and their function. *Cell* **2007**, *128*, 693−705.

(3) Bannister, A. J.; Kouzarides, T. Regulation of chromatin by histone modifications. *Cell Res.* **2011**, *21*, 381−395.
(4) Bhaumik, S. R.; Smith, E.; Shilatifard, A. Covalent modifications of histones during development and disease pathogenesis. *Nat. Struct. Mol. Biol.* **2007**, *14*, 1008−1016.
(5) Voigt, P.; Reinberg, D. Histone tails: ideal motifs for probing epigenetics through chemical biology approaches. *ChemBioChem* **2011**, *12*, 236−252.
(6) Taverna, S. D.; Li, H.; Ruthenburg, A. J.; Allis, C. D.; Patel, D. J. How chromatin-binding modules interpret histone modifications: lessons from professional pocket pickers. *Nat. Struct. Mol. Biol.* **2007**, *14*, 1025−1040.
(7) Allis, C. D.; Berger, S. L.; Cote, J.; Dent, S.; Jenuwein, T.; Kouzarides, T.; Pillus, L.; Reinberg, D.; Shi, Y.; Shiekhattar, R.; Shilatifard, A.; Workman, J. L.; Zhang, Y. New nomenclature for chromatin-modifying enzymes. *Cell* **2007**, *131*, 633−636.
(8) Egger, G.; Liang, G.; Jones, P. A. Epigenetics in human disease and prospects for epigenetic therapy. *Nature* **2004**, *429*, 457−463.
(9) Feinberg, A. P. Phenotypic plasticity and the epigenetics of human disease. *Nature* **2007**, *447*, 433−440.
(10) Portela, A.; Esteller, M. Epigenetic modifications and human disease. *Nat. Biotechnol.* **2010**, *28*, 1057−1068.
(11) Petronis, A. Epigenetics as a unifying principle in the aetiology of complex traits and diseases. *Nature* **2010**, *465*, 721−727.
(12) Rodriguez-Paredes, M.; Esteller, M. Cancer epigenetics reaches mainstream oncology. *Nat. Med.* **2011**, *17*, 330−339.
(13) Dawson, M. A.; Kouzarides, T. Cancer epigenetics: from mechanism to therapy. *Cell* **2012**, *150*, 12−27.
(14) You, J. S.; Jones, P. A. Cancer genetics and epigenetics: two sides of the same coin? *Cancer Cell* **2012**, *22*, 9−20.
(15) Varambally, S.; Dhanasekaran, S. M.; Zhou, M.; Barrettemgrt, T. R.; Kumar-Sinha, C.; Sanda, M. G.; Ghosh, D.; Pienta, K. J.; Sewalt, R. G. A. B.; Otte, A. P. The polycomb group protein EZH2 is involved in progression of prostate cancer. *Nature* **2002**, *419*, 624−629.
(16) Varier, R. A.; Timmers, H. T. M. Histone lysine methylation and demethylation pathways in cancer. *Biochim. Biophys. Acta, Rev. Cancer* **2011**, *1815*, 75−89.
(17) Lee, J.-S.; Smith, E.; Shilatifard, A. The language of histone crosstalk. *Cell* **2010**, *142*, 682−685.
(18) Chi, P.; Allis, C. D.; Wang, G. G. Covalent histone modifications: miswritten, misinterpreted and mis-erased in human cancers. *Nat. Rev. Cancer* **2010**, *10*, 457−469.
(19) Biel, M.; Wascholowski, V.; Giannis, A. Epigenetics—an epicenter of gene regulation: histones and histone-modifying enzymes. *Angew. Chem., Int. Ed.* **2005**, *44*, 3186−3216.
(20) Hellebrekers, D. M. E. I.; Griffioen, A. W.; van Engeland, M. Dual targeting of epigenetic therapy in cancer. *Biochim. Biophys. Acta, Rev. Cancer* **2007**, *1775*, 76−91.
(21) Cheng, X.; Blumenthal, R. M. Mammalian DNA methyltransferases: a structural perspective. *Structure* **2008**, *16*, 341−350.
(22) Chen, Z.-x.; Riggs, A. D. DNA methylation and demethylation in mammals. *J. Biol. Chem.* **2011**, *286*, 18347−18353.
(23) El-Osta, A. DNMT cooperativity: the developing links between methylation, chromatin structure and cancer. *BioEssays* **2003**, *25*, 1071−1084.
(24) Das, P. M.; Singal, R. DNA methylation and cancer. *J. Clin. Oncol.* **2004**, *22*, 4632−4642.
(25) Klose, R. J.; Bird, A. P. Genomic DNA methylation: the mark and its mediators. *Trends Biochem. Sci.* **2006**, *31*, 89−97.
(26) Jones, P. A.; Baylin, S. B. The epigenomics of cancer. *Cell* **2007**, *128*, 683−692.
(27) Feinberg, A. P. Epigenetics at the epicenter of modern medicine. *JAMA, J. Am. Med. Assoc.* **2008**, *299*, 1345−1350.
(28) Esteller, M. Epigenetics in Cancer. *N. Engl. J. Med.* **2008**, *358*, 1148−1159.
(29) Jurkowska, R. Z.; Jurkowski, T. P.; Jeltsch, A. Structure and function of mammalian DNA methyltransferases. *ChemBioChem* **2011**, *12*, 206−222.
(30) Altucci, L.; Leibowitz, M. D.; Ogilvie, K. M.; de Lera, A. R.; Gronemeyer, H. RAR and RXR modulation in cancer and metabolic disease. *Nat. Rev. Drug Discovery* **2007**, *6*, 793−810.
(31) Chen, J.; Odenike, O.; Rowley, J. D. Leukaemogenesis: more than mutant genes. *Nat. Rev. Cancer* **2010**, *10*, 23−36.
(32) Baylin, S. B. DNA methylation and gene silencing in cancer. *Nat. Clin. Pract. Oncol.* **2005**, *2*, S4−S11.
(33) Hodawadekar, S. C.; Marmorstein, R. Chemistry of acetyl transfer by histone modifying enzymes: structure, mechanism and implications for effector design. *Oncogene* **2007**, *26*, 5528−5540.
(34) De Ruijter, A. J. M.; Van Gennip, A. H.; Caron, H. N.; Kemp, S.; Van Kuilenburg, A. B. P. Histone deacetylases (HDACs): characterization of the classical HDAC family. *Biochem. J.* **2003**, *370*, 737−749.
(35) Ekwall, K. Genome-wide analysis of HDAC function. *Trends Genet.* **2005**, *21*, 608−615.
(36) Finkel, T.; Deng, C.-X.; Mostoslavsky, R. Recent progress in the biology and physiology of sirtuins. *Nature* **2009**, *460*, 587−591.
(37) Miller, T. A.; Witter, D. J.; Belvedere, S Histone deacetylase inhibitors. *J. Med. Chem.* **2003**, *46*, 5097−5114.
(38) Paris, M.; Porcelloni, M.; Binaschi, M.; Fattori, D. Histone deacetylase inhibitors: from bench to clinic. *J. Med. Chem.* **2008**, *51*, 1505−1529.
(39) Bieliauskas, A. V.; Pflum, M. K. H. Isoform-selective histone deacetylase inhibitors. *Chem. Soc. Rev.* **2008**, *37*, 1402−1413.
(40) Wang, D.; Helquist, P.; Wiest, O. Zinc binding in HDAC inhibitors: a DFT study. *J. Org. Chem.* **2008**, *72*, 5446−5449.
(41) Longo, V. D.; Kennedy, B. K. Sirtuins in aging and age-related disease. *Cell* **2006**, *126*, 257−268.
(42) Guarente, L. Sirtuins as potential targets for metabolic syndrome. *Nature* **2006**, *444*, 868−874.
(43) Liu, T.; Liu, P. Y.; Marshall, G. M. The critical role of the class III histone deacetylase SIRT1 in cancer. *Cancer Res.* **2009**, *69*, 1702−1705.
(44) Zhong, L.; D'Urso, A.; Toiber, D.; Sebastian, C.; Henry, R. E.; Vadysirisack, D. D.; Guimaraes, A.; Marinelli, B.; Wikstrom, J. D.; Nir, T.; Clish, C. B.; Vaitheesvaran, B.; Iliopoulos, O.; Kurland, I.; Dor, Y.; Weissleder, R.; Shirihai, O. S.; Ellisen, L. W.; Espinosa, J. M.; Mostoslavsky, R. The histone deacetylase SIRT6 regulates glucose homeostasis via Hif1α. *Cell* **2010**, *140*, 280−293.
(45) Lavu, S.; Boss, O.; Elliot, P. J.; Lambert, P. D. Sirtuins—novel therapeutic targets to treat age-associated disorders. *Nat. Rev. Drug Discovery* **2008**, *7*, 841−853.
(46) Kelly, T. K.; De Carvalho, D. D.; Jones, P. A. Epigenetic modifications as therapeutic targets. *Nat. Biotechnol.* **2010**, *28*, 1069−1078.
(47) Nebbioso, A.; Clarke, N.; Voltz, E.; Germain, E.; Ambrosino, C.; Bontempo, P.; Alvarez, R.; Schiavone, E. M.; Ferrara, F.; Bresciani, F.; Weisz, A.; de Lera, A. R.; Gronemeyer, H.; Altucci, L. Tumor-selective action of HDAC inhibitors involves TRAIL induction in acute myeloid leukemia cells. *Nat. Med.* **2005**, *11*, 77−84.
(48) Sippl, W.; Jung, M. *Epigenetic Targets in Drug Discovery*; Wiley-VCH: Weinheim, Germany, 2009; Vol. *42*.
(49) Szyf, M. Epigenetics, DNA methylation and chromatin modifying drugs. *Annu. Rev. Pharmacol. Toxicol.* **2009**, *49*, 243−263.
(50) Minucci, S.; Pelicci, P. G. Histone deacetylase inhibitors and the promise of epigenetic (and more) treatments for cancer. *Nat. Rev. Cancer* **2006**, *6*, 38−51.
(51) Minucci, S.; Pelicci, P. G. Histone deacetylase inhibitors and the promise of epigenetic (and more) treatments for cancer. *Nat. Rev. Cancer* **2006**, *6*, 38−51.
(52) Satterlee, J. S.; Schubeler, D.; Ng, H.-H. Tackling the epigenome: challenges and opportunities for collaboration. *Nat. Biotechnol.* **2010**, *28*, 1039−1044.
(53) Brueckner, B.; Lyko, F. DNA methyltransferase inhibitors: old and new drugs for an epigenetic cancer therapy. *Trends Pharmacol. Sci.* **2004**, *25*, 551−554.
(54) Kaminskas, E.; Farrell, A.; Abraham, S.; Baird, A.; Hsieh, L.-S.; Lee, S.-L.; Leighton, J. K.; Patel, H.; Rahman, A.; Sridhara, R.; Wang, Y.-C.; Pazdur, R. Approval summary: azacitidine for treatment of

myelodysplastic syndrome subtypes. *Clin. Cancer Res.* **2005**, *11*, 3604−3608.
(55) Shigematsu, N.; Ueda, H.; Takase, S.; Tanaka, H.; Yamamoto, K.; Tada, T. FR901228, a novel antitumor bicyclic depsipeptide produced by *Chromobacterium violaceum* No. 968. II. Structure determination. *J. Antibiot.* **1994**, *47*, 311−314.
(56) Newman, D. J. Natural products as leads to potential drugs: an old process or the new hope for drug discovery? *J. Med. Chem.* **2008**, *51*, 2589−2599.
(57) Koehn, F. E.; Carter, G. T. The evolving role of natural products in drug discovery. *Nat. Rev. Drug Discovery* **2005**, *4*, 206−220.
(58) Newkirk, T. L.; Bowers, A. A.; Williams, R. M. Discovery, biological activity, synthesis and potential therapeutic utility of naturally occurring histone deacetylase inhibitors. *Nat. Prod. Rep.* **2009**, *26*, 1293−1320.
(59) Álvarez, R.; Gronemeyer, H.; Altucci, L.; de Lera, A. R. Epigenetic multiple modulators. *Curr. Top. Med. Chem.* **2011**, *11*, 2749−2787.
(60) Gerwick, W. H.; Moore, B. S. Lessons from the past and charting the future of marine natural products drug discovery and chemical biology. *Chem. Biol.* **2012**, *19*, 85−98.
(61) Furumai, R.; Matsuyama, A.; Kobashi, N.; Lee, K. H.; Nishiyama, M.; Nakajima, H.; Tanaka, A.; Komatsu, Y.; Nishino, N.; Yoshida, M.; Horinouchi, S. FK228 (depsipeptide) as a natural prodrug that inhibits class I histone deacetylases. *Cancer Res.* **2002**, *62*, 4916−4921.
(62) Arabshahi, L.; Schmitz, F. J. Brominated tyrosine metabolites from an unidentified sponge. *J. Org. Chem.* **1987**, *52*, 3584−3586.
(63) Rodriguez, A. D.; Akee, R. K.; Scheuer, P. J. Two bromotyrosine-cysteine derived metabolites from a sponge. *Tetrahedron Lett.* **1987**, *28*, 4989−4992.
(64) Quiñoà, E.; Crews, P. Phenolic constituents of *Psammaplysilla*. *Tetrahedron Lett.* **1987**, *28*, 3229−3232.
(65) Piña, I. C.; Gautschi, J. T.; Wang, G. Y. S.; Sanders, M. L.; Schmitz, F. J.; France, D.; Cornell-Kennon, S.; Sambucetti, L. C.; Remiszewski, S. W.; Perez, L. B.; Bair, K. W.; Crews, P. Psammaplins from the sponge *Pseudoceratina purpurea*: inhibition of both histone deacetylase and DNA methyltransferase. *J. Org. Chem.* **2003**, *68*, 3866−3873.
(66) Park, Y.; Liu, Y.; Hong, J.; Lee, C. O.; Cho, H.; Kim, D. K.; Im, K. S.; Jung, J. H. New bromotyrosine derivatives from an association of two sponges, *Jaspis wondoensis* and *Poecillastra wondoensis*. *J. Nat. Prod.* **2003**, *66*, 1495−1498.
(67) Remiszewski, S. W. The discovery of NVP-LAQ824: from concept to clinic. *Curr. Med. Chem.* **2003**, *10*, 2393−2402.
(68) Amatori, S.; Bagaloni, I.; Donati, B.; Fanelli, M. DNA demethylating antineoplastic strategies. *Genes Cancer* **2010**, *1*, 197−209.
(69) Baud, M. G. J.; Leiser, T.; Meyer-Almes, F.-J.; Fuchter, M. J. New synthetic strategies towards psammaplin A, access to natural product analogues for biological evaluation. *Org. Biomol. Chem.* **2011**, *9*, 659−662.
(70) Kim, H. J.; Kim, J. H.; Chie, E. K.; Da Young, P.; Kim, I. A.; Kim, I. H. DNMT (DNA methyltransferase) inhibitors radiosensitize human cancer cells by suppressing DNA repair activity. *Radiat. Oncol.* **2012**, *7*, 39.
(71) Baud, M. G. J.; Leiser, T.; Haus, P.; Samlal, S.; Wong, A. C.; Wood, R. J.; Petrucci, V.; Gunaratnam, M.; Hughes, S. M.; Buluwela, L.; Turlais, F.; Neidle, S.; Meyer-Almes, F.-J.; White, A. J. P.; Fuchter, M. J. Defining the mechanism of action and enzymatic selectivity of psammaplin A against its epigenetic targets. *J. Med. Chem.* **2012**, *55*, 1731−1750.
(72) García, J.; Franci, G.; Pereira, R.; Benedetti, R.; Nebbioso, A.; Rodríguez-Barrios, F.; Gronemeyer, H.; Altucci, L.; de Lera, A. R. Epigenetic profiling of the antitumor natural product psammaplin A and its analogues. *Bioorg. Med. Chem.* **2011**, *19*, 3637−3649.
(73) Belinsky, S. A.; Grimes, M. J.; Picchi, M. A.; Mitchell, H. D.; Stidley, C. A.; Tesfaigzi, Y.; Channell, M. M.; Liu, Y.; Casero, R. A.; Baylin, S. B.; Reed, M. D.; Tellez, C. S.; March, T. H. Combination therapy with Vidaza and Entinostat suppresses tumor growth and reprograms the epigenome in an orthotopic lung cancer model. *Cancer Res.* **2011**, *71*, 454−462.
(74) Nebbioso, A.; Pereira, R.; Khanwalkar, H.; Matarese, F.; García-Rodríguez, J.; Miceli, M.; Logie, C.; Kedinger, V.; Ferrara, F.; Stunnenberg, H. G.; de Lera, A. R.; Gronemeyer, H.; Altucci, L. *Mol. Cancer Ther.* **2011**, *10*, 2394−2404.
(75) Dai, Y.; Guo, Y.; Guo, J.; Pease, L. J.; Li, J.; Marcotte, P. A.; Glaser, K. B.; Tapang, P.; Albert, D. H.; Richardson, P. L.; Davidsen, S. K.; Michaelides, M. R. Indole amide hydroxamic acids as potent inhibitors of histone deacetylases. *Bioorg. Med. Chem. Lett.* **2003**, *13*, 1897−190.
(76) Dai, Y.; Guo, Y.; Curtin, M. L.; Li, J.; Pease, L. J.; Guo, J.; Marcotte, P. A.; Glaser, K. B.; Davidsen, S. K.; Michaelides, M. R. A novel series of histone deacetylase inhibitors incorporating hetero aromatic ring systems as connection units. *Bioorg. Med. Chem. Lett.* **2003**, *13*, 3817−3820.
(77) Gilchrist, T. L.; Roberts, T. G. Addition and cycloaddition reactions of the electrophilic vinyl nitroso compounds 3-nitrosobut-3-en-2-one, 2-nitrosopropenal, and ethyl 2-nitrosopropenoate. *J. Chem. Soc., Perkin Trans. 1* **1983**, 1283−1292.
(78) Moyer, M. P.; Shiurba, J. F.; Rapoport, H. Metal−halogen exchange of bromoindoles. A route to substituted indoles. *J. Org. Chem.* **1986**, *51*, 5106−5110.
(79) Nicolaou, K. C.; Chen, D. Y. K.; Huang, X.; Ling, T.; Bella, M.; Snyder, S. A. Chemistry and biology of diazonamide A: first total synthesis and confirmation of the true structure. *J. Am. Chem. Soc.* **2004**, *126*, 12888−12896.
(80) Stadlwieser, J. F.; Dambaur, M. E. Convenient synthesis of 1*H*-indol-1-yl boronates via palladium(0)-catalyzed borylation of bromo-1*H*-indoles with pinacolborane. *Helv. Chim. Acta* **2006**, *89*, 936−946.
(81) Zhu, G.; Yang, F.; Balachandran, R.; Hook, P.; Vallee, R. B.; Curran, D. P.; Day, B. W. Synthesis and biological evaluation of purealin and analogues as cytoplasmic dynein heavy chain inhibitors. *J. Med. Chem.* **2006**, *49*, 2063−20766.
(82) Kotoku, N.; Tsujita, H.; Hiramatsu, A.; Mori, C.; Koizumi, N.; Kobayashi, M. Efficient total synthesis of bastadin 6, an anti-angiogenic brominated tyrosine-derived metabolite from marine sponge. *Tetrahedron* **2005**, *61*, 7211−7218.
(83) Reddy, A. S.; Kumar, M. S.; Reddy, G. R. A convenient method for the preparation of hydroxamic acids. *Tetrahedron Lett.* **2000**, *41*, 6285−6288.
(84) Hoshino, O.; Murakata, M.; Yamada, K. A convenient synthesis of a bromotyrosine derived metabolite, psammaplin A, from *Psammaplysilla* sp. *Bioorg. Med. Chem. Lett.* **1992**, *2*, 1561−1562.
(85) Nicolaou, K. C.; Hughes, R.; Pfefferkorn, J. A.; Barluenga, S.; Roecker, A. J. Combinatorial synthesis through bisulfide exchange: discovery of potent psammaplin A type antibacterial agents active against methicillin-resistant *Staphylococcus aureus* (MRSA). *Chem.—Eur. J.* **2001**, *7*, 4280−4295.
(86) Pfammatter, M. J.; Siljegovic, V.; Darbre, T.; Keese, R. Synthesis of ω-substituted alkanethiols and (bromomethyl)methylthiomalonates. *Helv. Chim. Acta* **2001**, *84*, 678−689.
(87) Schneider, P. H.; Schrekker, H. S.; Silveira, C. C.; Wessjohann, L. A.; Braga, A. L. First generation cysteine- and methionine-derived oxazolidine and thiazolidine ligands for palladium-catalyzed asymmetric allylations. *Eur. J. Org. Chem.* **2004**, 2715−2722.
(88) Plate, R.; Nivard, R. J. F.; Ottenheijm, H. C. J. Conversion of *N*-hydroxytryptophans into α,β-dehydrotryptophan. An approach to the neoechinulin series. *J. Chem. Soc., Perkin Trans. 1* **1987**, 2473−2480.
(89) Hermkens, P. H. H.; van Maarseveen, J. H.; Cobben, P. L. H. M.; Ottenheijm, H. C. J.; Kruse, C. G.; Scheerent, H. W. Syntheses of 1,3-disubstituted *N*-oxy-[beta]-carbolines by the Pictet−Spengler reactions of *N*-oxy-tryptophan and -tryptamine derivatives. *Tetrahedron* **1990**, *46*, 833−846.
(90) Kumar, V.; Kaur, S.; Kumar, S. $ZrCl_4$ catalyzed highly selective and efficient Michael addition of heterocyclic enamines with [alpha],[beta]-unsaturated olefins. *Tetrahedron Lett.* **2006**, *47*, 7001−7005.
(91) Datta, J.; Ghoshal, K.; Denny, W. A.; Gamage, S. A.; Brooke, D. G.; Phiasivongsa, P.; Redkar, S.; Jacob, S. T. A new class of quinoline-

based DNA hypomethylating agents reactivates tumor suppressor genes by blocking DNA methyltransferase 1 activity and inducing its degradation. *Cancer Res.* **2009**, *69*, 4277−4285.
(92) Solomon, J. M.; Pasupuleti, R.; Xu, L.; McDonagh, T.; Curtis, R.; DiStefano, P. S.; Huber, L. J. Inhibition of SIRT1 catalytic activity increases p53 acetylation but does not alter cell survival following DNA damage. *Mol. Cell. Biol.* **2006**, *26*, 28−38.
(93) Lara, E.; Mai, A.; Calvanese, V.; Altucci, L.; López-Nieva, P.; Martínez-Chantar, M. L.; Varela-Rey, M.; Rotili, D.; Nebbioso, A.; Ropero, S.; Montoya, G.; Oyarzabal, J.; Velasco, S.; Serrano, M.; Witt, M.; Villar-Garea, A.; Inhof, A.; Mato, J. M.; Esteller, M.; Fraga, M. F. Salermide, a sirtuin inhibitor with a strong cancer-specific proapoptotic effect. *Oncogene* **2009**, *28*, 781−791.
(94) Vaquero, A.; Scher, M. B.; Lee, D. H.; Sutton, A.; Cheng, H.-L.; Alt, F. W.; Serrano, L.; Sternglanz, R.; Reinberg, D. SIRT2 is a histone deacetylase with preference for histone H4 Lys 16 during mitosis. *Genes Dev.* **2006**, *20*, 1256−1261.
(95) Pruitt, K.; Zinn, R. L.; Ohm, J. E.; McGarvey, K. M.; Kang, S. H.; Watkins, D. N.; Herman, J. G.; Baylin, S. B. *PLoS Genet.* **2006**, *2*, e40.
(96) Yuan, J.; Pu, M.; Zhang, Z.; Lou, Z. Histone H3-K56 acetylation is important for genomic stability in mammals. *Cell Cycle* **2009**, *8*, 1747−1753.
(97) Verdine, G. L. The flip side of DNA methylation. *Cell* **1994**, *76*, 197.
(98) Bowers, A.; West, N.; Taunton, J.; Schreiber, S. L.; Bradner, J. E.; Williams, R. M. Total synthesis and biological mode of action of largazole: a potent class I histone deacetylase inhibitor. *J. Am. Chem. Soc.* **2008**, *130*, 11219−11222.
(99) Bowers, A. A.; Greshock, T. J.; West, N.; Estiu, G.; Schreiber, S. L.; Wiest, O.; Williams, R. M.; Bradner, J. E. Synthesis and conformation−activity relationships of the peptide isosteres of FK228 and largazole. *J. Am. Chem. Soc.* **2009**, *131*, 2900−2905.
(100) Saito, G.; Swanson, J. A.; Lee, K.-D. Drug delivery strategy utilizing conjugation via reversible disulfide linkages: role and site of cellular reducing activities. *Adv. Drug Delivery Rev.* **2003**, *55*, 199−215.
(101) Somoza, J. R.; Skene, R. J.; Katz, B. A.; Mol, C.; Ho, J. D.; Jennings, A. J.; Luong, C.; Arvai, A.; Buggy, J. J.; Chi, E.; Tang, J.; Sang, B. C.; Verner, E.; Wynands, R.; Leahy, E. M.; Dougan, D. R.; Snell, G.; Navre, M.; Knuth, M. W.; Swanson, R. V.; McRee, D. E.; Tari, L. W. Structural snapshots of human HDAC8 provide insights into the class I histone deacetylases. *Structure* **2004**, *12*, 1325−1334.
(102) Taori, K.; Paul, V. J.; Luesch, H. Structure and activity of largazole, a potent antiproliferative agent from the floridian marine cyanobacterium *Symploca* sp. *J. Am. Chem. Soc.* **2008**, *130*, 1806−1807.
(103) Suzuki, T.; Kouketsu, A.; Itoh, Y.; Hisakawa, S.; Maeda, S.; Yoshida, M.; Nakagawa, H.; Miyata, N. Highly potent and selective histone deacetylase 6 inhibitors designed based on a small-molecular substrate. *J. Med. Chem.* **2006**, *49*, 4809−4812.
(104) Itoh, Y.; Suzuki, T.; Kouketsu, A.; Suzuki, N.; Maeda, S.; Yoshida, M.; Nakagawa, H.; Miyata, N. Design, synthesis, structure−selectivity relationship, and effect on human cancer cells of a novel series of histone deacetylase 6-selective inhibitors. *J. Med. Chem.* **2007**, *50*, 5425−5438.
(105) Suzuki, T.; Hisakawa, S.; Itoh, Y.; Maruyama, S.; Kurotaki, M.; Nakagawa, H.; Miyata, N. Identification of a potent and stable antiproliferative agent by the prodrug formation of a thiolate histone deacetylase inhibitor. *Bioorg. Med. Chem. Lett.* **2007**, *17*, 1558−1561.
(106) Nishino, N.; Jose, B.; Okamura, S.; Ebisusaki, S.; Kato, T.; Sumida, Y.; Yoshida, M. Cyclic tetrapeptides bearing a sulfhydryl group potently inhibit histone deacetylases. *Org. Lett.* **2003**, *5*, 5079−5082.
(107) Rautio, J.; Kumpulainen, H.; Heimbach, T.; Oliyai, R.; Oh, D.; Järvinen, T.; Savolainen, J. Prodrugs: design and clinical applications. *Nat. Rev. Drug Discovery* **2008**, *7*, 255−270.
(108) Bach, R. D.; Dmitrenko, O.; Thorpe, C. Mechanism of thiolate−disulfide interchange reactions in biochemistry. *J. Org. Chem.* **2008**, *73*, 12−21.
(109) Dehmel, F.; Weinbrenner, S.; Julius, H.; Ciossek, T.; Maier, T.; Stengel, T.; Fettis, K.; Burkhardt, C.; Wieland, H.; Beckers, T. Trithiocarbonates as a novel class of HDAC inhibitors: SAR studies, isoenzyme selectivity, and pharmacological profiles. *J. Med. Chem.* **2008**, *51*, 3985−4001.
(110) Kozikowski, A. P.; Chen, Y.; Gaysin, A.; Chen, B.; D'Annibale, M. A.; Suto, C. M.; Langley, B. C. Functional differences in epigenetic modulators—superiority of mercaptoacetamide-based histone deacetylase inhibitors relative to hydroxamates in cortical neuron neuroprotection studies. *J. Med. Chem.* **2007**, *50*, 3054−3061.
(111) Hassig, C. A.; Symons, K. T.; Guo, X.; Nguyen, P.-M.; Annable, T.; Wash, P. L.; Payne, J. E.; Jenkins, D. A.; Bonnefous, C.; Trotter, C.; Wang, Y.; Anzola, J. V.; Milkova, E. L.; Hoffman, T. Z.; Dozier, S. J.; Wiley, B. M.; Saven, A.; Malecha, J. W.; Davis, R. L.; Muhammad, J.; Shiau, A. K.; Noble, S. A.; Rao, T. S.; Smith, N. D.; Hager, J. H. KD5170, a novel mercaptoketone-based histone deacetylase inhibitor that exhibits broad spectrum antitumor activity in vitro and in vivo. *Mol. Cancer Ther.* **2008**, *7*, 1054−1065.
(112) Suzuki, T.; Matsuura, A.; Kouketsu, A.; Hisakawa, S.; Nakagawa, H.; Miyata, N. Design and synthesis of non-hydroxamate histone deacetylase inhibitors: identification of a selective histone acetylating agent. *Bioorg. Med. Chem.* **2005**, *13*, 4332−4342.
(113) Morphy, R.; Rankovic, Z. Designed multiple ligands. An emerging drug discovery paradigm. *J. Med. Chem.* **2005**, *48*, 6523−6543.
(114) Frisch, M. J.; Trucks, G. W.; Schlegel, H. B.; Scuseria, G. E.; Robb, M. A.; Cheeseman, J. R.; Montgomery, J. A., Jr.; Vreven, T.; Kudin, K. N.; Burant, J. C.; Millam, J. M.; Iyengar, S. S.; Tomasi, J.; Barone, V.; Mennucci, B.; Cossi, M.; Scalmani, G.; Rega, N.; Petersson, G. A.; Nakatsuji, H.; Hada, M.; Ehara, M.; Toyota, K.; Fukuda, R.; Hasegawa, J.; Ishida, M.; Nakajima, T.; Honda, Y.; Kitao, O.; Nakai, H.; Klene, M.; Li, X.; Knox, J. E.; Hratchian, H. P.; Cross, J. B.; Bakken, V.; Adamo, C.; Jaramillo, J.; Gomperts, R.; Stratmann, R. E.; Yazyev, O.; Austin, A. J.; Cammi, R.; Pomelli, C.; Ochterski, J. W.; Ayala, P. Y.; Morokuma, K.; Voth, G. A.; Salvador, P.; Dannenberg, J. J.; Zakrzewski, V. G.; Dapprich, S.; Daniels, A. D.; Strain, M. C.; Farkas, O.; Malick, D. K.; Rabuck, A. D.; Raghavachari, K.; Foresman, J. B.; Ortiz, J. V.; Cui, Q.; Baboul, A. G.; Clifford, S.; Cioslowski, J.; Stefanov, B. B.; Liu, G.; Liashenko, A.; Piskorz, P.; Komaromi, I.; Martin, R.L.; Fox, D. J.; Keith, T.; Al-Laham, M. A.; Peng, C. Y.; Nanayakkara, A.; Challacombe, M.; Gill, P. M. W.; Johnson, B.; Chen, W.; Wong, M. W.; Gonzalez, C.; Pople, J.A. *Gaussian 03*, revision D.02; Gaussian, Inc.: Wallingford, CT, 2004.
(115) Bayly, C. I.; Cieplak, P.; Cornell, W. D.; Kollman, P. A. A well-behaved electrostatic potential based method using charge restraints for deriving atomic charges: the RESP model. *J. Phys. Chem.* **1993**, *97*, 10269−10280.
(116) Cornell, W. D.; Cieplak, P.; Bayly, C. I.; Gould, I. R.; Merz, K. M.; Ferguson, D. M.; Spellmeyer, D. C.; Fox, T.; Caldwell, J. W.; Kollman, P. A. A second generation force field for the simulation of proteins, nucleic acids, and organic molecules. *J. Am. Chem. Soc.* **1995**, *117*, 5179−5197.
(117) Rodríguez-Barrios, F.; Pérez, C.; Lobatón, E.; Velázquez, S.; Chamorro, C.; San-Félix, A.; Pérez-Pérez, M. J.; Camarasa, M. J.; Pelemans, H.; Balzarini, J.; Gago, F. Identification of a putative binding site for [2′,5′-bis-*O*-(*tert*-butyldimethylsilyl)-*β*-D-ribofuranosyl]-3′-spiro-5″-(4″-amino-1″,2″-oxathiole-2″,2″-dioxide)thymine (TSAO) Derivatives at the p51-p66 Interface of HIV-1 Reverse Transcriptase. *J. Med. Chem.* **2001**, *44*, 1853−1865.
(118) Morris, G. M.; Goodsell, D. S.; Halliday, R. S.; Huey, R.; Hart, W. E.; Belew, R. K.; Olson, A. J. Automated docking using Lamarckian genetic algorithm and an empirical binding free energy function. *J. Comput. Chem.* **1998**, *19*, 1639−1662.
(119) Morris, G. M.; Goodsell, D. S.; Huey, R.; Hart, W. E.; Halliday, S.; Belew, R.; Olson, A. J. *AutoDock, Automated Docking of Flexible Ligands to Receptors*, version 3.0; The Scripps Research Institute: La Jolla, CA, 1999.
(120) Goodford, P. J. A computational procedure for determining energetically favorable binding sites on biologically important macromolecules. *J. Med. Chem.* **1985**, *28*, 849−857.
(121) Åqvist, J. Ion−water interaction potentials derived from free energy perturbation simulations. *J. Phys. Chem.* **1990**, *94*, 8021−8024.

(122) Jorgensen, W. L.; Chandrasekhar, J.; Madura, J. D. Comparison of simple potential functions for simulating liquid water. *J. Chem. Phys.* **1983**, *79*, 926−935.
(123) Case, D. A.; Darden, T. A.; Cheatham, T. E., III; Simmerling, C. L.; Wang, J.; Duke, R. E.; Luo, R.; Merz, K. M.; Wang, B.; Pearlman, D. A.; Crowley, M.; Brozell, S.; Tsui, V.; Gohlke, H.; Mongan, J.; Hornak, V.; Cui, G.; Beroza, P.; Schafmeister, C.; Caldwell, J. W.; Ross, W. S.; Kollman, P. A. *AMBER 8*; University of California, San Francisco, 2004.
(124) Ryckaert, J. P.; Ciccoti, G.; Berendsen, H. J. C. Numerical integration of the Cartesian equations of motion of a system with constraints: molecular dynamics of *n*-alkanes. *J. Comput. Phys.* **1977**, *23*, 327−341.